Macaque V1

Myelin

Nissl

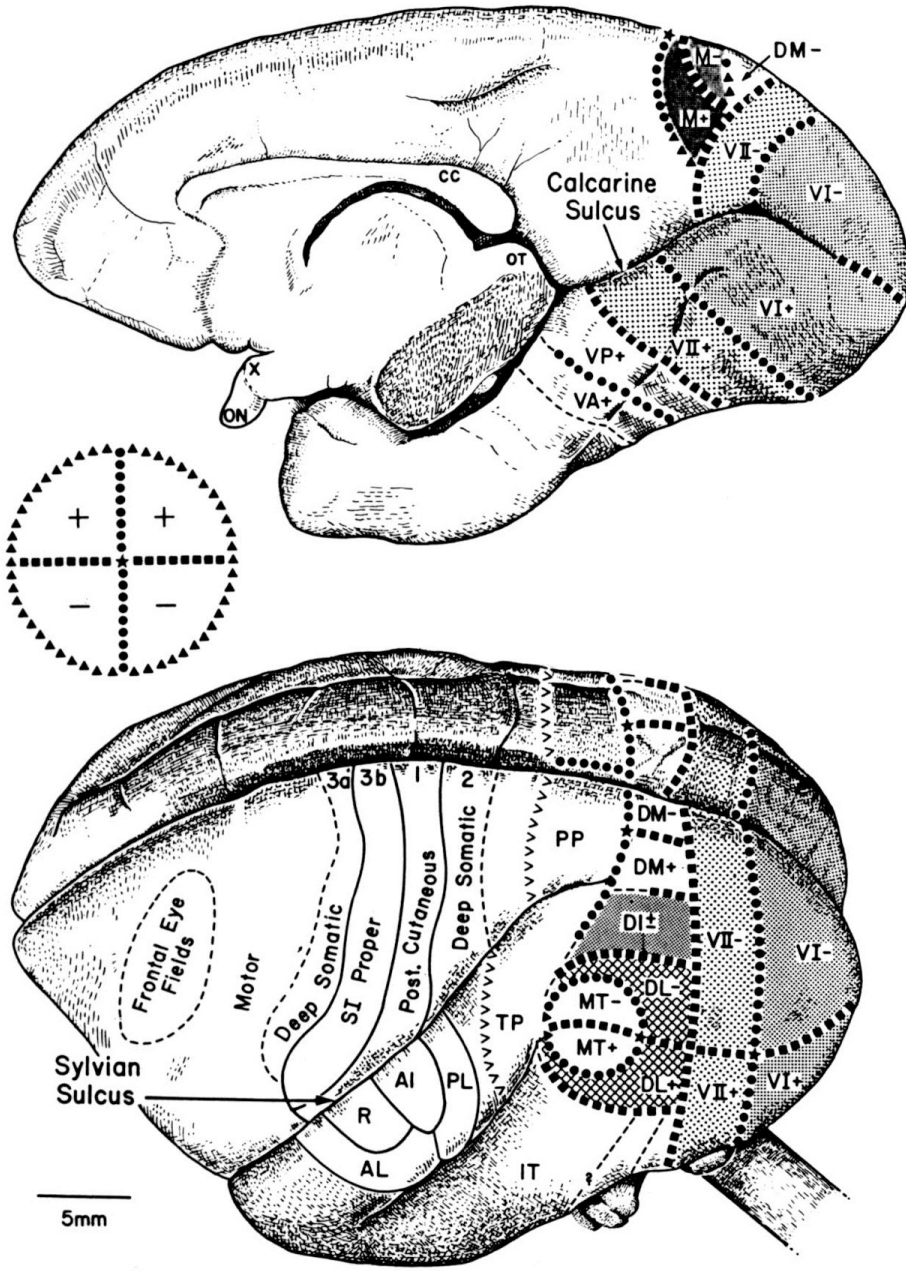

Allman & Kaas, 1981

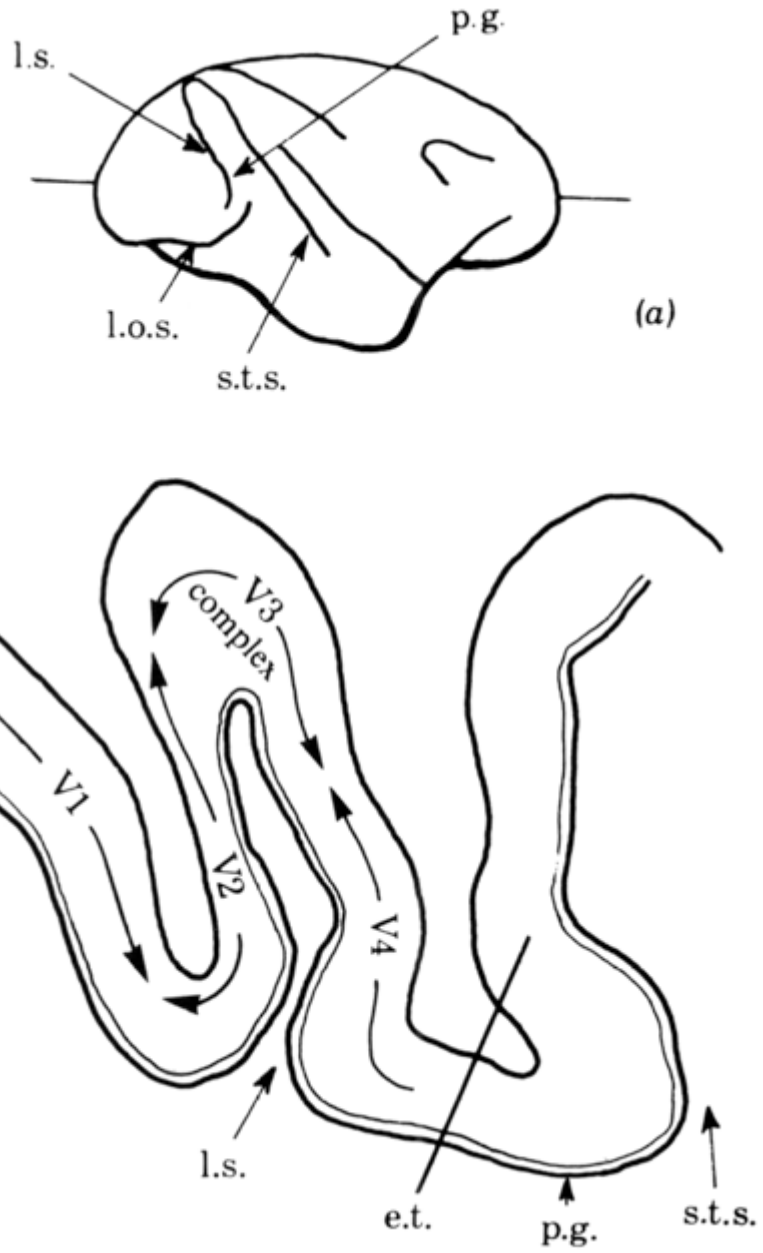

Zeki, 1978

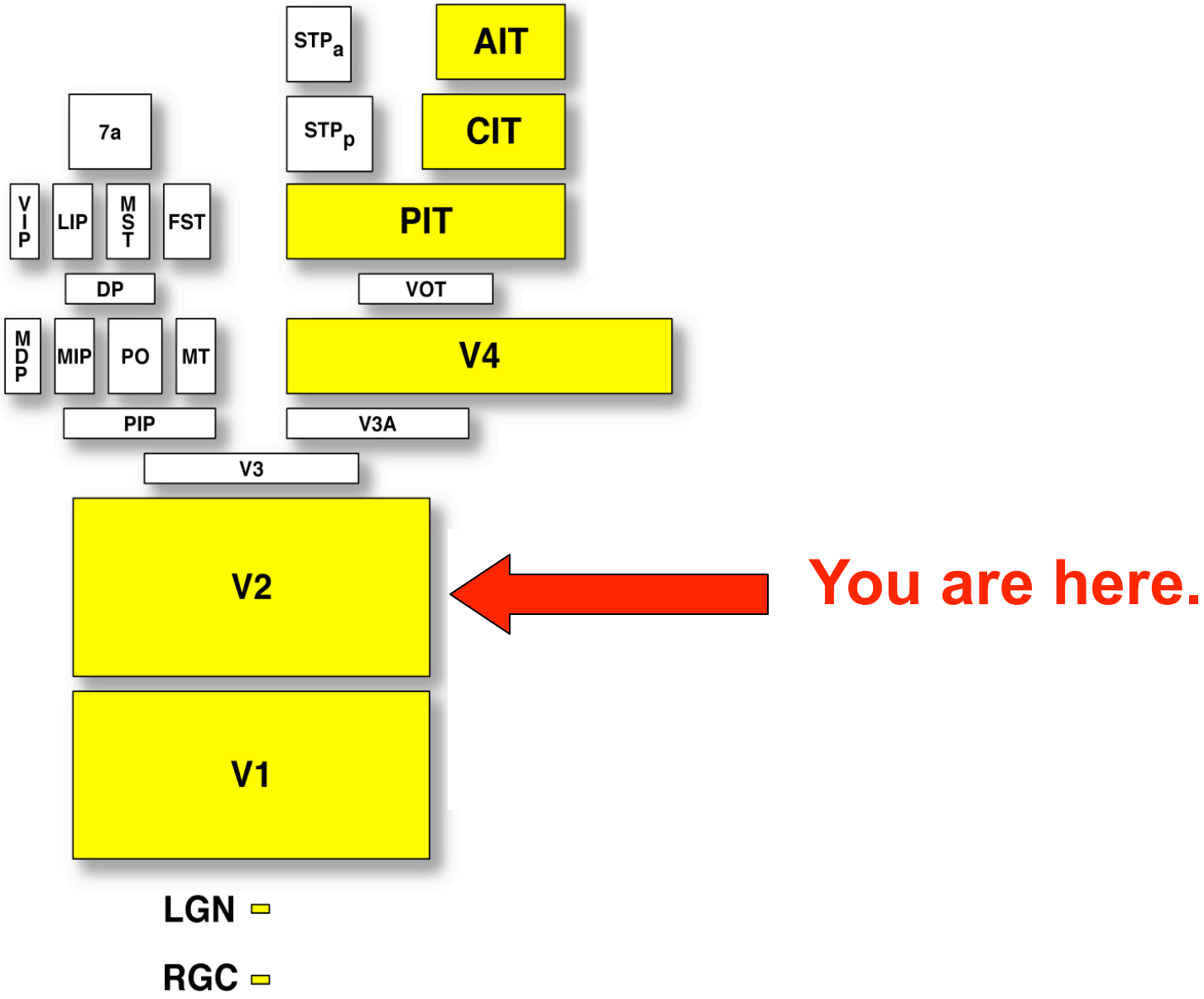
STP a
AIT
7a
STP p
CIT
VIP
LIP
MST
FST
PIT
DP
VOT
MDP
MIP
PO
MT
V4
PIP
V3A
V3
V2
V1
LGN
RGC
You are here.

Macaque V1 patches and V2 stripes. A montage prepared from tissue sections cut tangentially to the cortical surface reveals characteristic patterns of endogenous metabolic activity when processed for CO. (*Bottom*) In V1 a fine array of patches is visible. (*Top*) In V2 a more irregular pattern is present, consisting of pale, thin (*arrows*) and thick (*brackets*) stripes arranged in repeating cycles.

Sincich, LC and Horton, JC. 2005
Annu. Rev. Neurosci. 28: 303–26

Cytochrome oxidase labelled stripes in a flattened section of macaque monkey area V2.

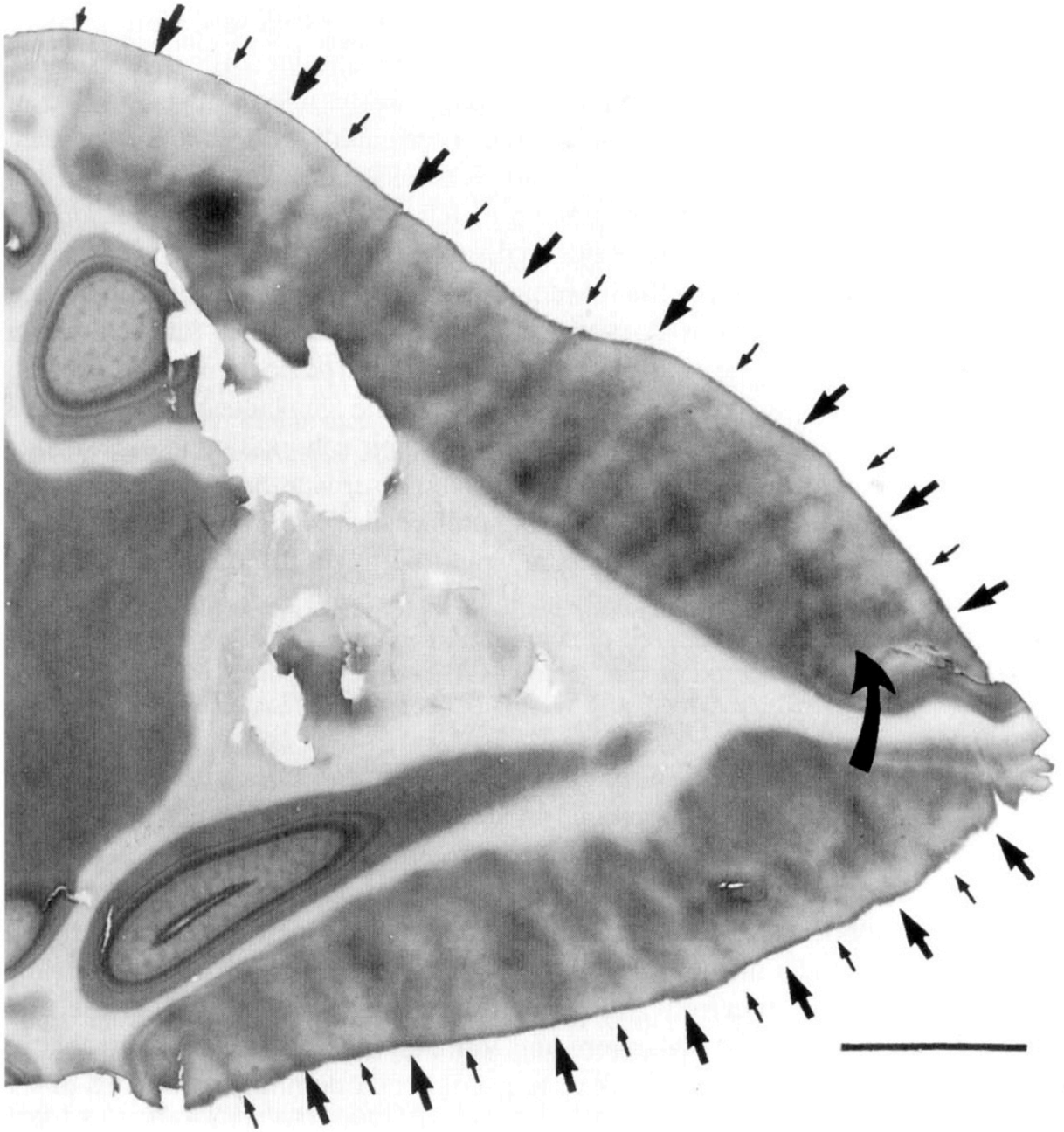

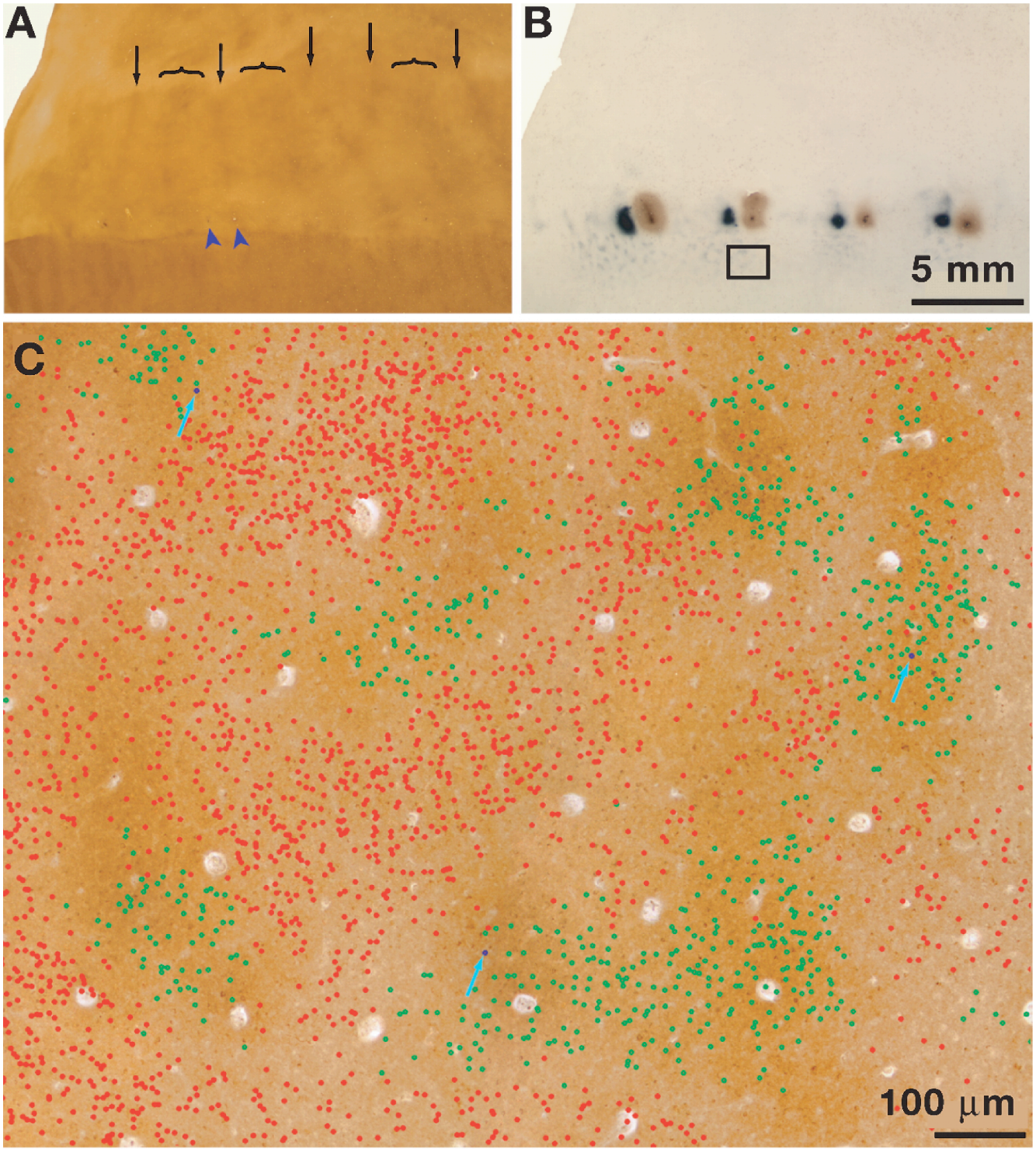

Segregation of V1-to-V2 projections. (*A*) Single CO-stained section from layer 4 in V2, showing the stripe pattern (*brackets, thick stripes; arrows, thin stripes*). One of the thin stripes splits to form a "Y"; such stripe bifurcations occasionally interrupt the regular stripe sequence. Blue arrowheads indicate the location of a CTB-Au injection in a pale stripe (*left*) and a WGA-HRP injection in a thin stripe (*right*). (*B*) A section more superficial to the one shown in (*A*), processed for both tracers. Black box is the area where cells are plotted and shown at higher power below. (*C*) Cells counted in box are superimposed onto the CO pattern from an adjacent section. Neurons projecting to the thin stripe (*green*, n = 703) were located in CO patches, whereas those projecting to the pale stripe (*red*, n = 2058) were situated in the interpatches. Of the 2761 cells in this single section, 3 were double-labeled (*blue, arrows*), demonstrating the high degree of segregation between these two pathways.

Sincich & Horton (2005)

Parallel visual pathways reconsidered

Cross-talk within V1

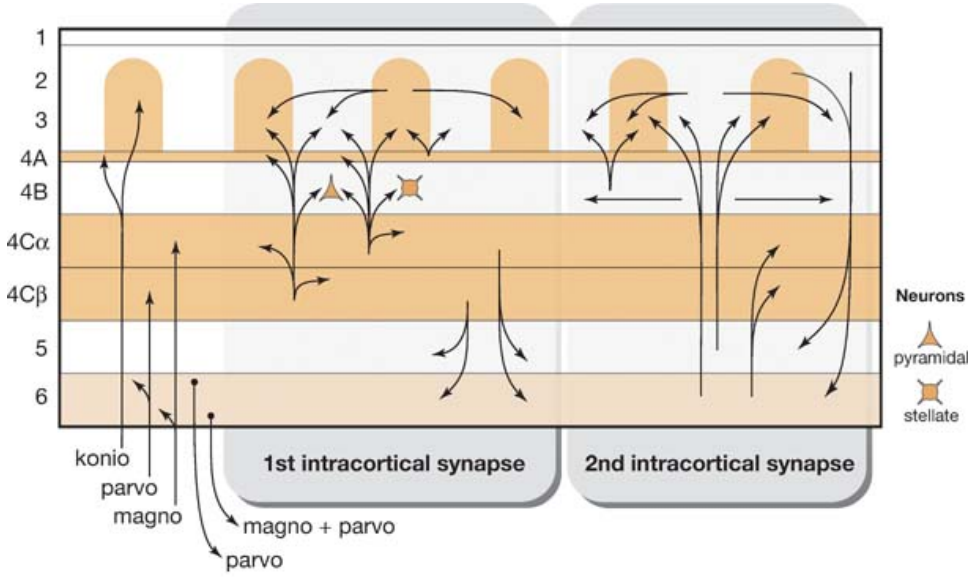

Sincich, LC and Horton, JC. 2005
Annu. Rev. Neurosci. 28: 303–26

V1-V2 projections not segregated

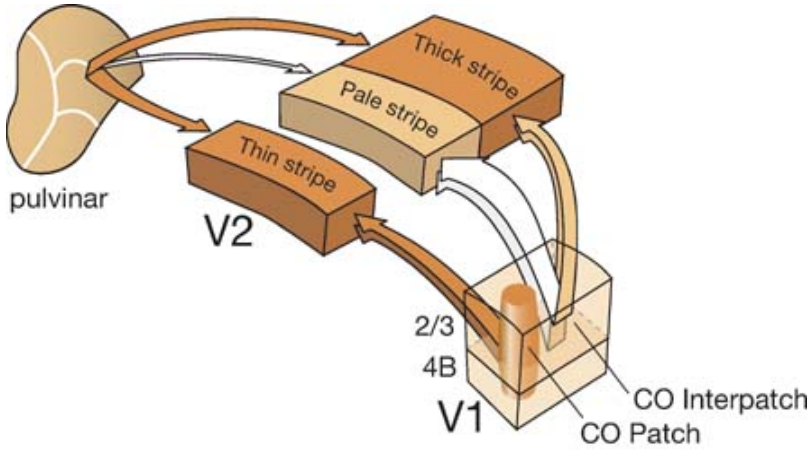

Sincich, LC and Horton, JC. 2005
Annu. Rev. Neurosci. 28: 303–26

Sincich & Horton (2005)

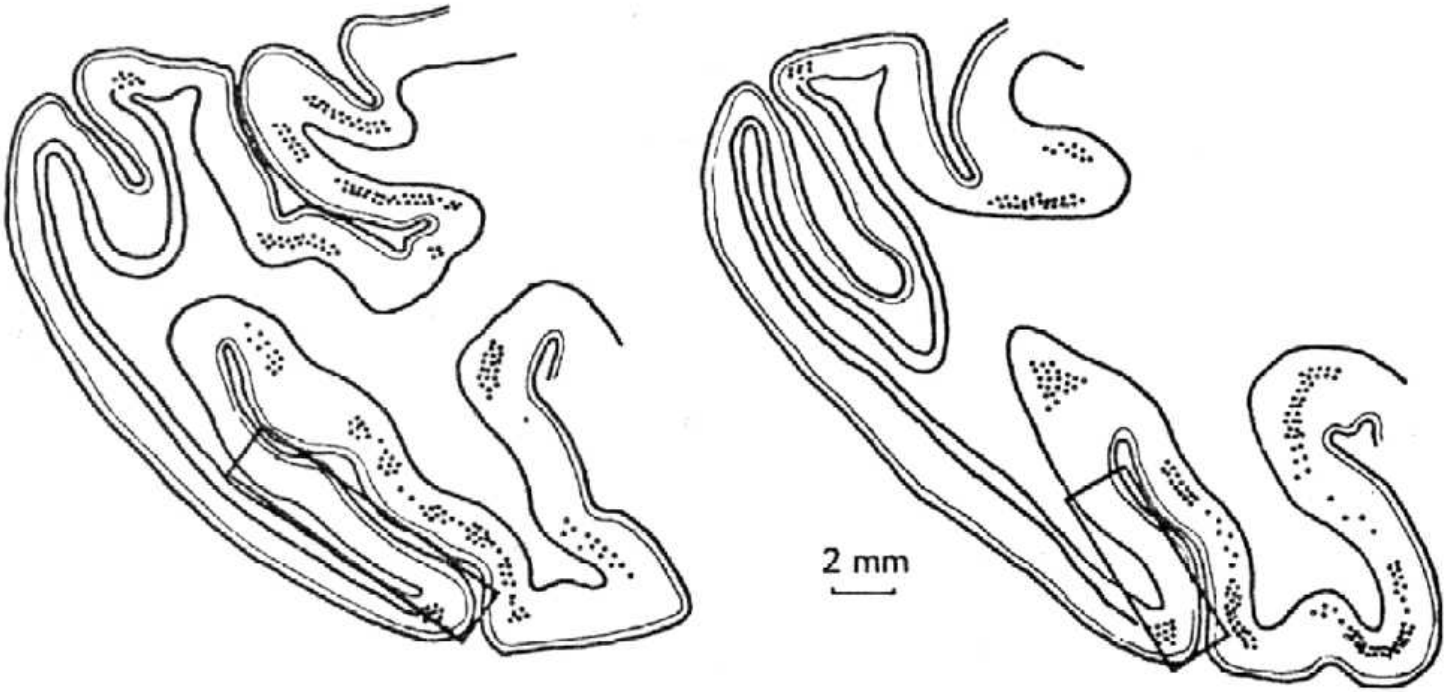

Area V2

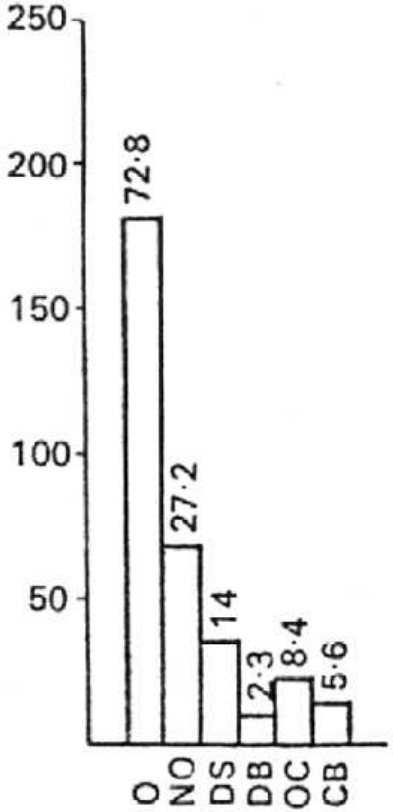

Semir Zeki

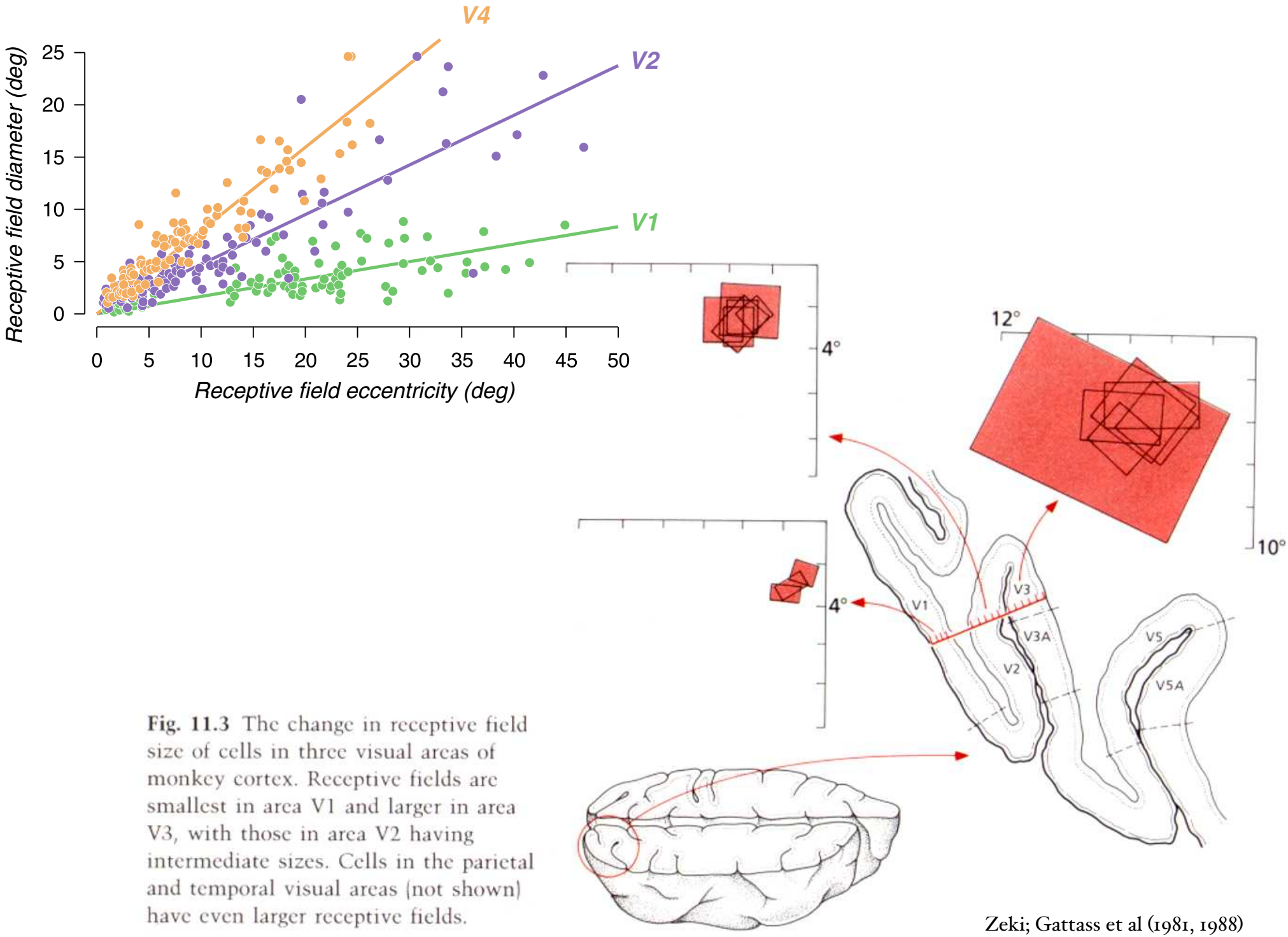

Fig. 11.3 The change in receptive field size of cells in three visual areas of monkey cortex. Receptive fields are smallest in area V1 and larger in area V3, with those in area V2 having intermediate sizes. Cells in the parietal and temporal visual areas (not shown) have even larger receptive fields.

Zeki; Gattass et al (1981, 1988)

Functional compartments in V2 (T'so et al 2001)

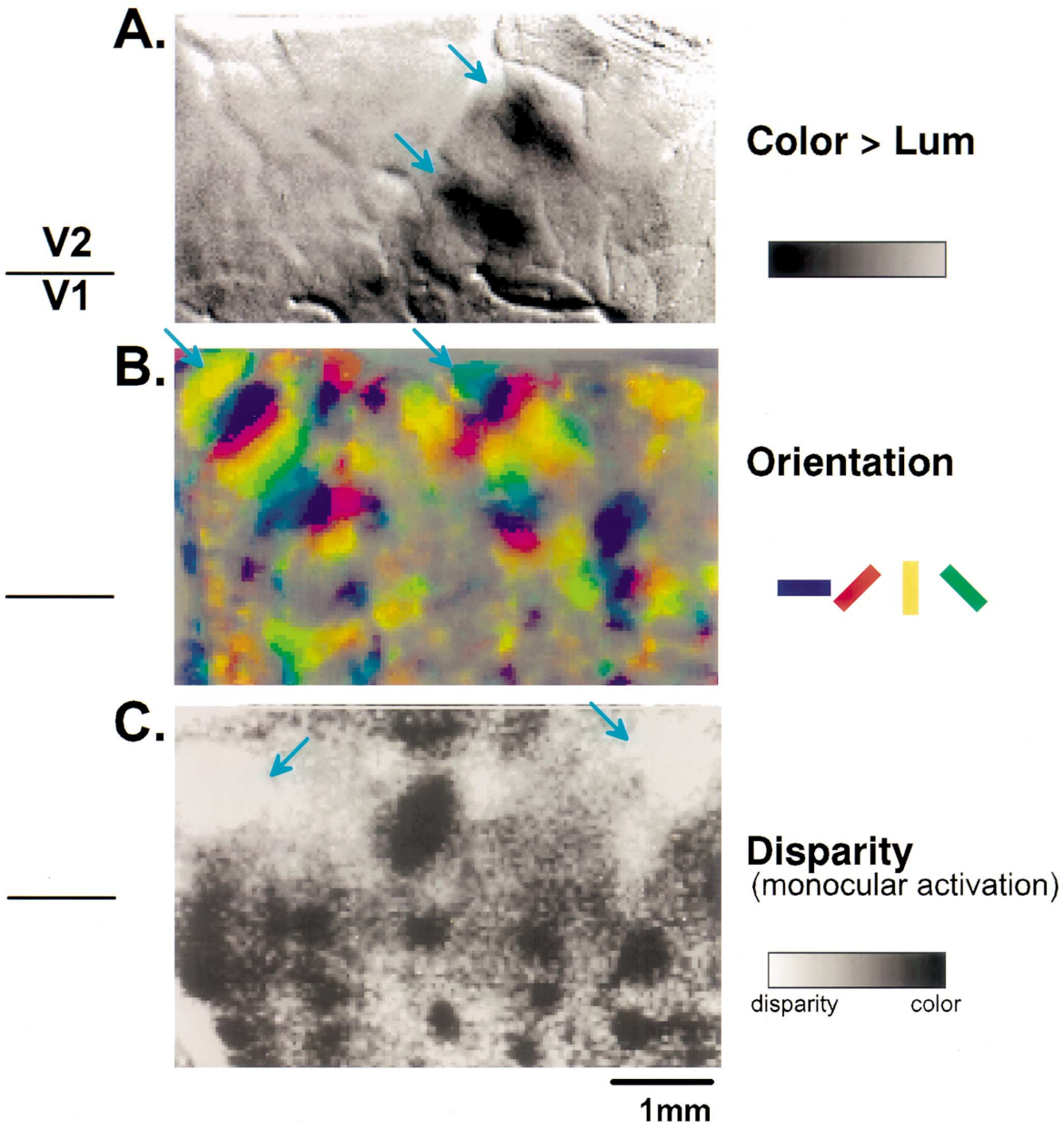

Fig. 10. Subcompartments for color, orientation and disparity within stripes of V2. The three optical images were obtained from different animals. (A) Color-preferring and luminance-preferring subcompartments within a single thin stripe. (B) Pseudo-color coded image of orientation selectivity in V2, showing domains of orientation (blue arrows indicate zones containing pale and thick stripes, large patches of saturated colors), separated by regions of little apparent organization for orientation (thin stripes, lacking patches of saturated color). Color code: blue = horizontal, red = 45°, yellow = vertical, green = 135°. (C) Patches of tuned excitatory disparity cells (white patches, left blue arrow) within thick stripes. Also patches of color cells (the dark patches, right blue arrow) can be seen within thin stripes of V2. Note the similarity of the geometry of the subcompartments, 0.7–1.5 mm in size, regardless of functional type, whereas subcompartments for color (blobs) or (iso)orientation in V1 are smaller than those in V2, at $\sim$0.2 mm in size.

Functional compartments in V2 (Lu et al 2010)

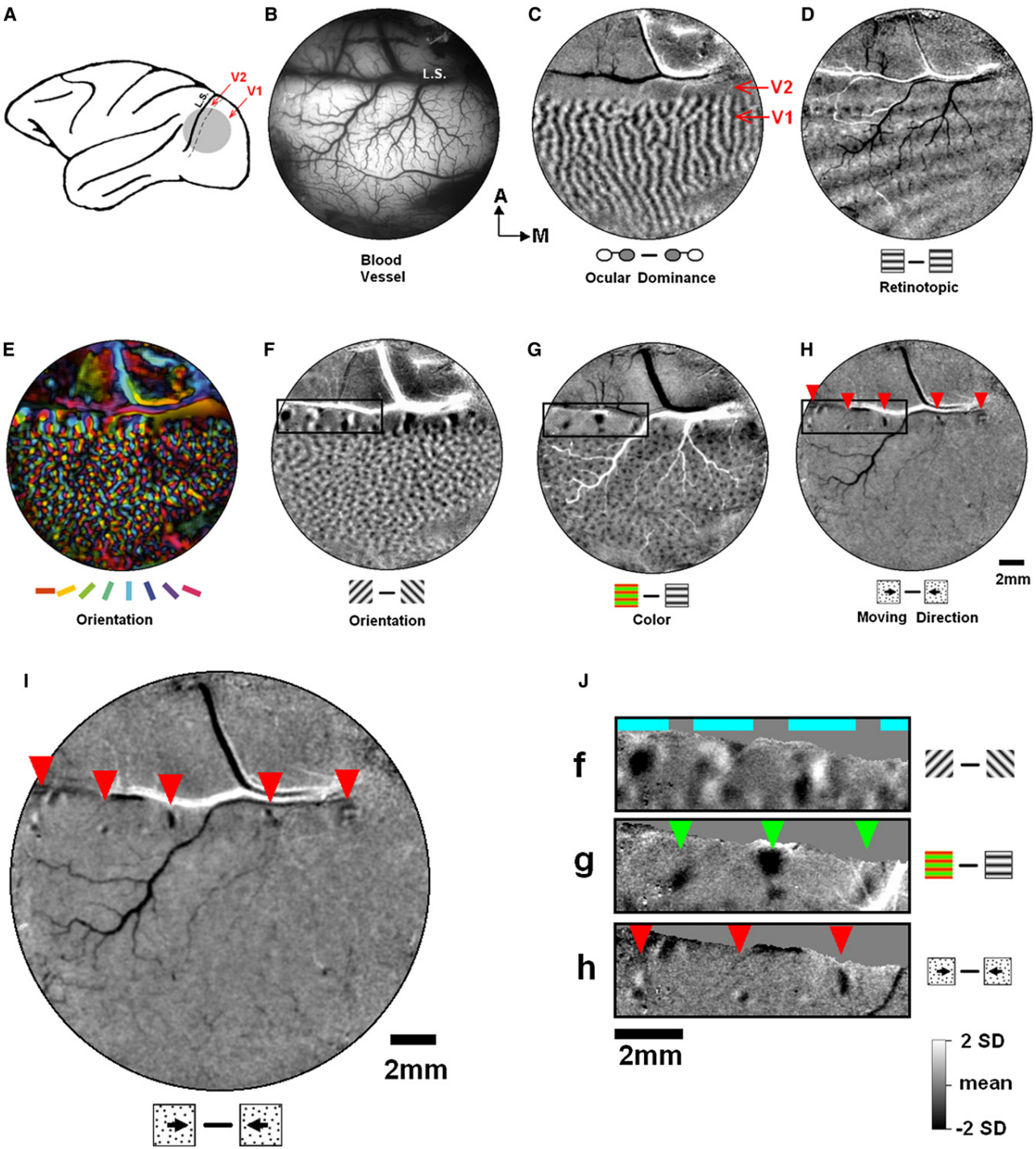

(A) Illustration of a macaque brain and the approximate location of imaging area. L.S., location of lunate sulcus.
\(B) Surface blood vessel pattern of the imaging area.
(C) Ocular dominance map (left-eye minus right-eye stimulation) reveals ocular dominance columns in V1 and lack thereof in V2. The imageable area of V2 is located between the V1/V2 border and the lunate sulcus.
(D) Retinotopic mapping (subtraction of two stationary phase-shifted vertical squarewave gratings) reveals cortical representation of vertical lines in the visual field. Left side of the image is closer to the fovea and has higher cortical magnification.
(E) Orientation vector map. Different colors represent different orientation preferences
(F) Orientation map (45-135 deg gratings) reveals locations of orientation-selective domains corresponding to thick/pale stripe locations in V2 (indicated by cyan bars in top panel of J).
(G) Color map (isoluminant red/green minus luminance gratings) reveals blobs in V1 and color preference domains corresponding to thin stripe locations in V2 (indicated by green arrowheads in middle panel of J).
(H) Motion direction map (rightward minus leftward drifting random dots). Red arrowheads: areas in V2 with directional response preference. No directional preference domains are seen in V1 and other parts of V2. (I) Enlarged view of (H).
(J) f, g, and h: Enlarged view of boxed regions of V2 shown in (F), (G), and (H), respectively.
Strong blood vessel noise overlying large vessel in lunate sulcus is replaced with even gray (top portion of each panel). Thick/pale stripes (indicated by cyan bars) contain orientation preference domains (f). Thin stripes (indicated by green arrowheads) contain color preference domains (g). Note that color preference regions (green arrowheads in g) occur in regions with poor orientation selectivity (even gray zones aligned with spaces between cyan bars in f) and interdigitate with orientation-selective regions. Directional domains (h, red arrow- heads) fall within thick/ pale stripe zones and avoid thin stripe zones. Maps (C)–(J) are displayed using the gray scale shown on the lower-right corner (SD: standard deviation of pixel distributions for each individual maps).

Effects of V2 lesions (Merigan et al 1993)

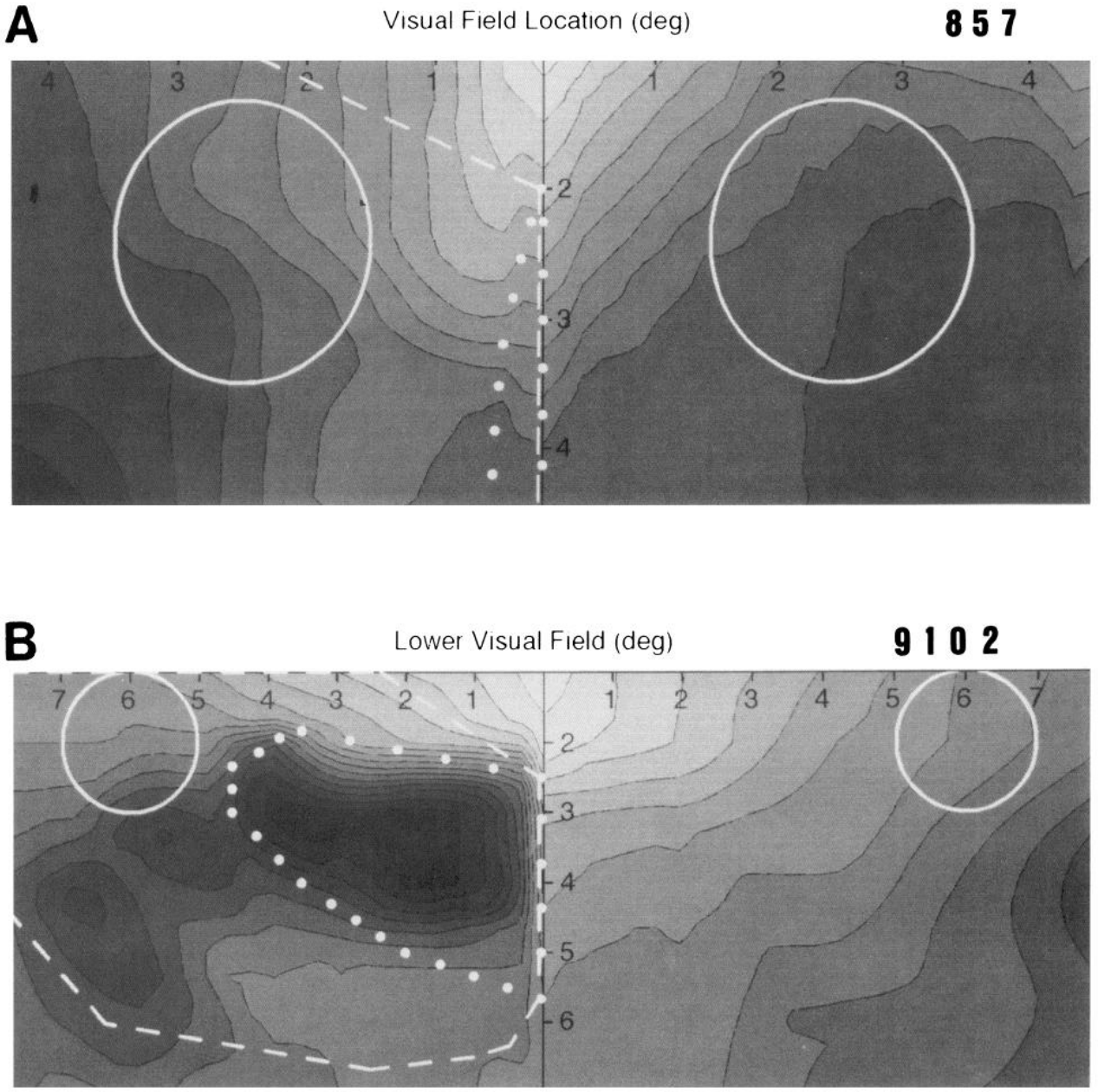

Figure 7. Visual acuity across the lower visual field of monkeys 857 and 9102. Acuity was measured at 2° intervals in monkey 857, and with 1° spacing in monkey 9102. The *vertical axis* corresponds to the vertical meridian of the visual field, and the *horizontal axis* is 1° below the horizontal meridian. The highest acuity was at the origin of the axes, and it was approximately the same in monkey 857 and in monkey 9102. Successive contour lines represent about a 10% decrease from this acuity. *Dotted lines* show the location of inadvertent damage to cortical area V1, and *dashed lines* damage to area V2. The *circles* represent the location and approximate extent of the test locations for contrast sensitivity and orientation of lines of dots or texture elements.

Effects of V2 lesions (Merigan et al 1993)

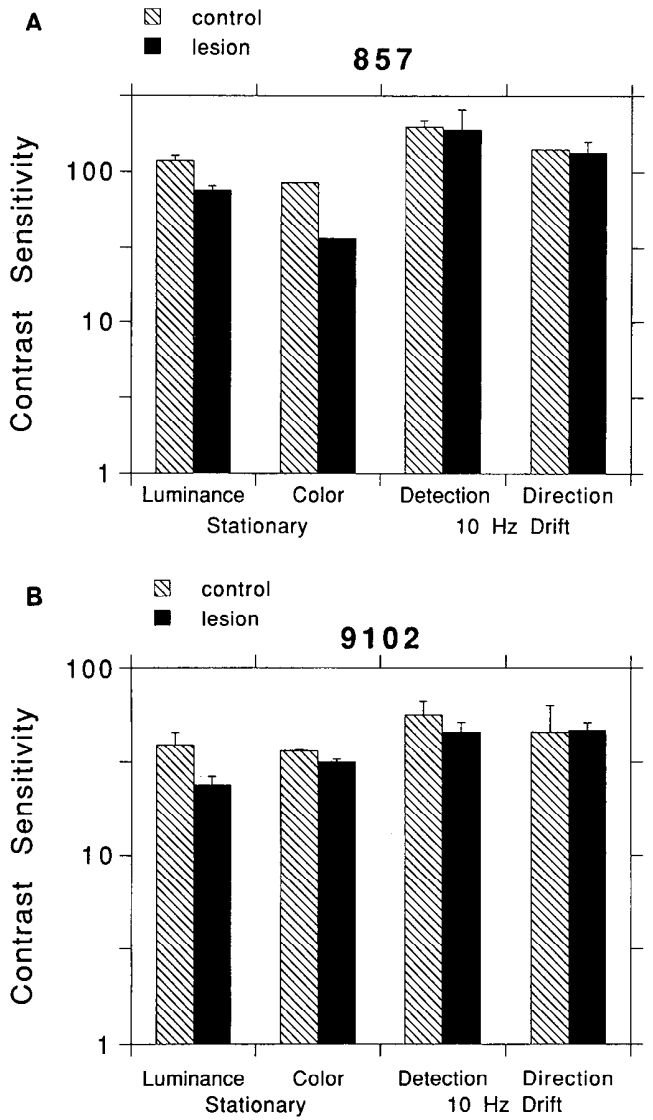

Figure 8. Contrast sensitivity of monkeys 857 and 9102 in control and V2 lesion locations (see Fig. 5 for visual field locus) for four types of Gabor stimuli. *Luminance* sensitivity was measured with stationary, 1 cycle/degree grating patches; *Color* sensitivity with stationary, 1 cycle/degree isoluminant red–green grating patches; *Detection* with 10 Hz, rightward drifting, 1 cycle/degree grating patches; and *Direction* with identical grating patches that drifted either right or left. The value shown for *Color* is chromatic contrast sensitivity (sum of the modulation of middle- and long-wavelength cones), and for the other tests is Michaelson contrast ($L_{max} - L_{min}/L_{max} + L_{min}$). The only significant difference was color contrast sensitivity for monkey 857 ($t = 22$, df = 1, $p > 0.05$). Error bars are ±SEM.

Effects of V2 lesions (Merigan et al 1993)

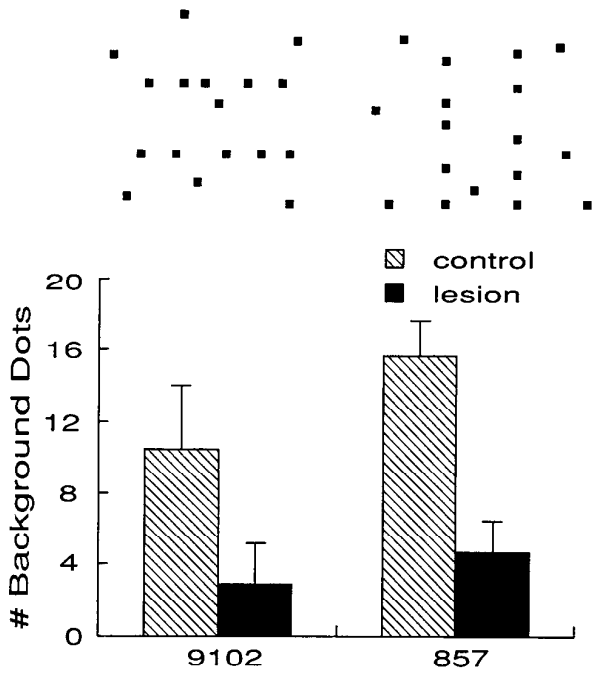

Figure 9. The number of background dots that brought the discrimination illustrated above the data to threshold performance. Results are shown for both monkeys in control and V2 lesion locations. On each trial only a single stimulus was presented. The stimulus shown to the *left* above the data has two horizontal lines of dots masked by seven background dots and indicated that a left response was correct. That to the *right* has two vertical lines of dots masked by seven background dots and indicates that a right response was correct. Stimuli indicating left and right responses are shown in the same way in Figures 10–13. Error bars are ±SEM. The lesion effect was significant for monkey 857 (t = 15, df = 1, $p > 0.05$).

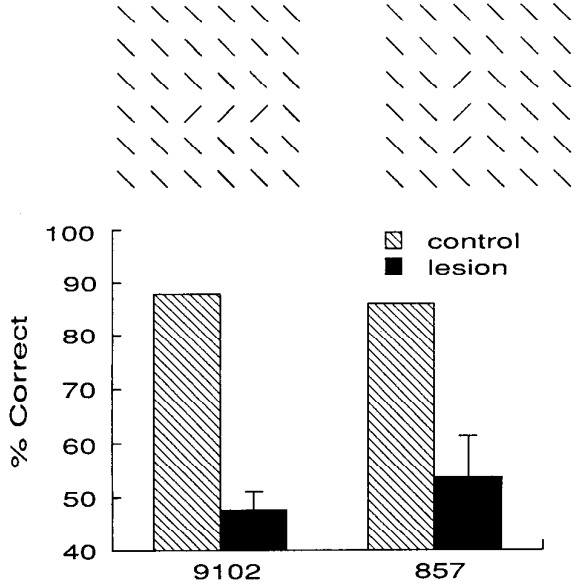

Figure 10. Percent correct performance for the two monkeys in control and V2 lesion locations for the discrimination task illustrated above the data. The stimulus to the *right* has a vertical row of right-oblique lines, and that to the *left* has a horizontal row. The monkey was required to identify the orientation of the row of differently oriented segments. Error bars are ±SEM. Both lesion effects were significant (t = 21, 23; df = 1; $p > 0.05$).

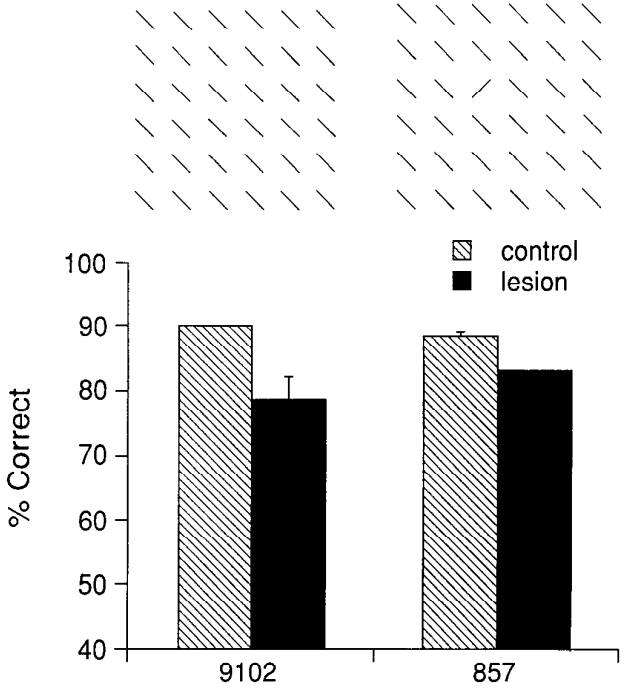

Figure 11. Percent correct performance on a discrimination used to determine if the monkey could detect differently oriented line segments. Performance is shown for both control and V2 lesion locations. Error bars are ±SEM. The effect of the lesion was significant for monkey 857 (t = 11, df = 1, $p > 0.05$).

Orientation selectivity in V1

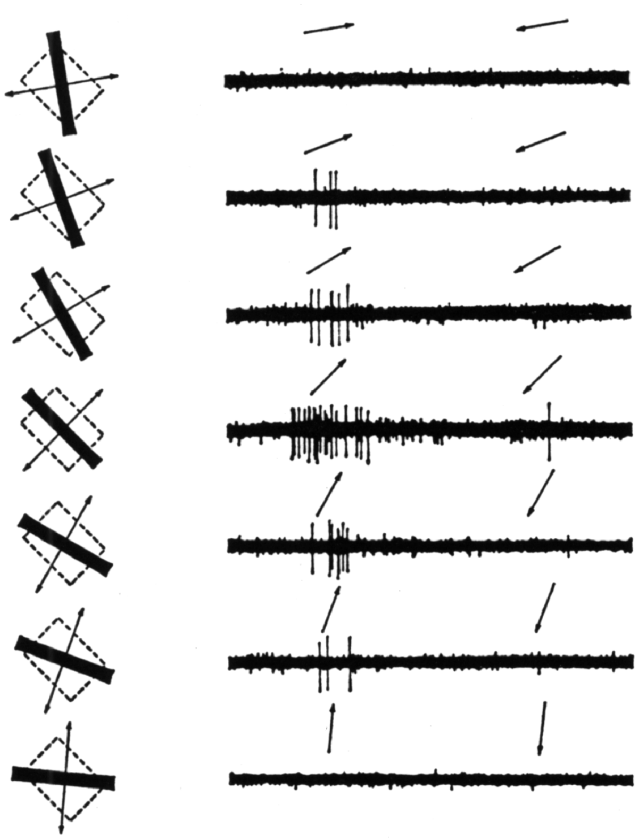

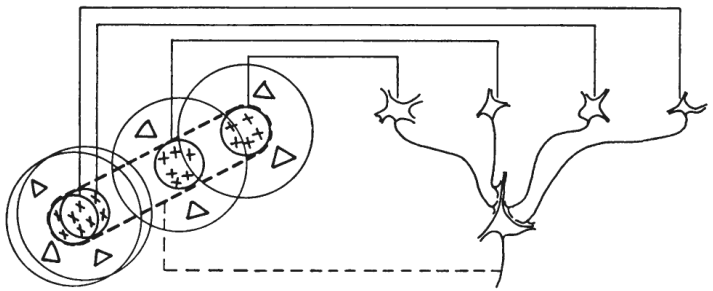

Hubel & Wiesel (1962, 1965, 1968)

RECEPTIVE FIELDS AND FUNCTIONAL ARCHITECTURE IN TWO NONSTRIATE VISUAL AREAS (18 AND 19) OF THE CAT[1]

DAVID H. HUBEL AND TORSTEN N. WIESEL
Neurophysiology Laboratory, Department of Pharmacology, Harvard Medical School, Boston, Massachusetts

(Received for publication August 24, 1964)

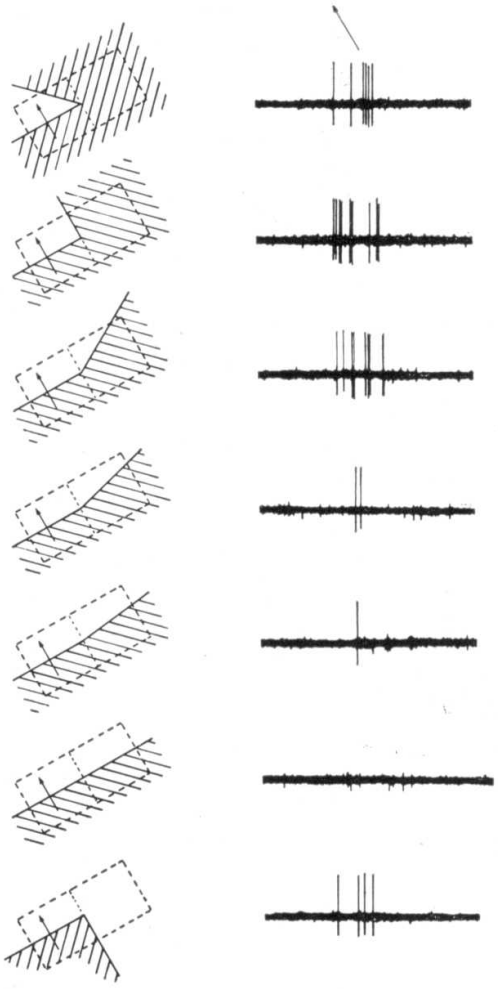

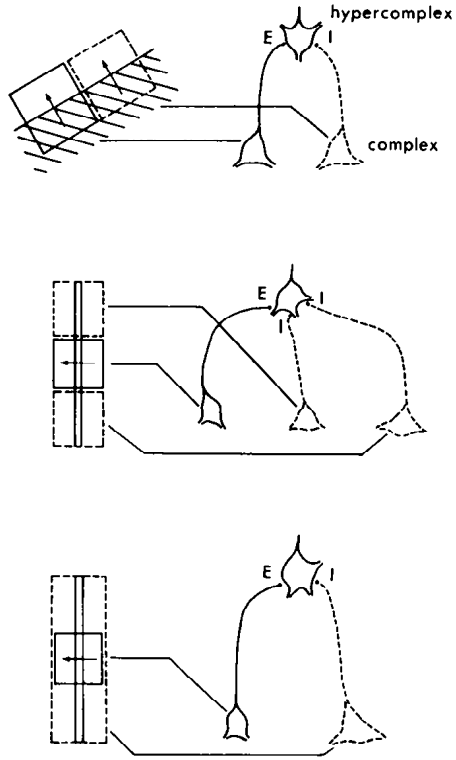

Structure of V2 receptive fields

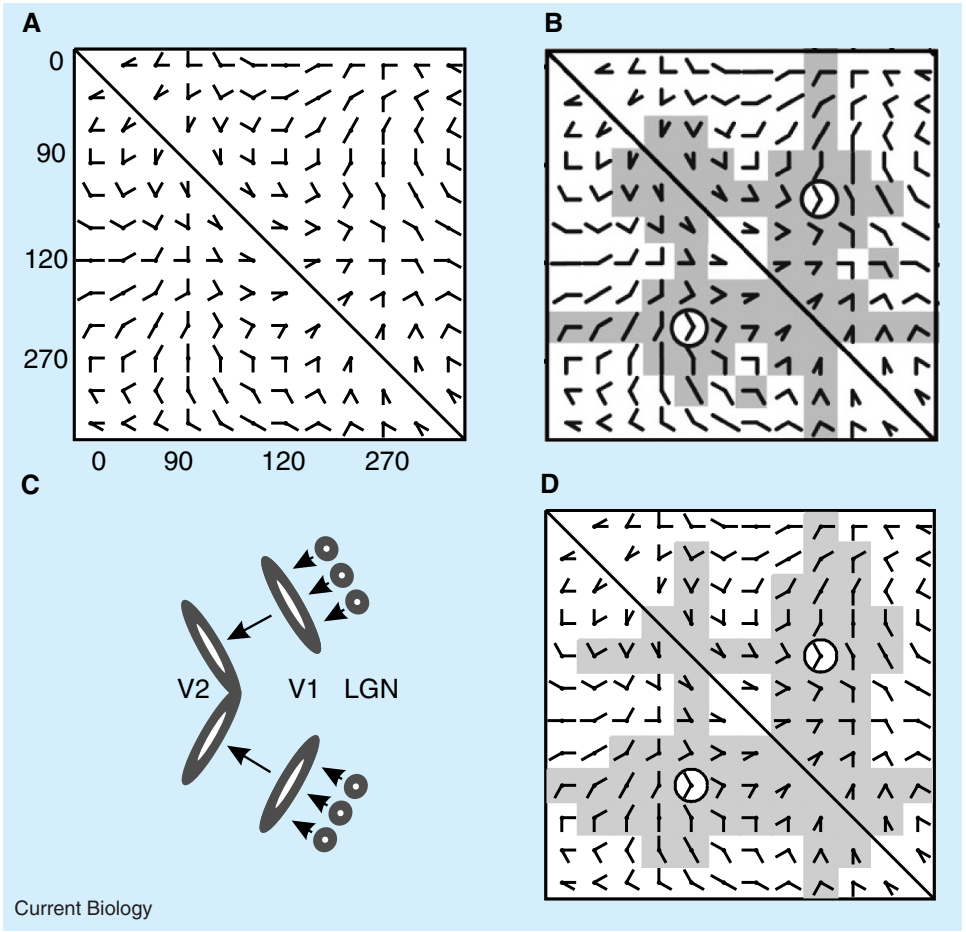

Boynton & Hegde, 2004; Ito & Komatsu, 2004;
Willmore, Prenger & Gallant, 2010

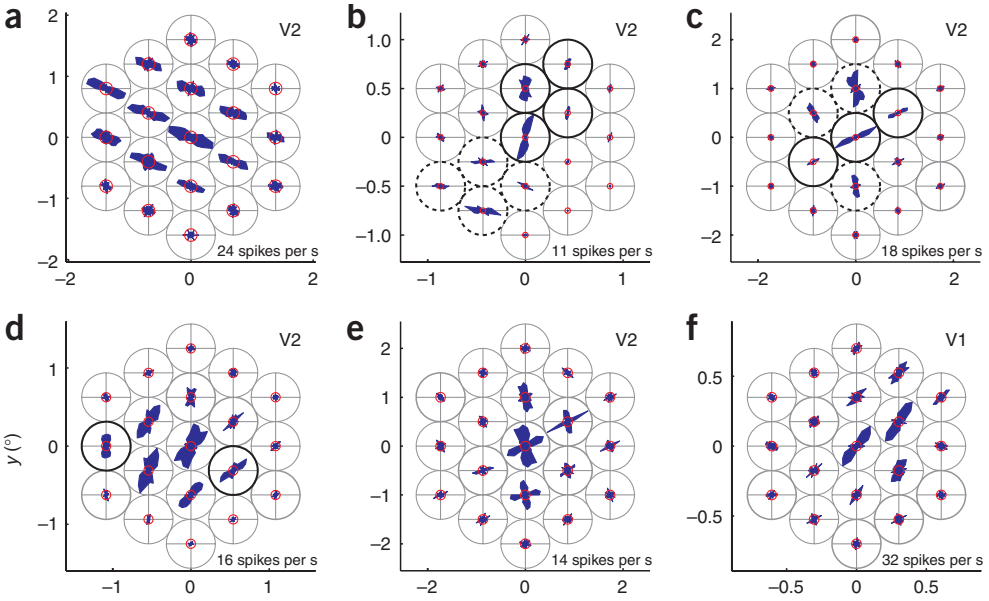

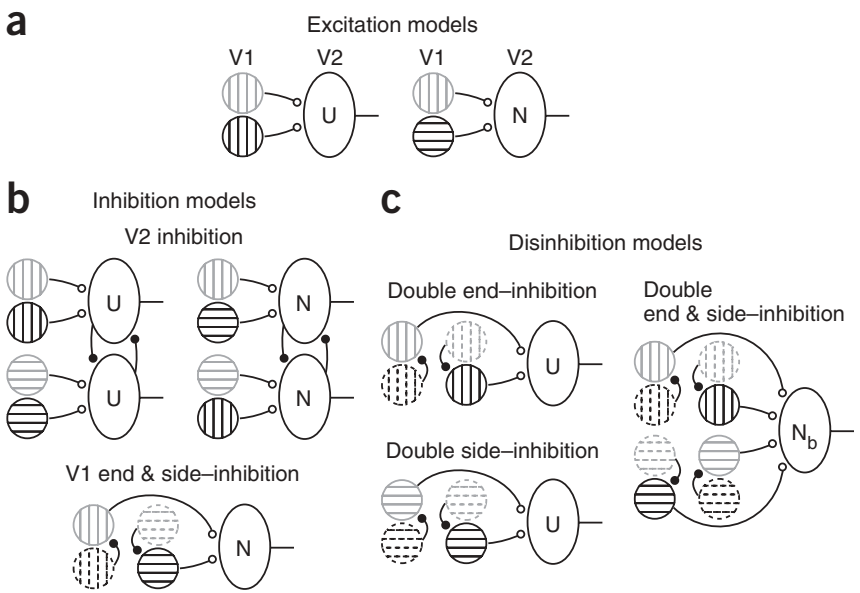

Anzai, Peng & Van Essen, 2007

V2 responses to nonconventional form stimuli (Hegde and Van Essen, 2002)

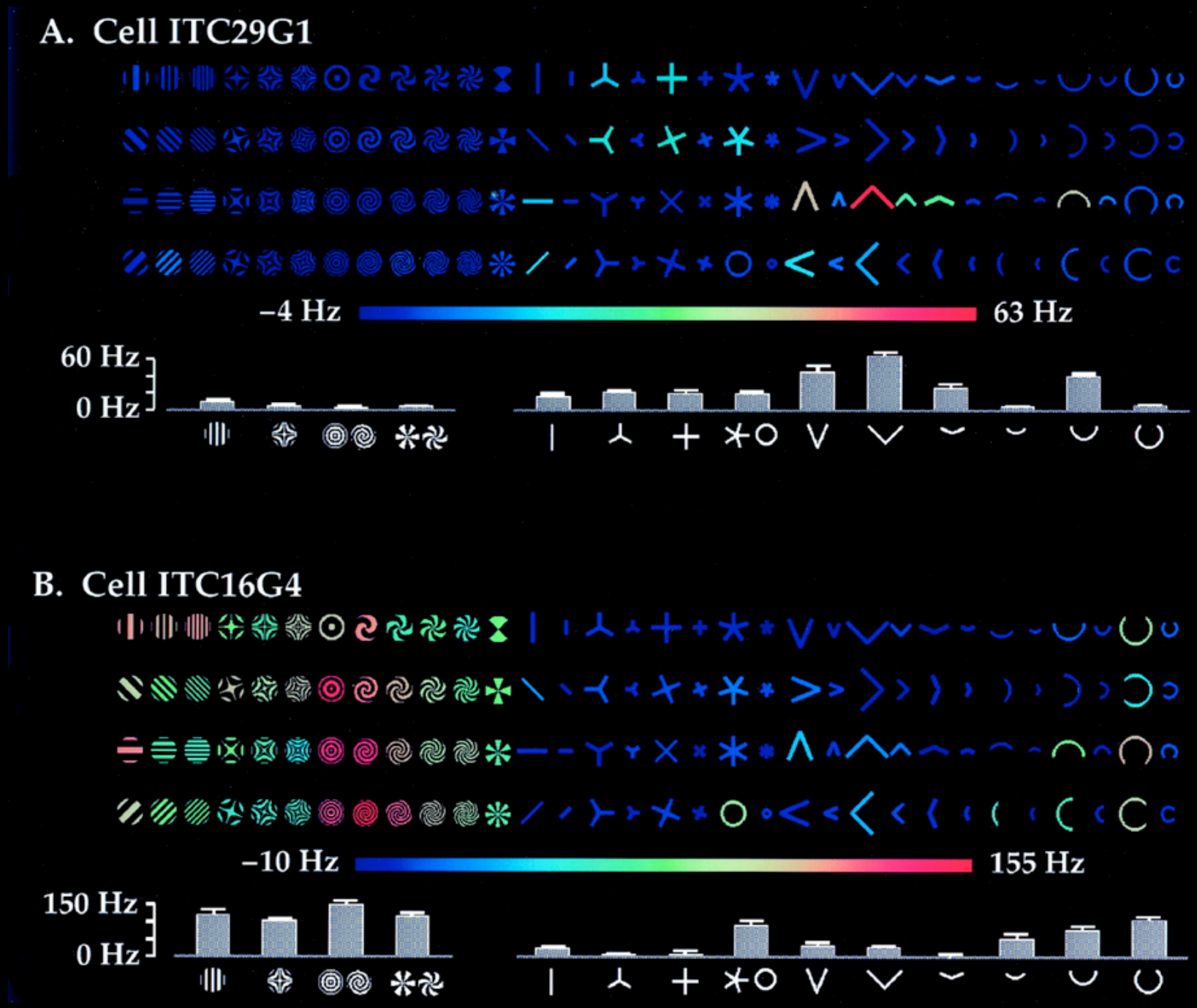

Structure of V2 receptive fields: curves, spirals, and angles

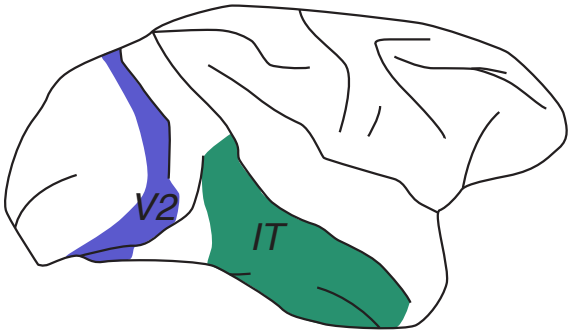

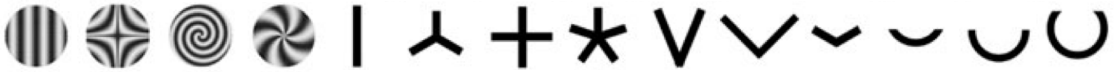

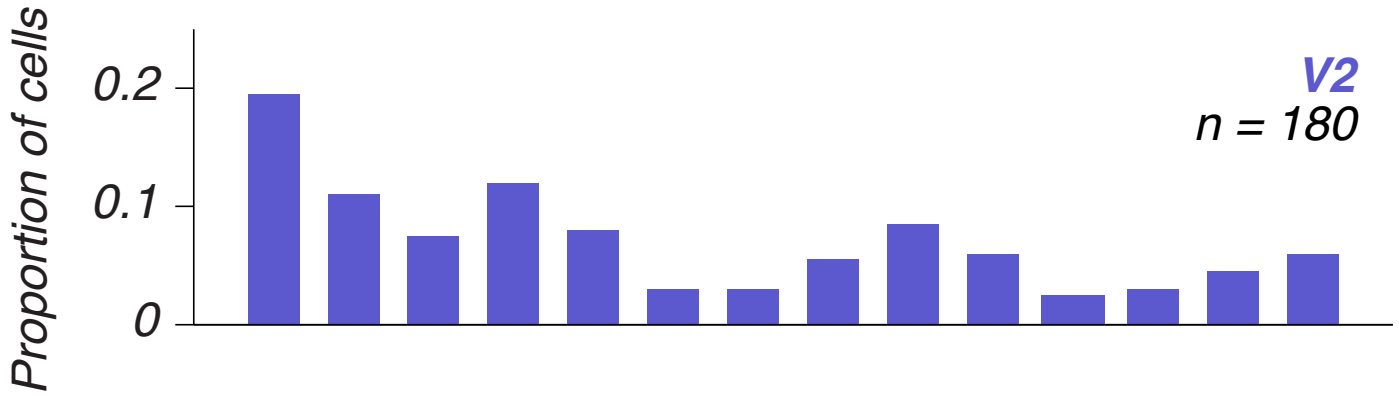

Hegde & Van Essen, 2007

Structure of V2 receptive fields: curves, spirals, and angles

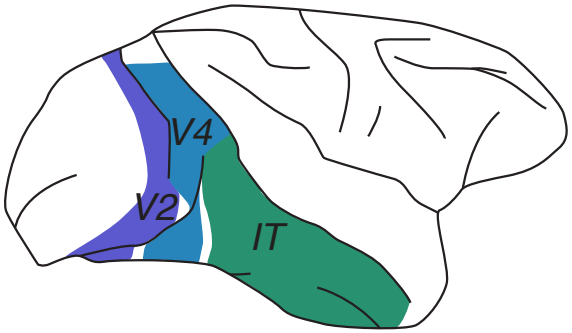

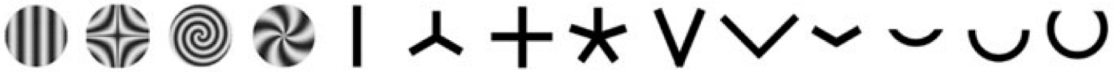

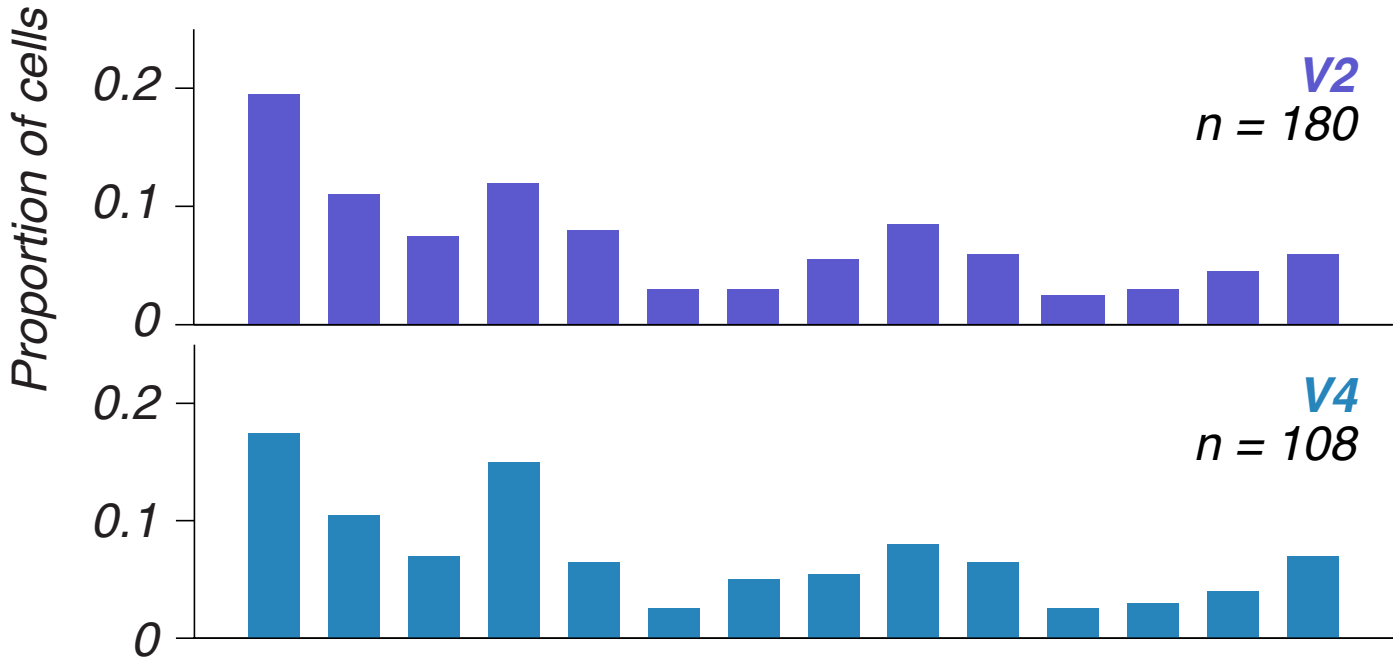

Hegde & Van Essen, 2007

Structure of V2 receptive fields: curves, spirals, and angles

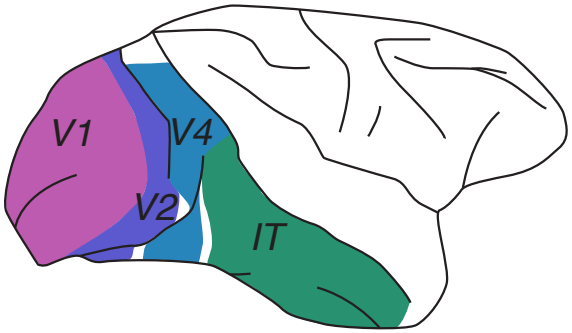

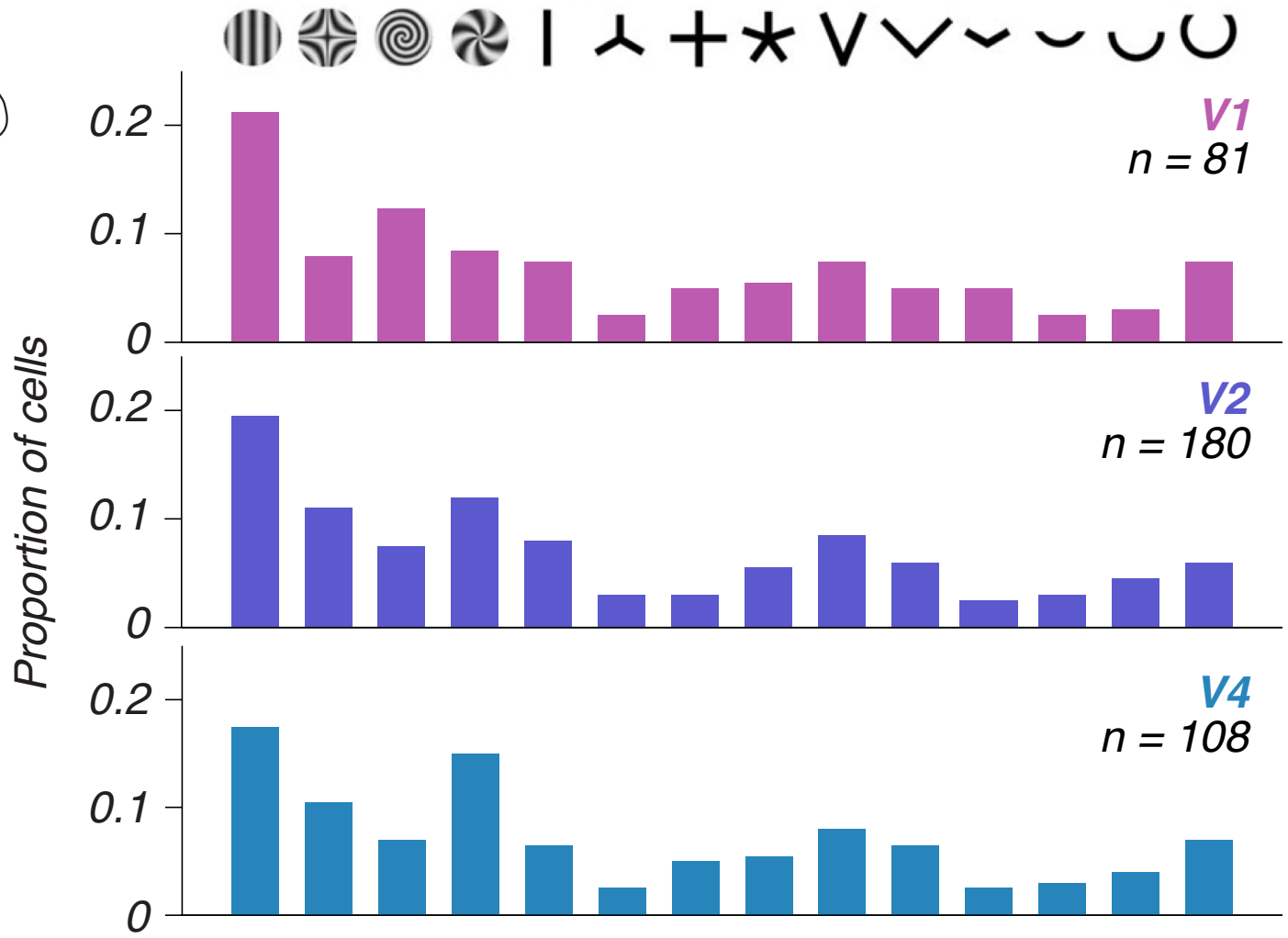

Hegde & Van Essen, 2007

Things


Stuff

Seeing things and stuff

People see stuff

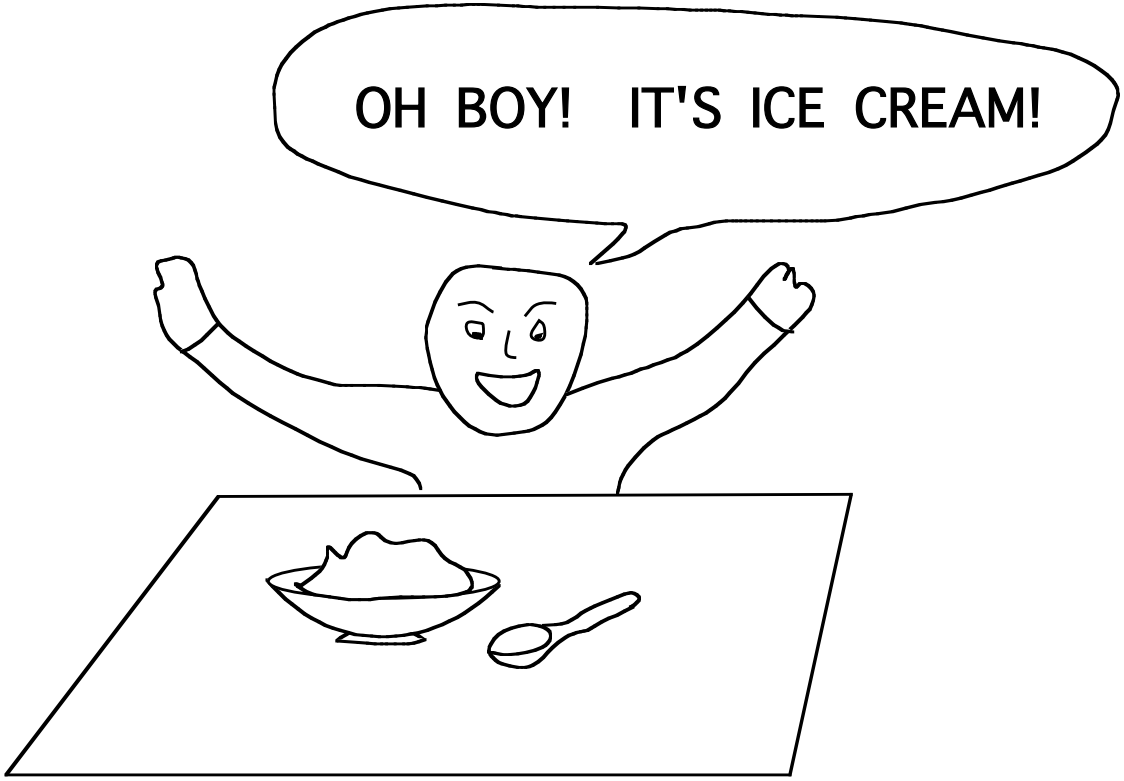

Adelson (2001)

Seeing things and stuff

Machines see things

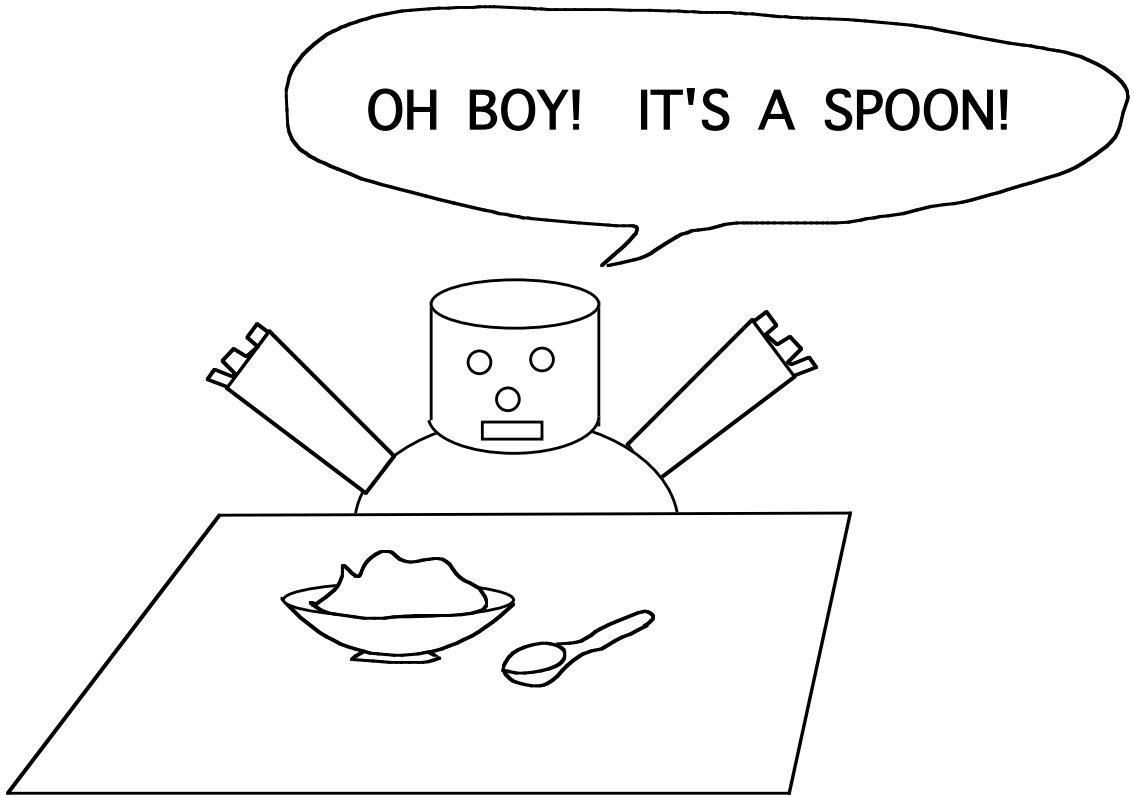

Adelson (2001)

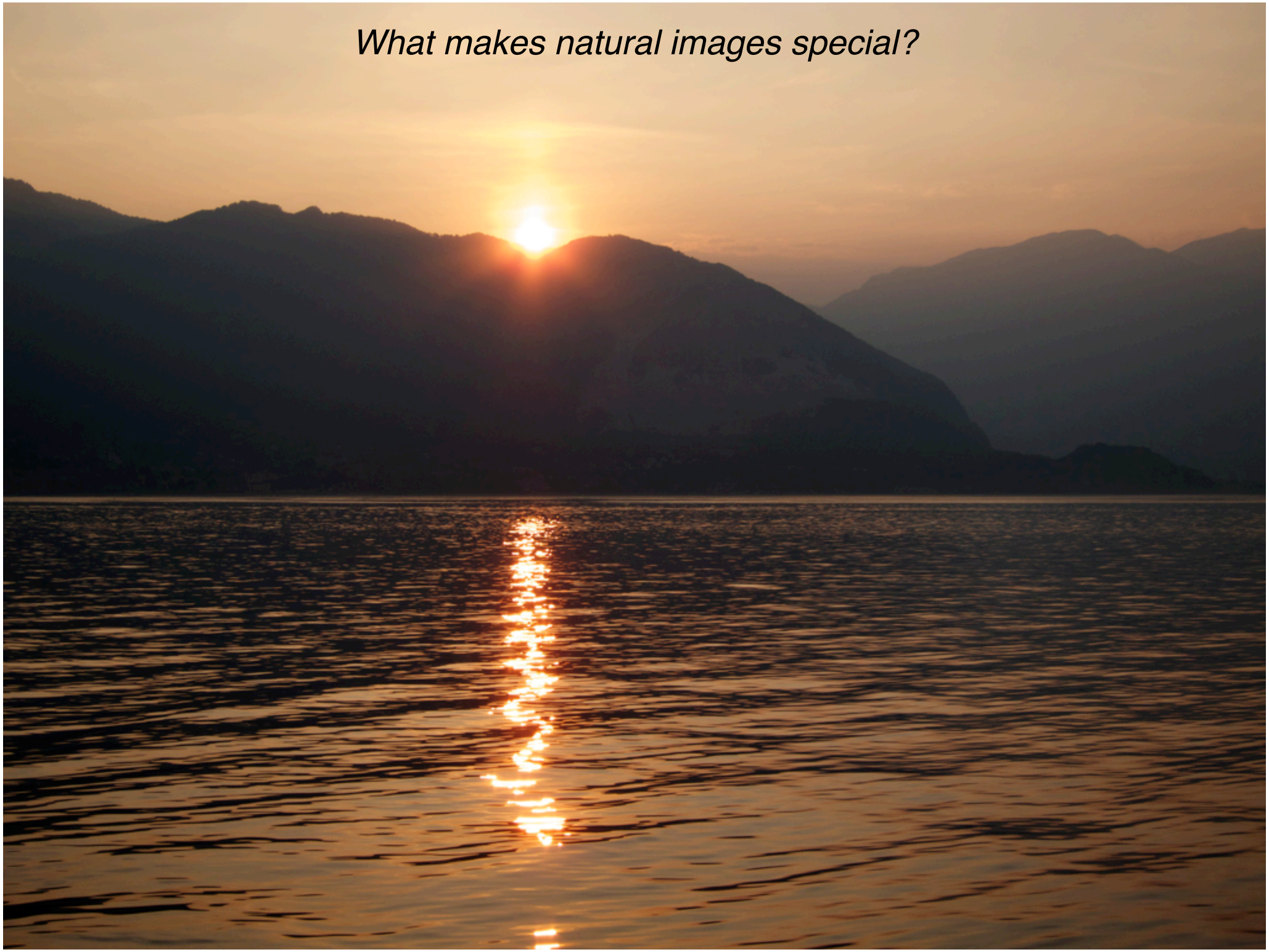
What makes natural images special?

What makes natural images special?

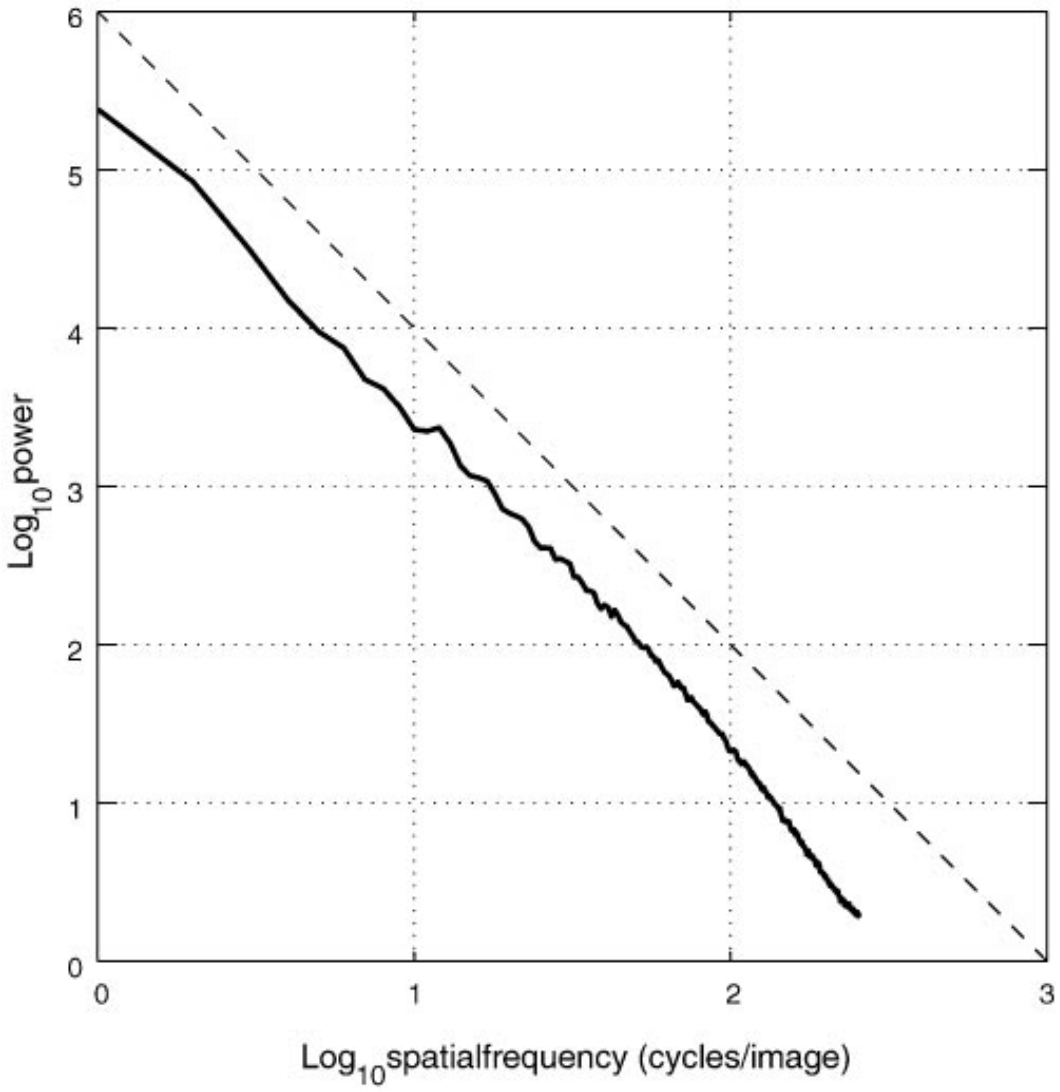

Figure 4 Power spectrum of a natural image (solid line) averaged over all orientations, compared with $1/f^2$ (dashed line).

Simoncelli & Olshausen (2001)

What makes natural images special?

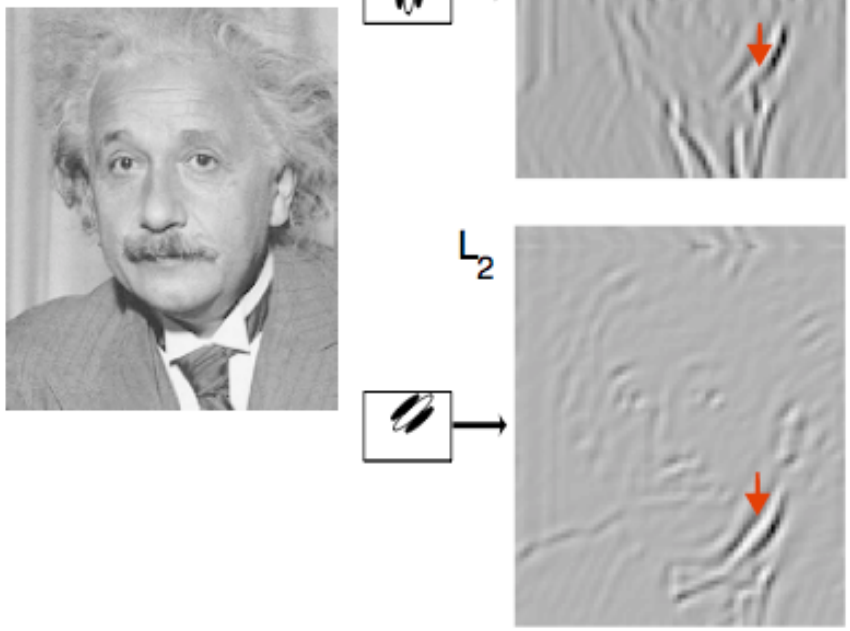

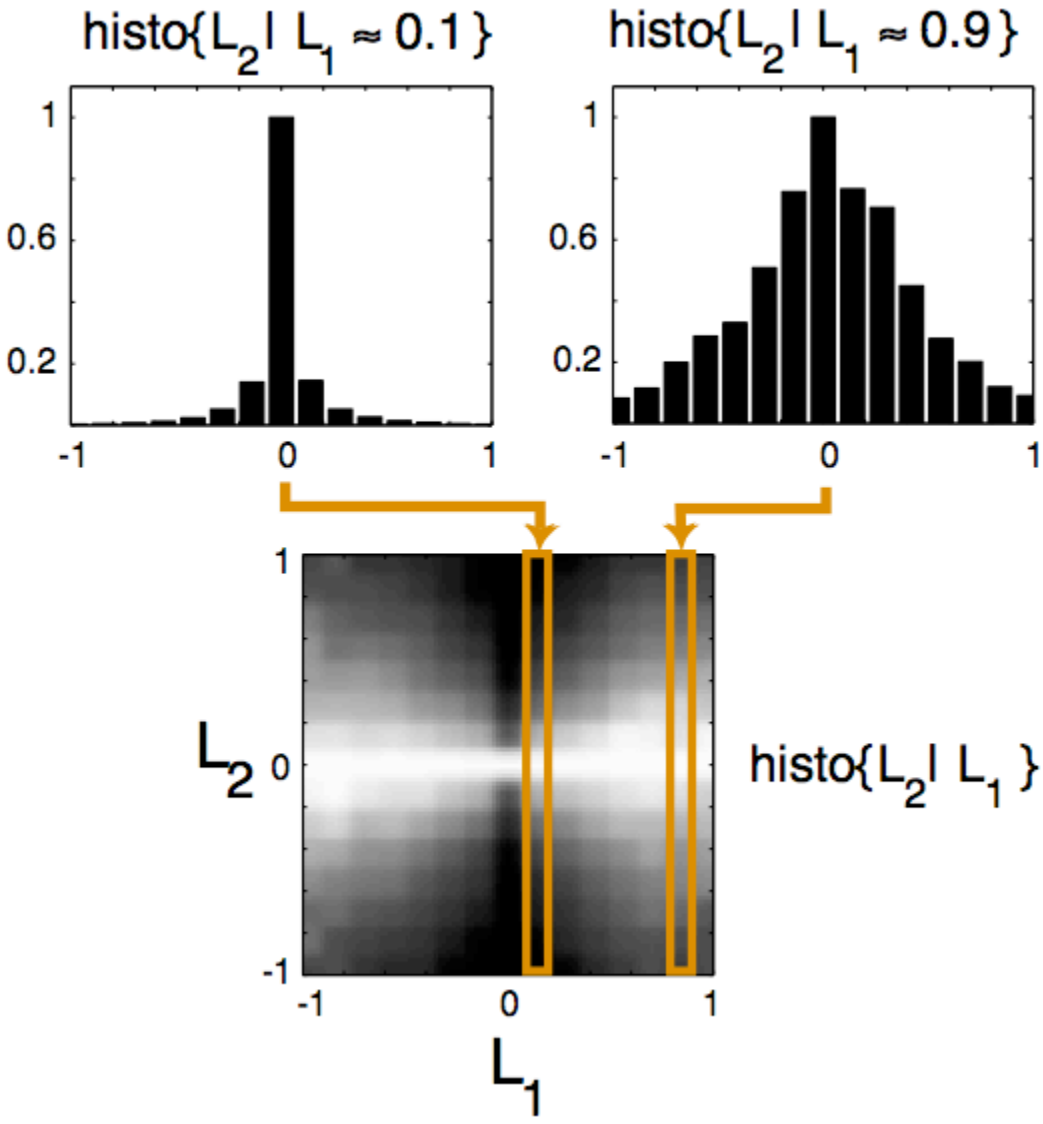

Schwartz & Simoncelli (2001)

Texture analysis and synthesis

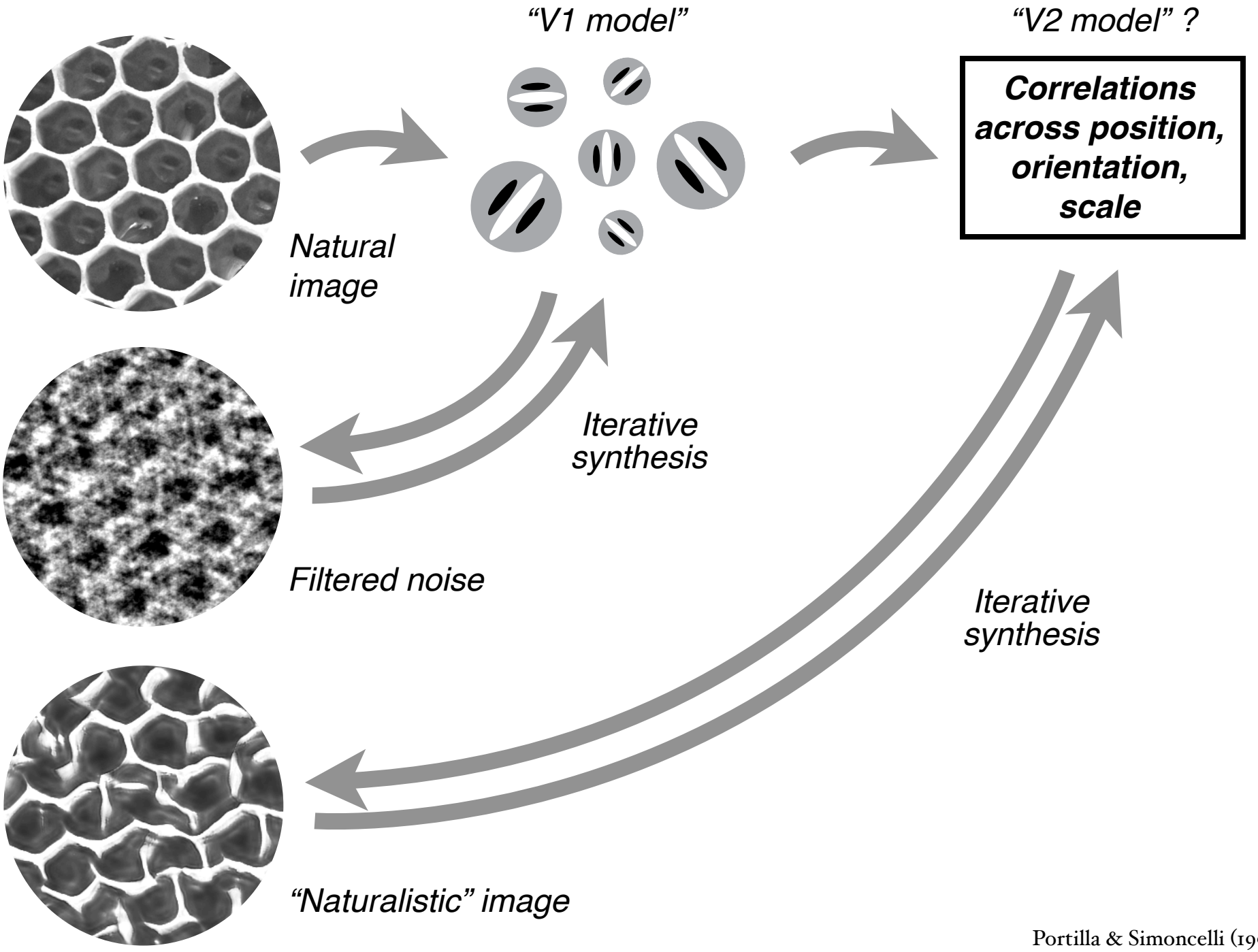

Portilla & Simoncelli (1999, 2000)

Texture analysis and synthesis

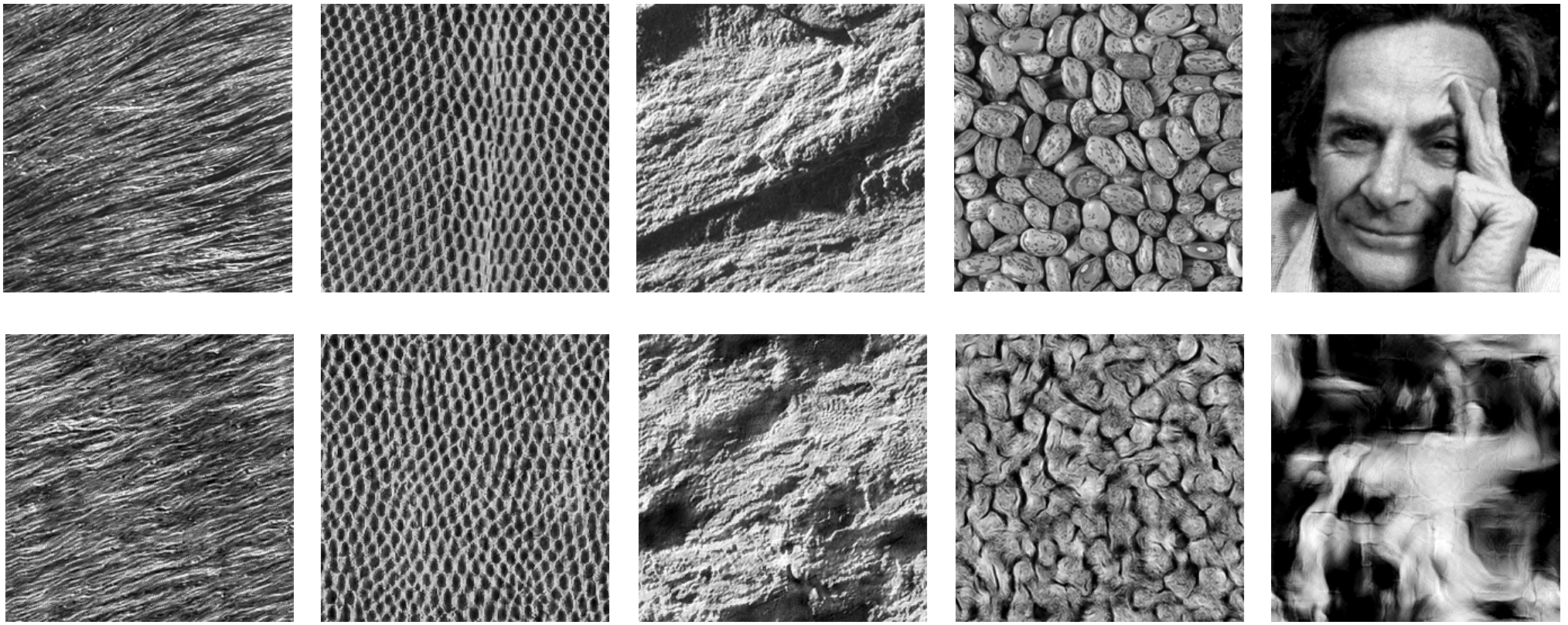

Portilla & Simoncelli (1999, 2000)

Let us say that to the extent that visible objects are different and far apart, they are **forms**. *To the extent that they are similar and congregated they are a* **texture**. *A man has form; a crowd has man-texture. A leaf has form; an arbor has leaf texture, and so on.*

Lettvin, 1976

Why V2?

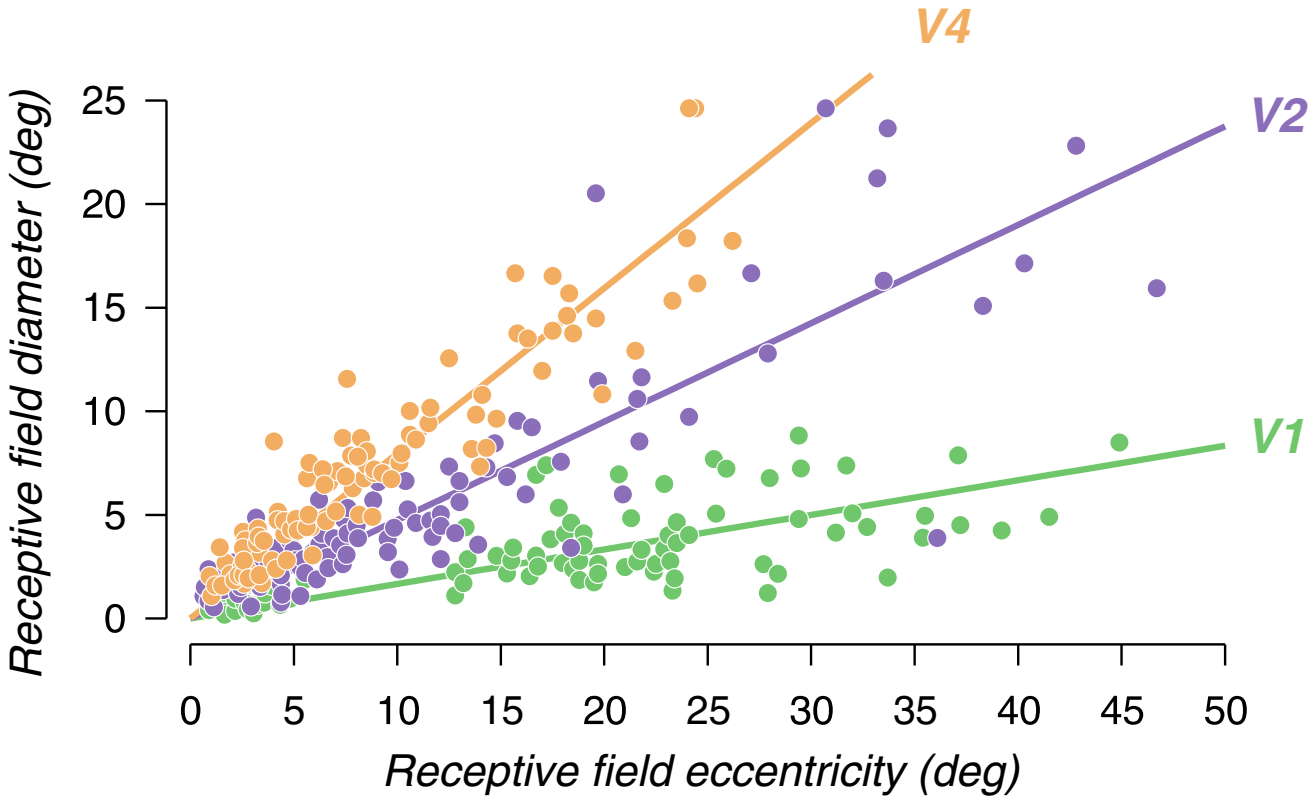

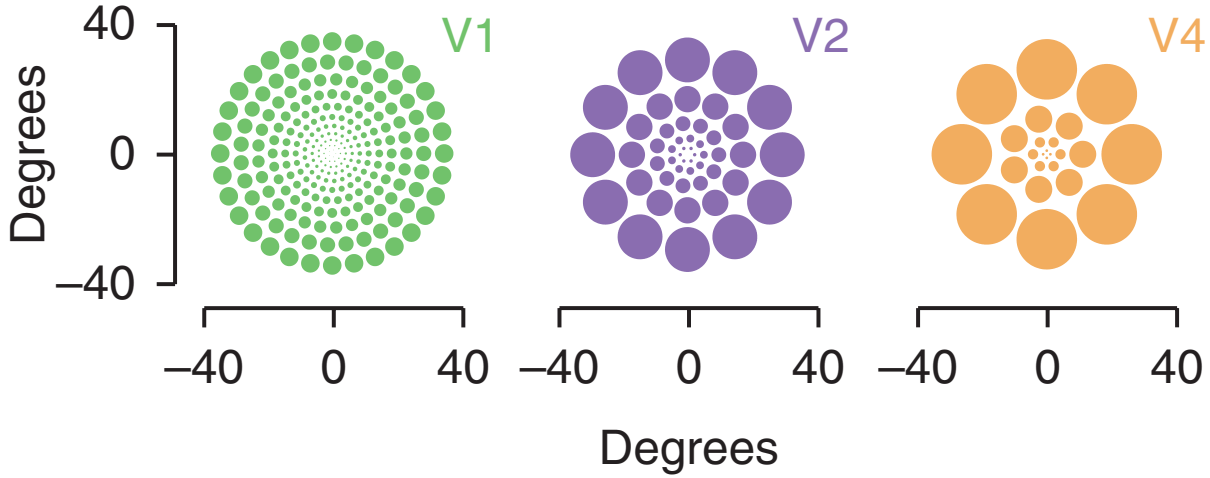

Freeman & Simoncelli (2011)


Why V2?
Jeremy Freeman

15 texture families

Naturalistic

Filtered noise

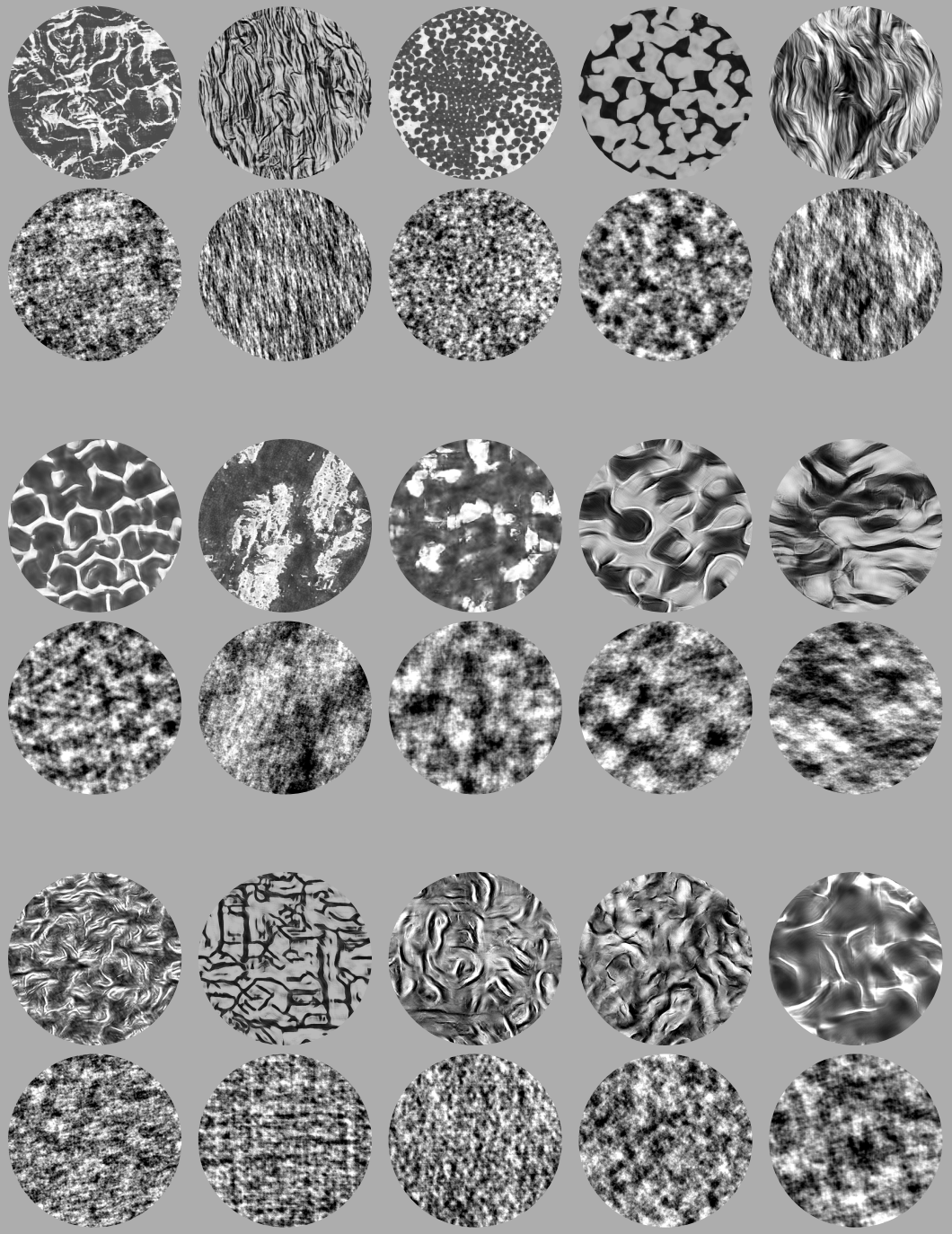

Freeman, Ziemba et al (2013)

"Naturalness" modulates responses in V2 but not V1 neurons

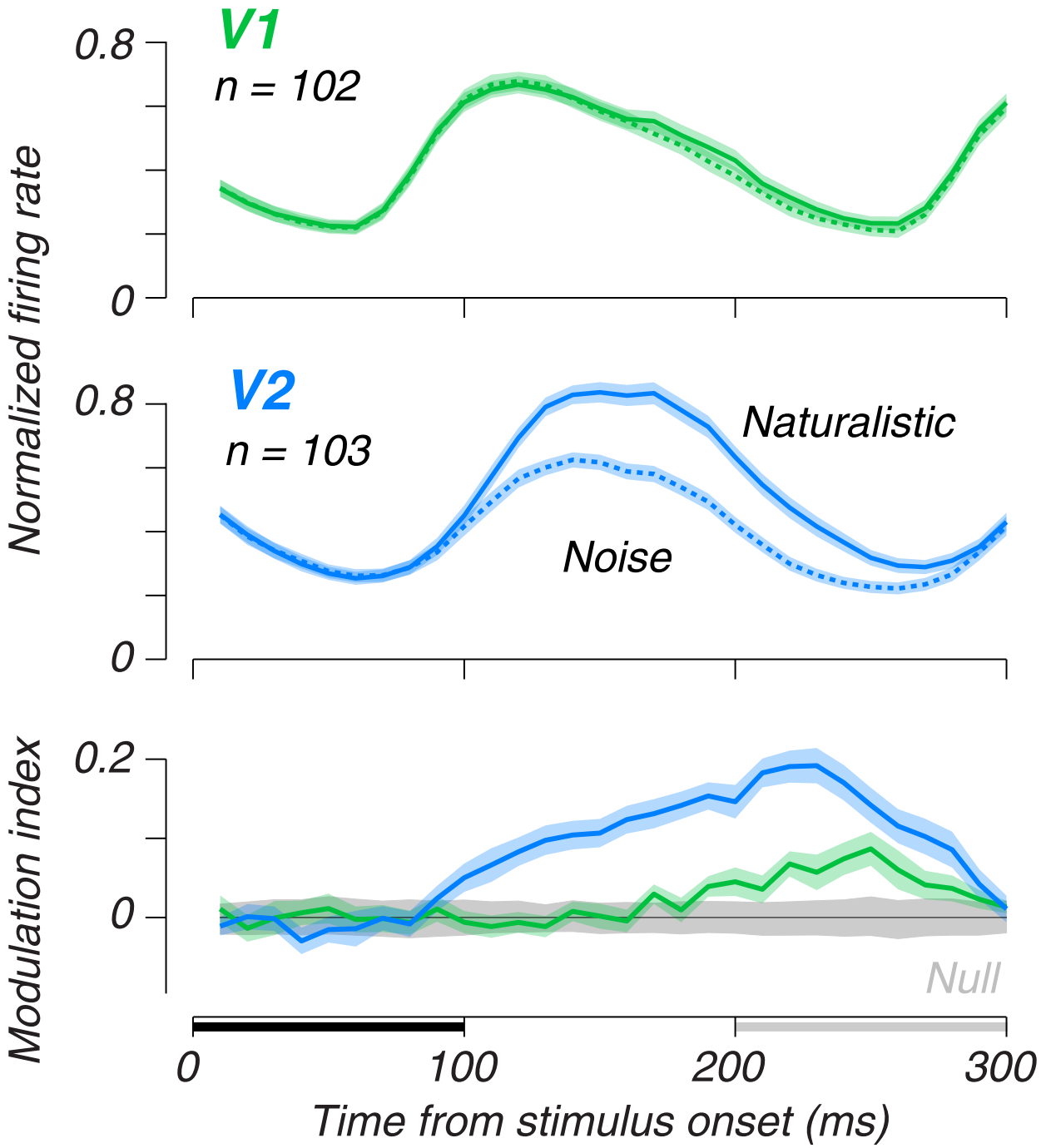

Freeman, Ziemba et al (2013)

"Naturalness" enhances responses in 63% of V2 but only 15% of V1 neurons

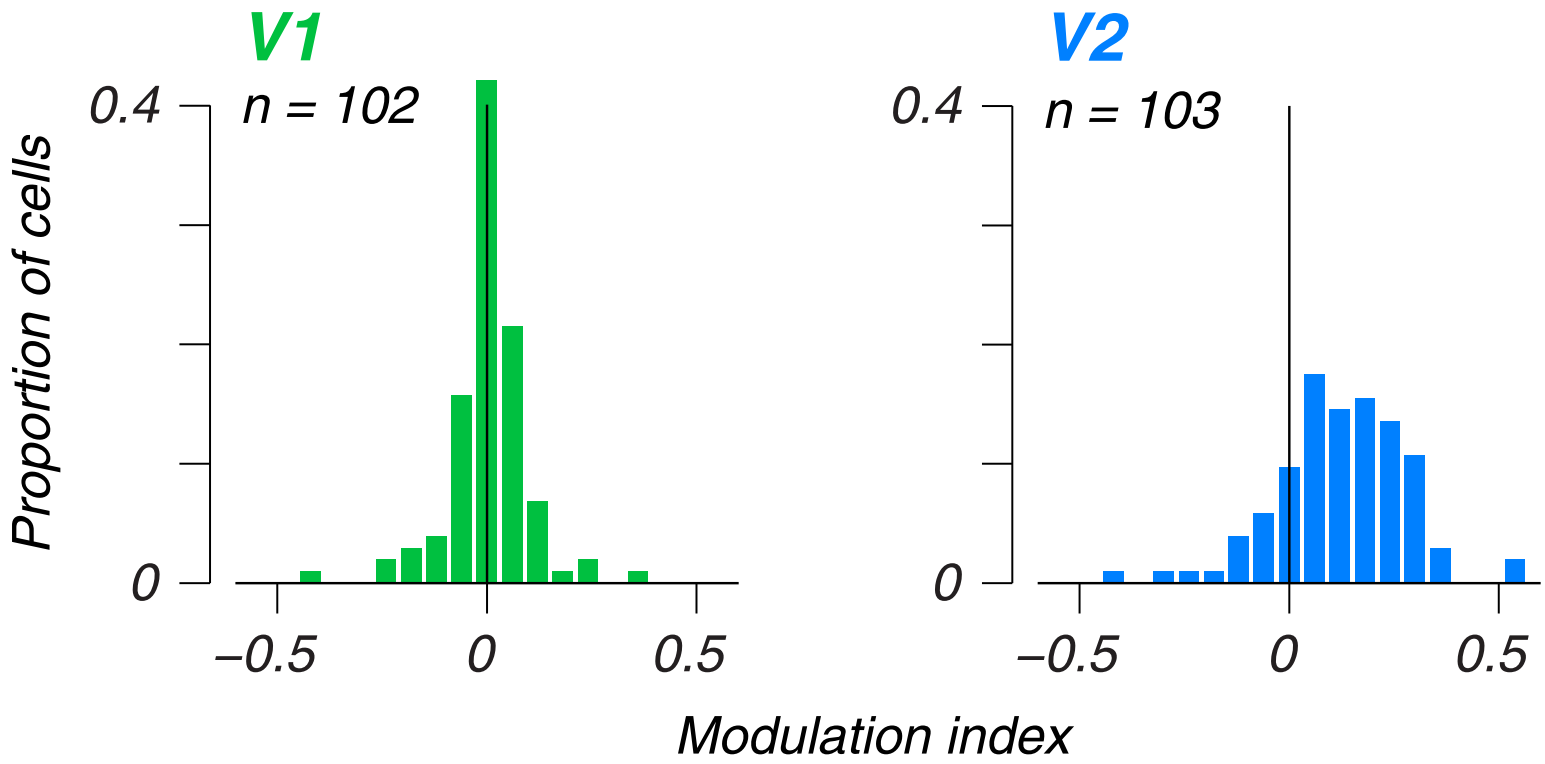

Freeman, Ziemba et al (2013)

Differences between naturalistic and noise responses first emerge in human V2

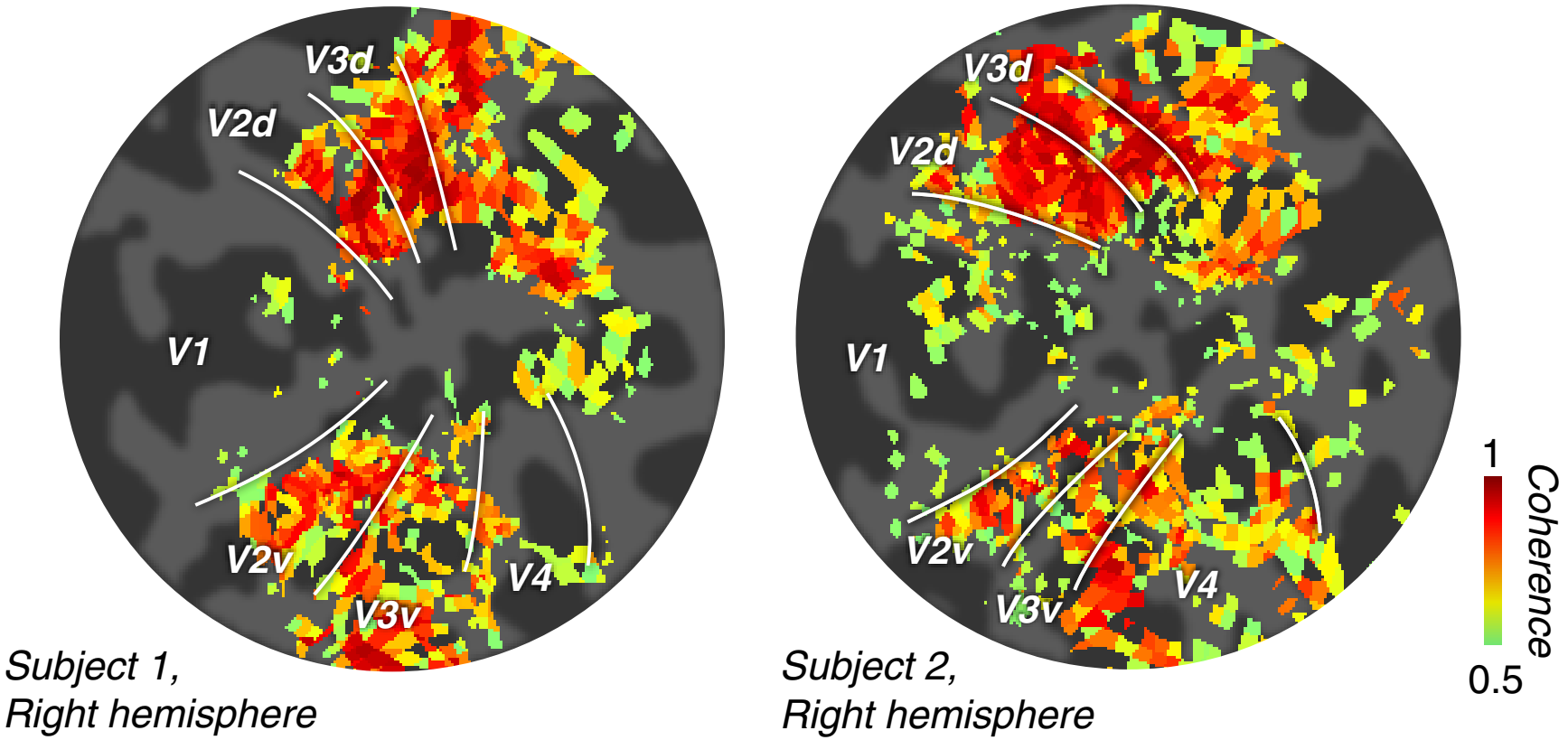

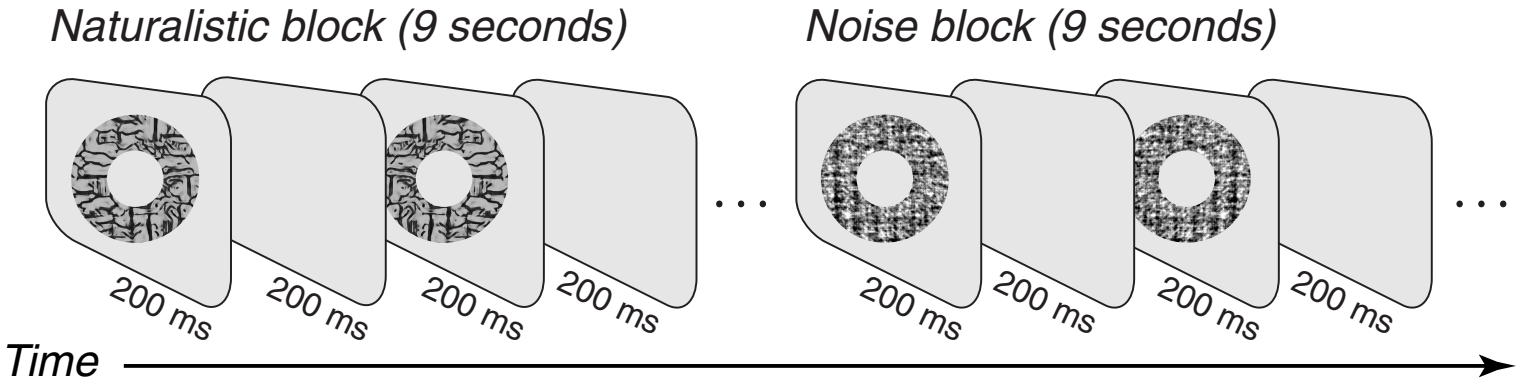

Freeman, Ziemba et al (2013)

Border ownership signals in macaque V2 (Zhou et al, 2000)

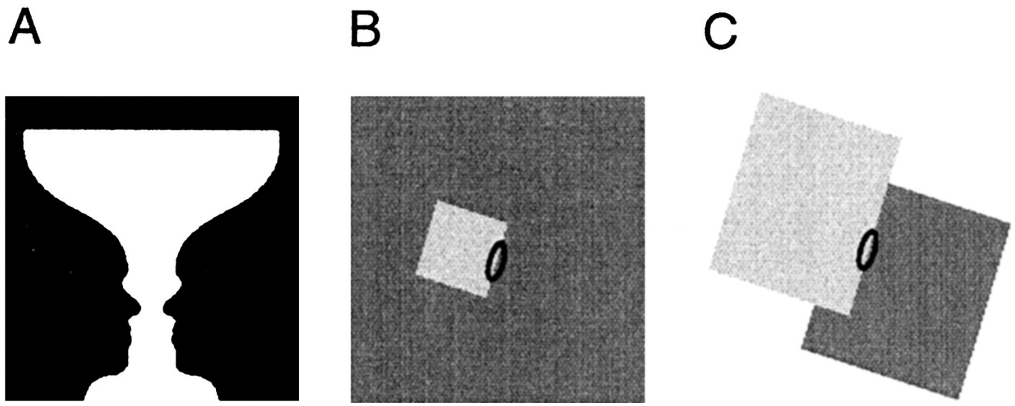

Perception of border ownership. *A*, Rubin's vase (Rubin, 1915). This well known ambiguous figure demonstrates the tendency of the visual system to interpret contrast borders as occluding contours and to assign them to one of the adjacent regions. In this example, figure-ground cues have been carefully balanced, but the black and white regions are generally not perceived as adjacent; instead, perception switches back and forth, and the borders belong either to the vase or to the faces. *B*, Isolated regions of contrast are generally perceived as "figures", that is, objects seen against a background. *C*, This display is generally perceived as two overlapping rectangles rather than a rectangle adjacent to an L-shaped object.

V1 and V2 responses to real and anomalous contours (Von der Heydt and Peterhans, 1989)

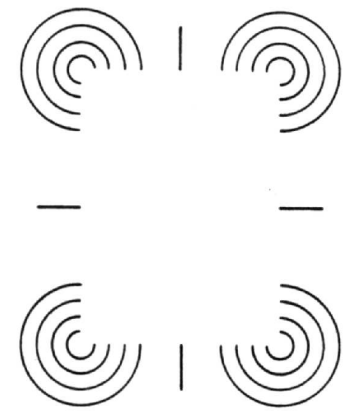

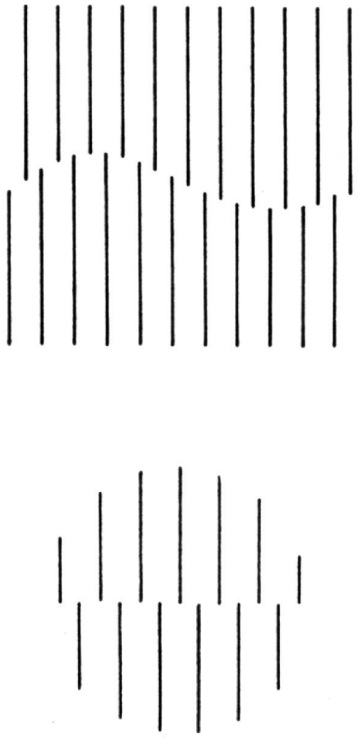

V1

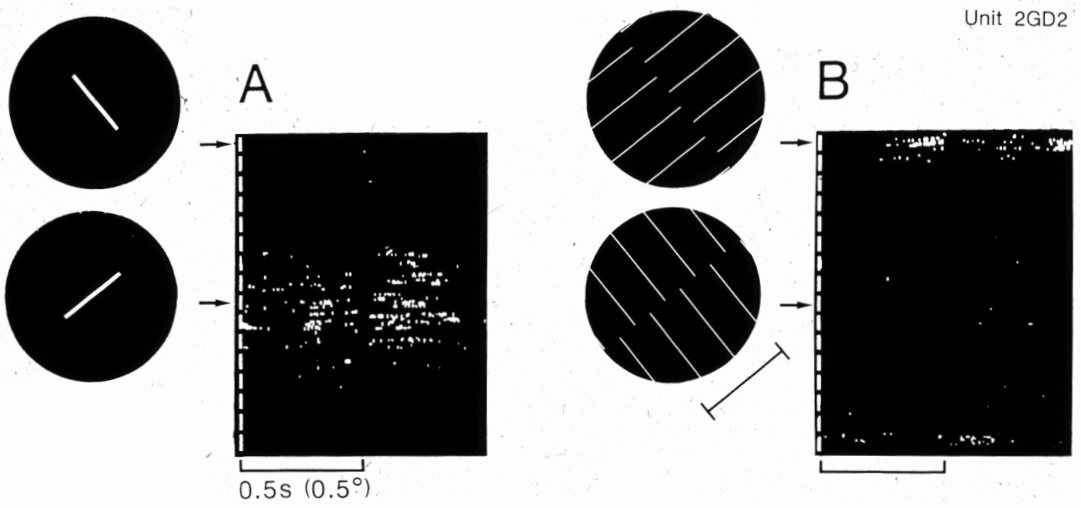

V2

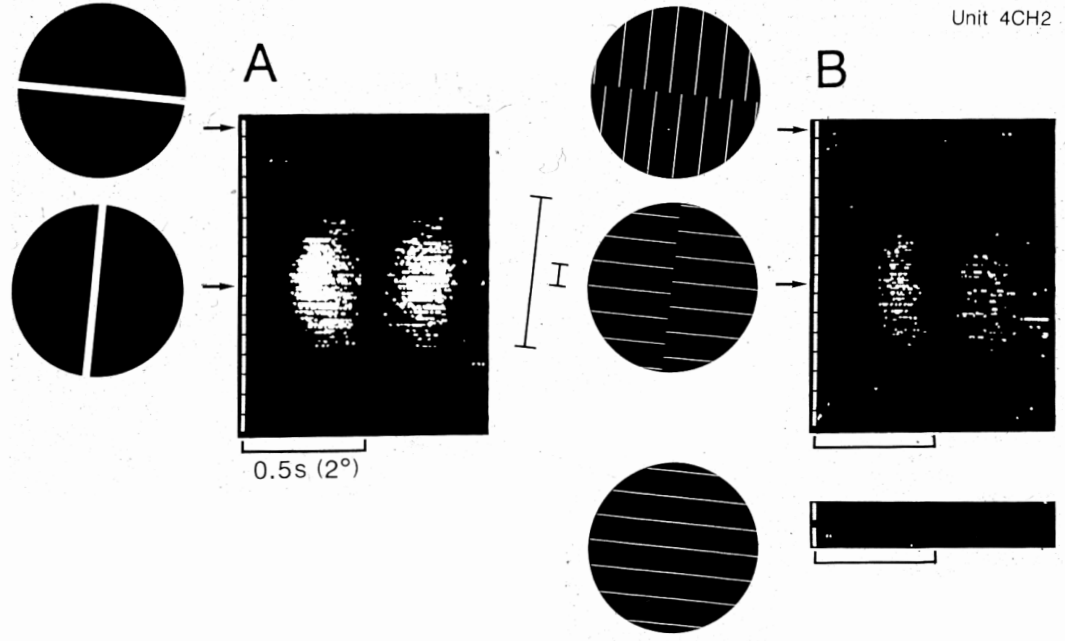

V1 and V2 responses to real and anomalous contours (Von der Heydt and Peterhans, 1989)

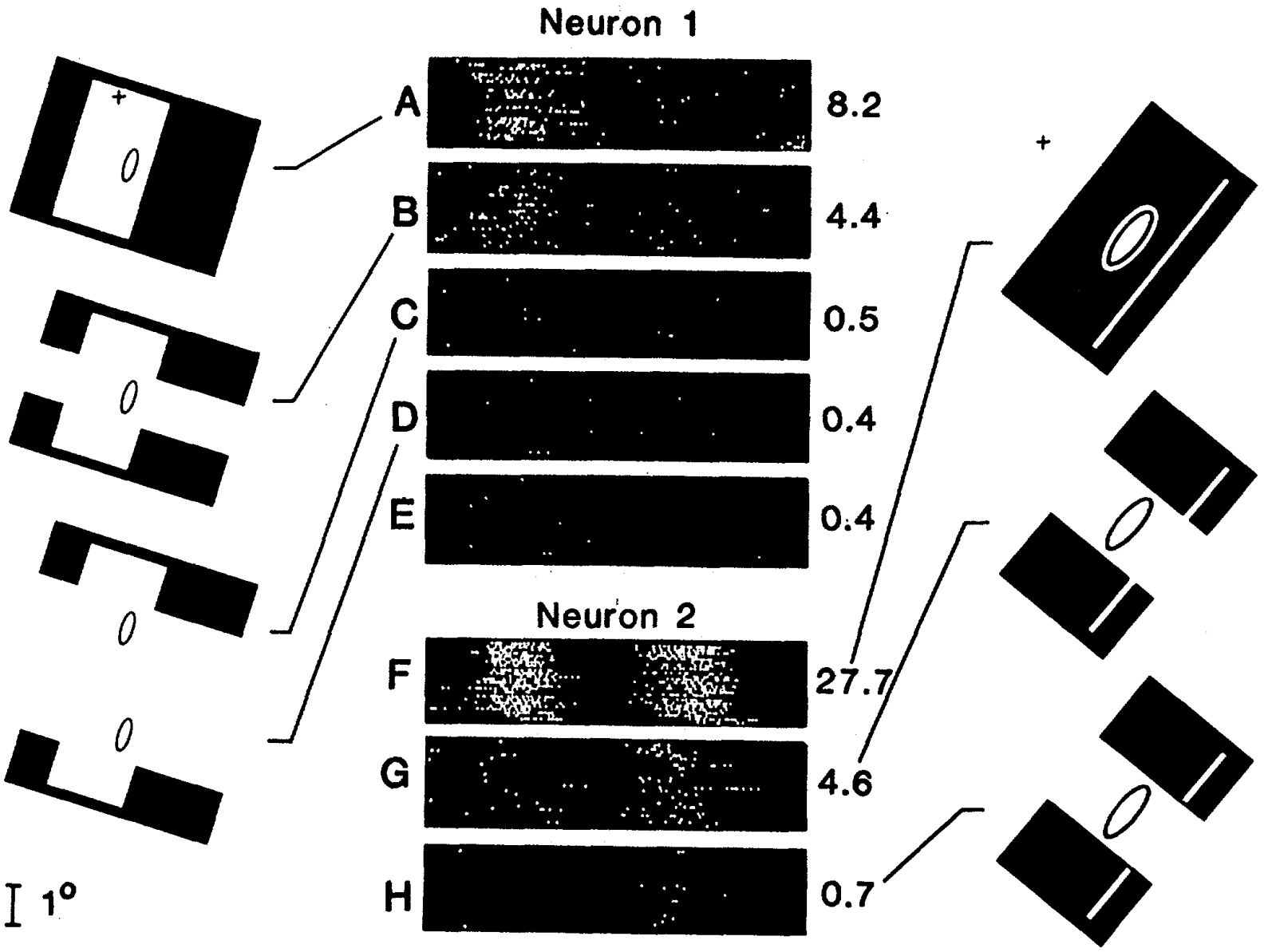

V1 and V2 responses to real and anomalous contours (Von der Heydt and Peterhans, 1989)

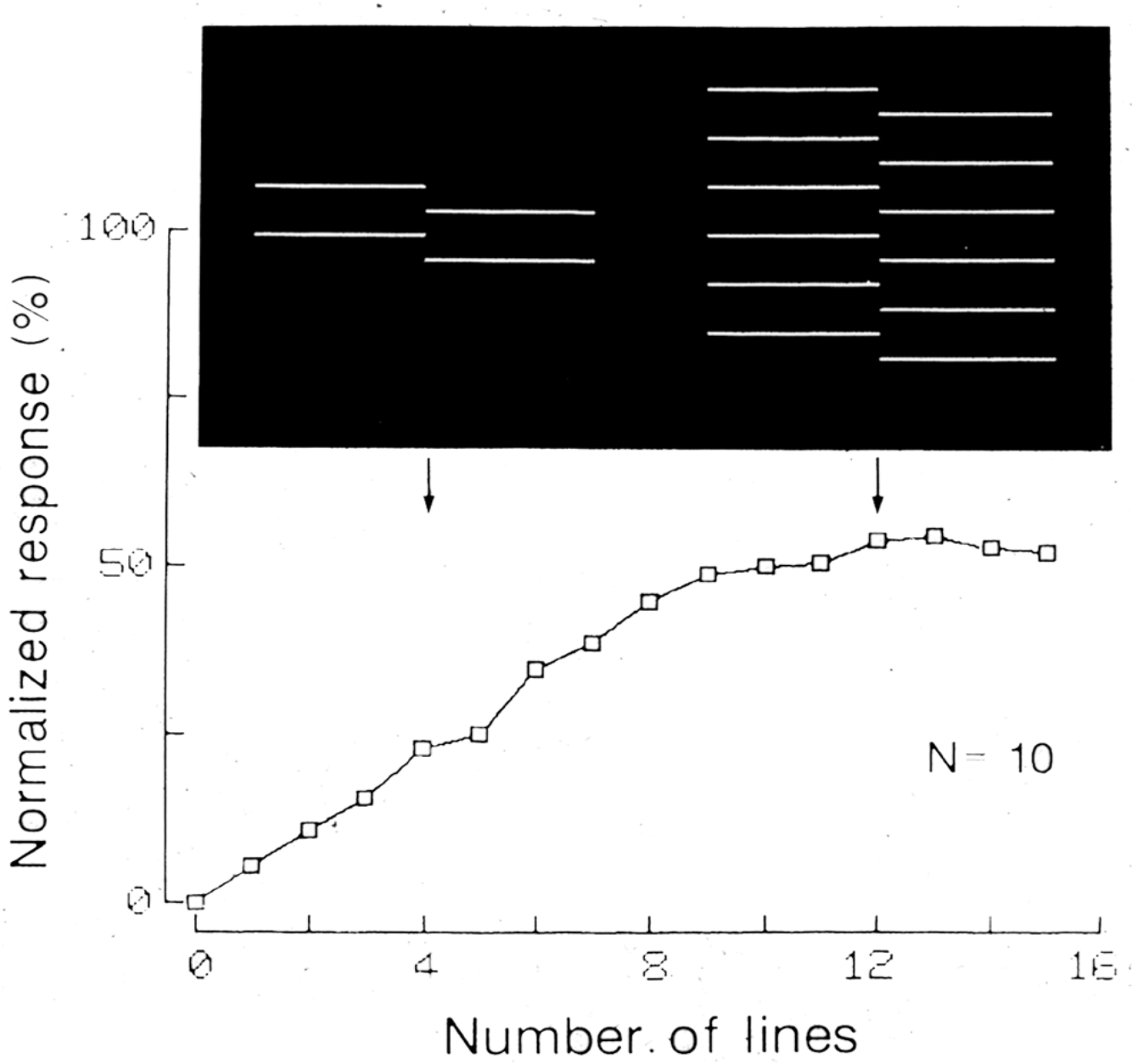

Border ownership signals in macaque V2 (Zhou et al, 2000)

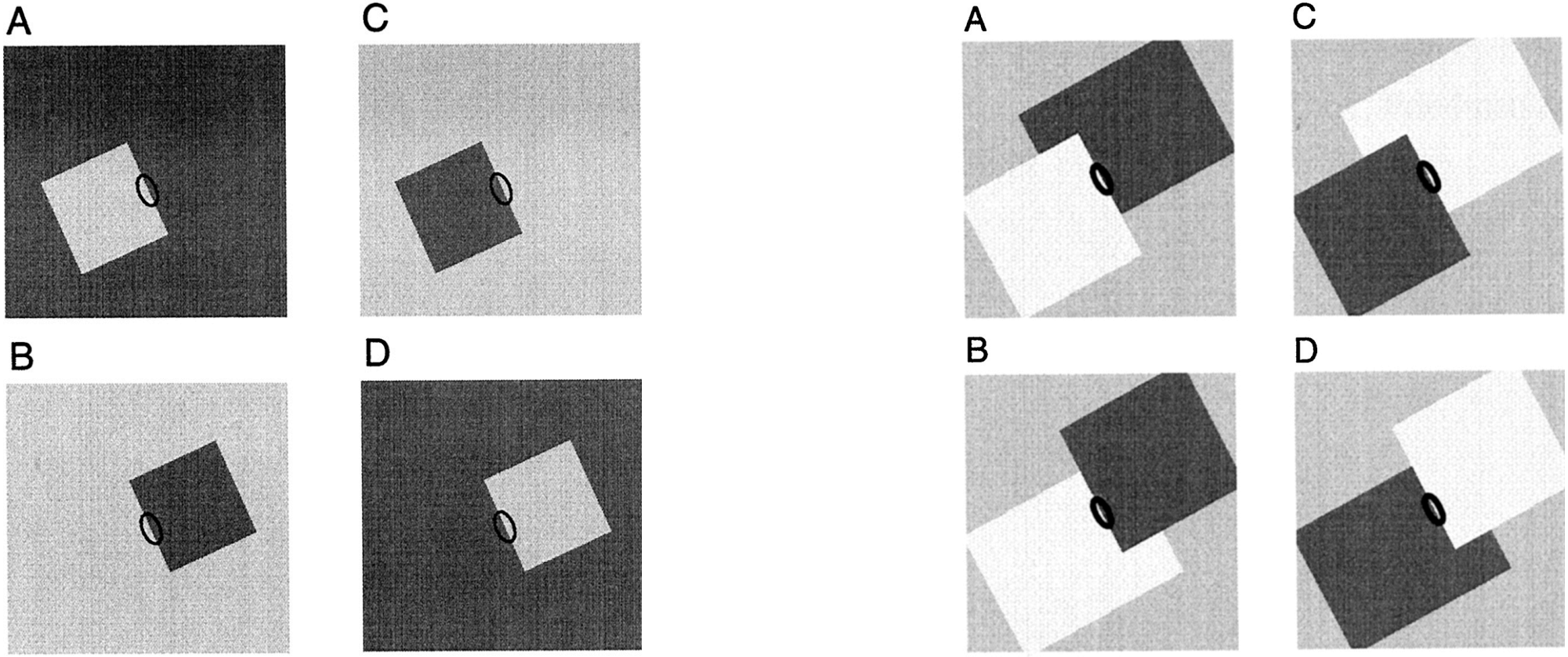

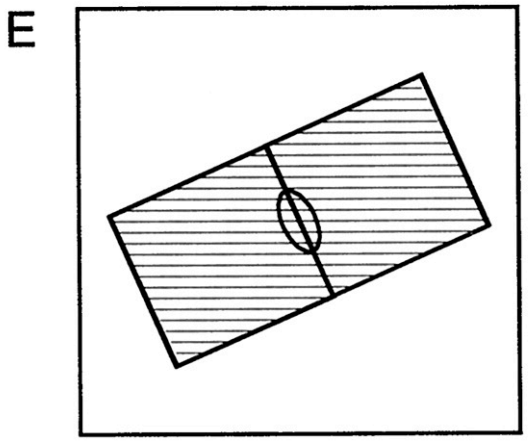

Standard tests for determining the effect of border ownership on edge responses.
On the left: in *A* and *B*, identical contrast edges are presented in the receptive field (*ellipses*), but in *A*, the edge is the right side of a dark square, in *B*, it is the left side of a light square. The relation is analogous between *C* and *D*, with reversed contrasts. *E*, The *hatched region* indicates the neighborhood of the receptive field in which displays *A* and *B* (or *C* and *D*) are identical.

On the right: Overlapping figure test. In each of these displays two regions of approximately the same area are presented on either side of the receptive field (*ellipses*).

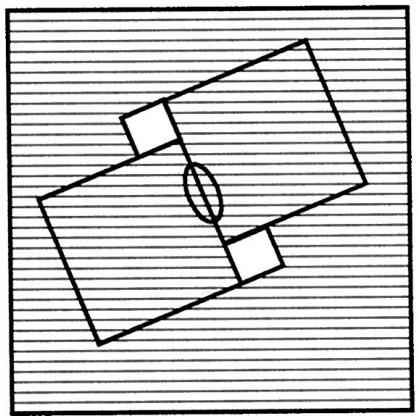

Border ownership signals in macaque V2 (Zhou et al, 2000)

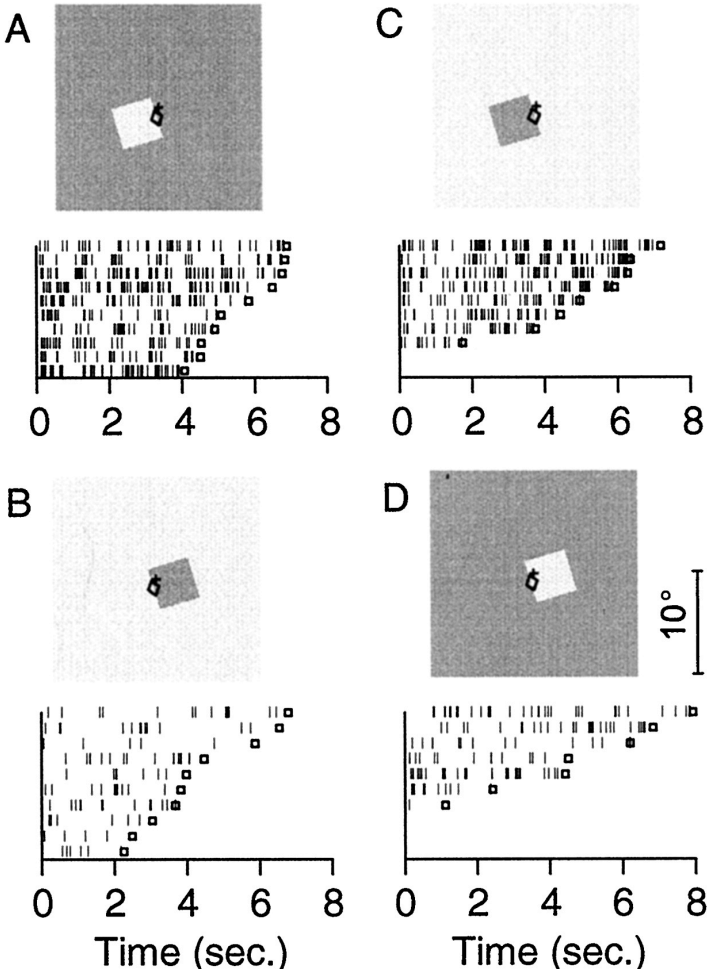

Example of border-ownership coding in a cell of area V2. The stimuli are shown at the *top*, and event plots of the corresponding responses are shown at the *bottom*. The *ellipses* indicate the location and orientation of the receptive field, and the *crosses* show the position of the fixation target. In the event plots, *small vertical lines* represent the times of action potentials, relative to the moment of lever pulling (which generally indicated the beginning of fixation). *Small squares* indicate the times of target flip (end of fixation).

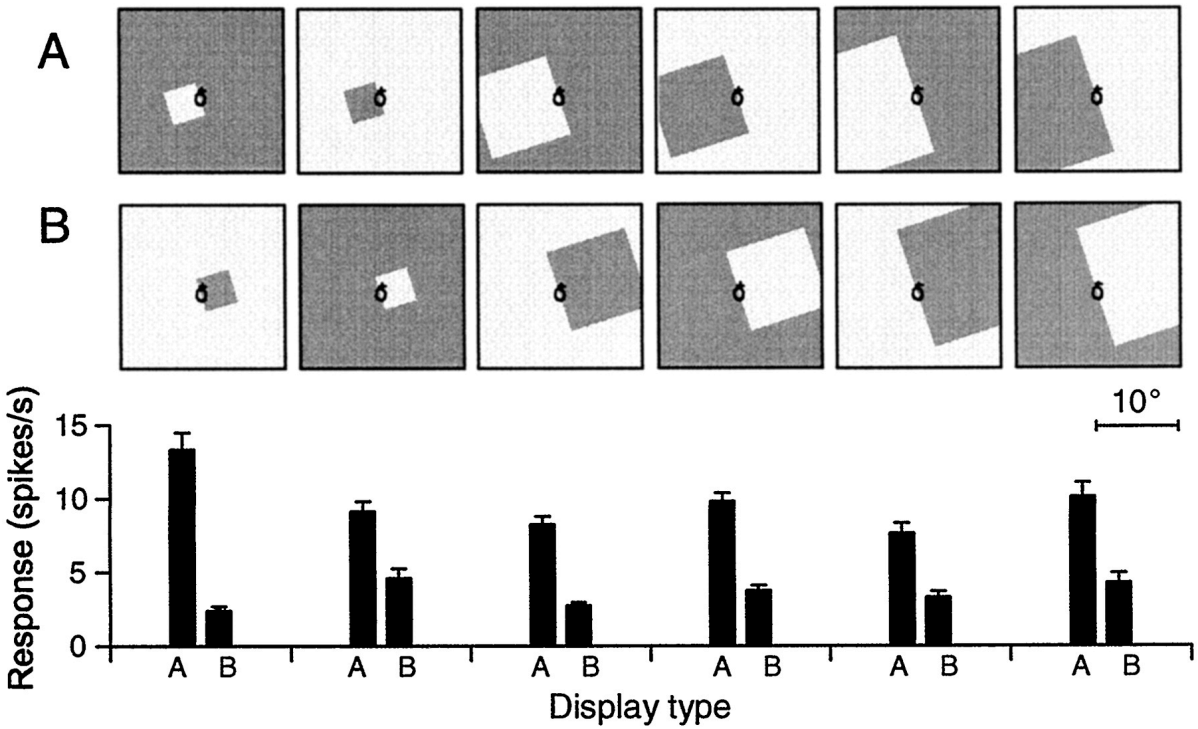

Size invariance of border-ownership coding. The same V2 cell. Rows *A* and *B* show the stimuli, with pairs of locally identical stimuli juxtaposed. Conventions as in Figure 4. Bar graphs below show mean firing rates and SEs of the corresponding responses. Square sizes: 1 and 2, 4°; 3 and 4, 10°; 5 and 6, 15°. For each size, and for either contrast polarity, the responses were stronger when the square was located on the left side of the receptive field.

Border ownership signals in macaque V2 (Zhou et al, 2000)

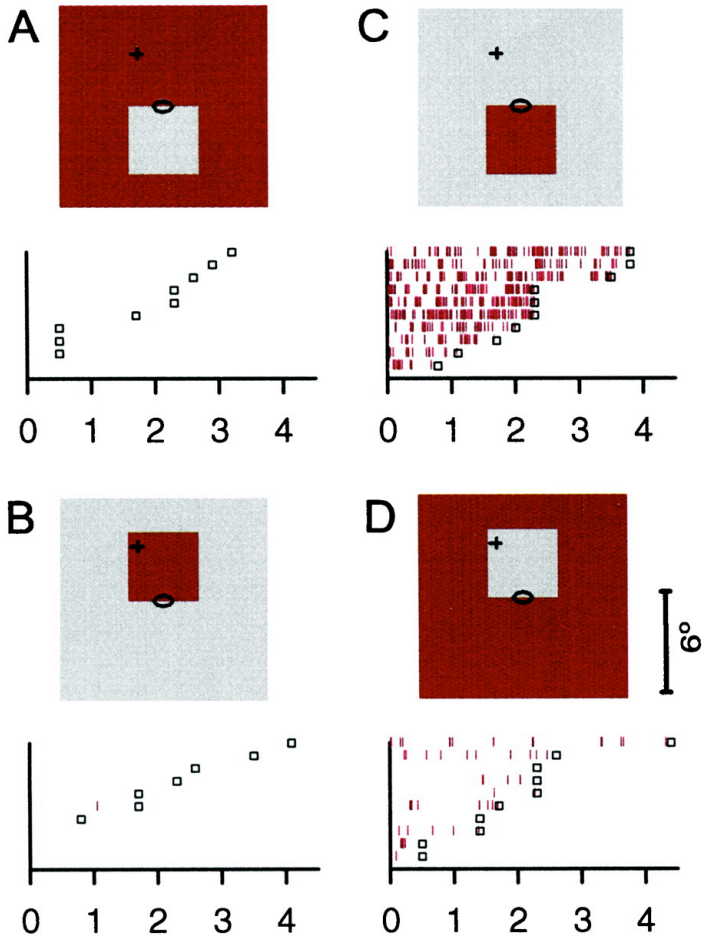

Example of simultaneous coding of border-ownership and edge-contrast polarity. This cell of area V2 was color-selective with a preference for dark, reddish colors (see Fig. 8). *Brown* and *gray* were used for the test. Conventions are the same as for Figure 4. The cell responded to the *top* edge of a *brown square* (*C*), but hardly at all to the *bottom* edge of a gray square (*D*), although in both cases the same *gray-brown* color boundary was presented in the receptive field. The cell did not respond at all to edges of the reversed contrast (*A, B*). Square size, 4°; length of minimum response field, 1.4°; location in visual field (1.4°, 3.0°).

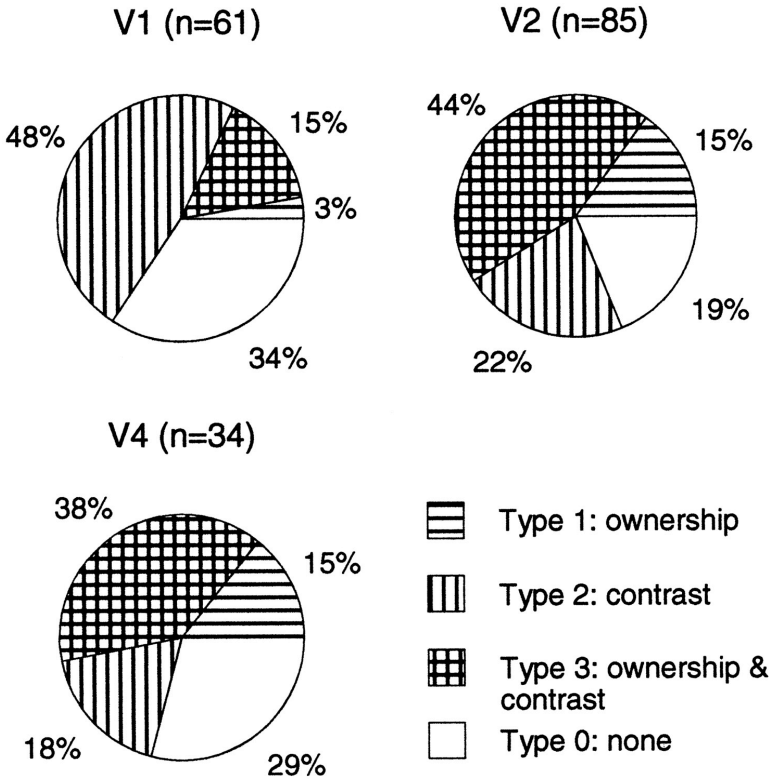

The distributions of the types of contour responses found in cortical areas V1, V2, and V4. Classification based on two-factor ANOVA. *Ownership*, Responses modulated according to side of ownership; *contrast*, responses modulated according to local contrast polarity; *ownership & contrast*, modulation by either factor; *none*, no modulation. In V2 and V4, more than half of the cells showed border-ownership modulation.

Persistence of border-ownership signals in V2 (O'Herron & von der Heydt, 2009)

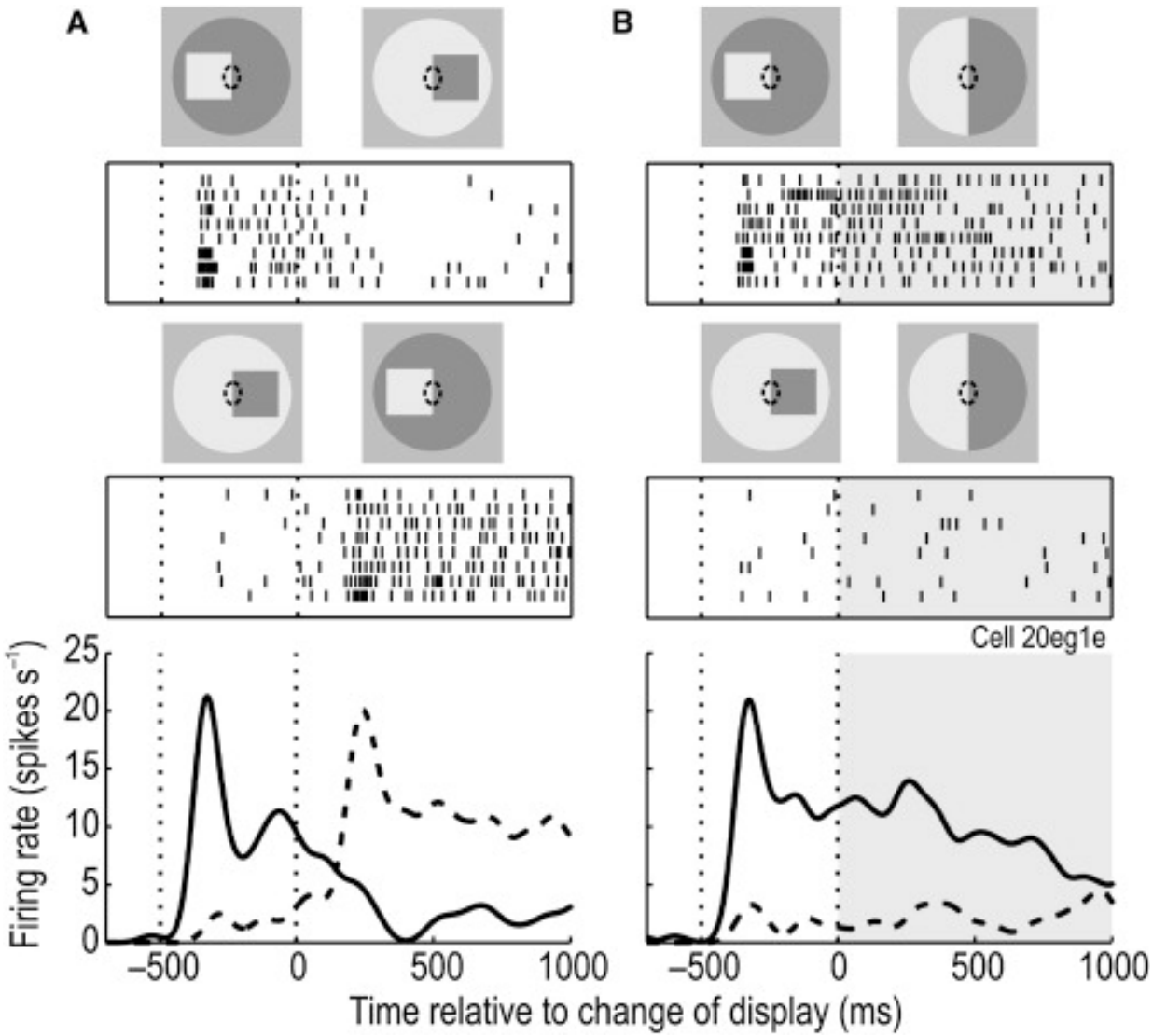

Transfer of border ownership across saccades (O'Herron & von der Heydt, 2013)

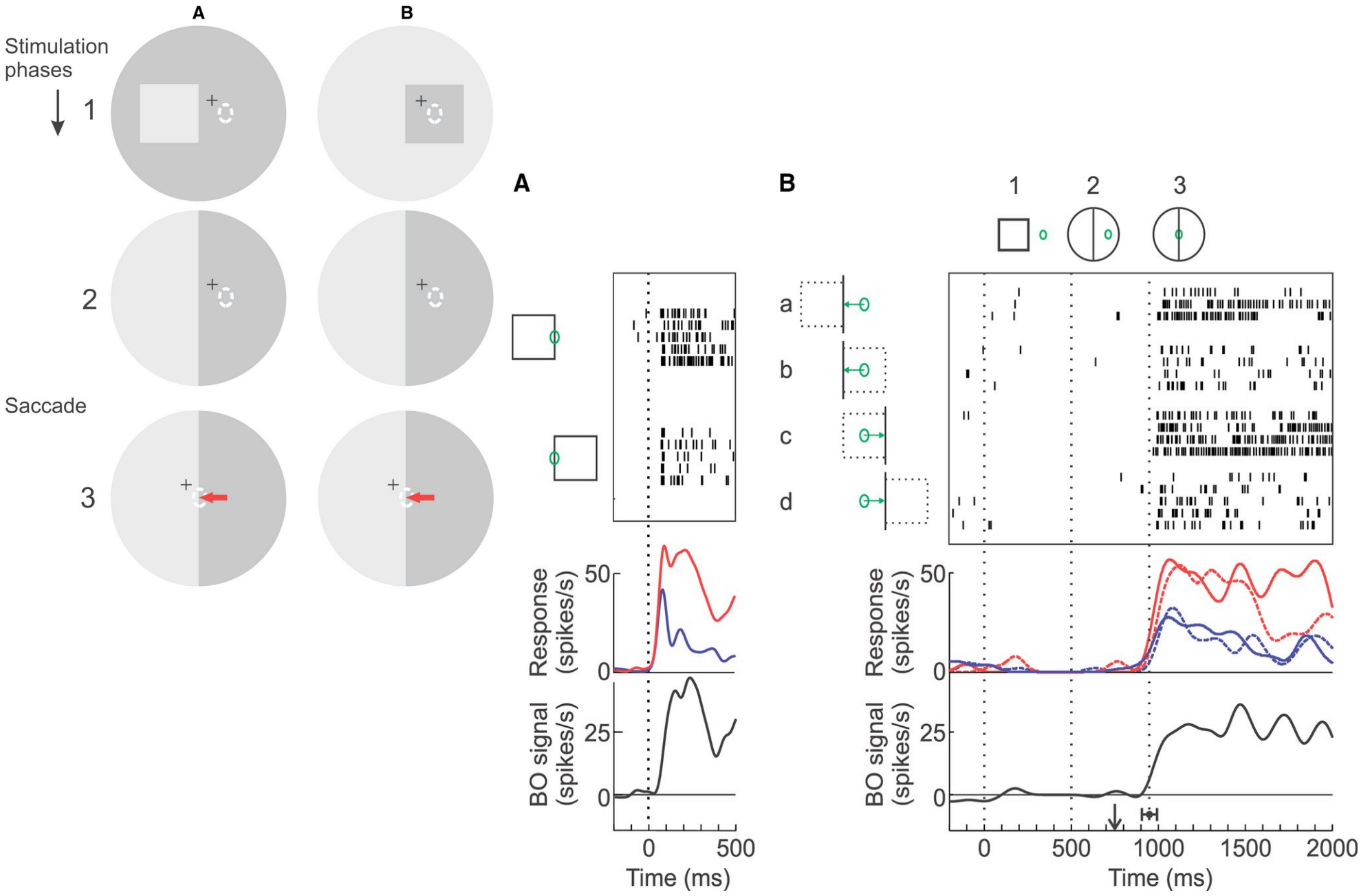

Transfer of border ownership across saccades: population response
(O'Herron & von der Heydt, 2013)

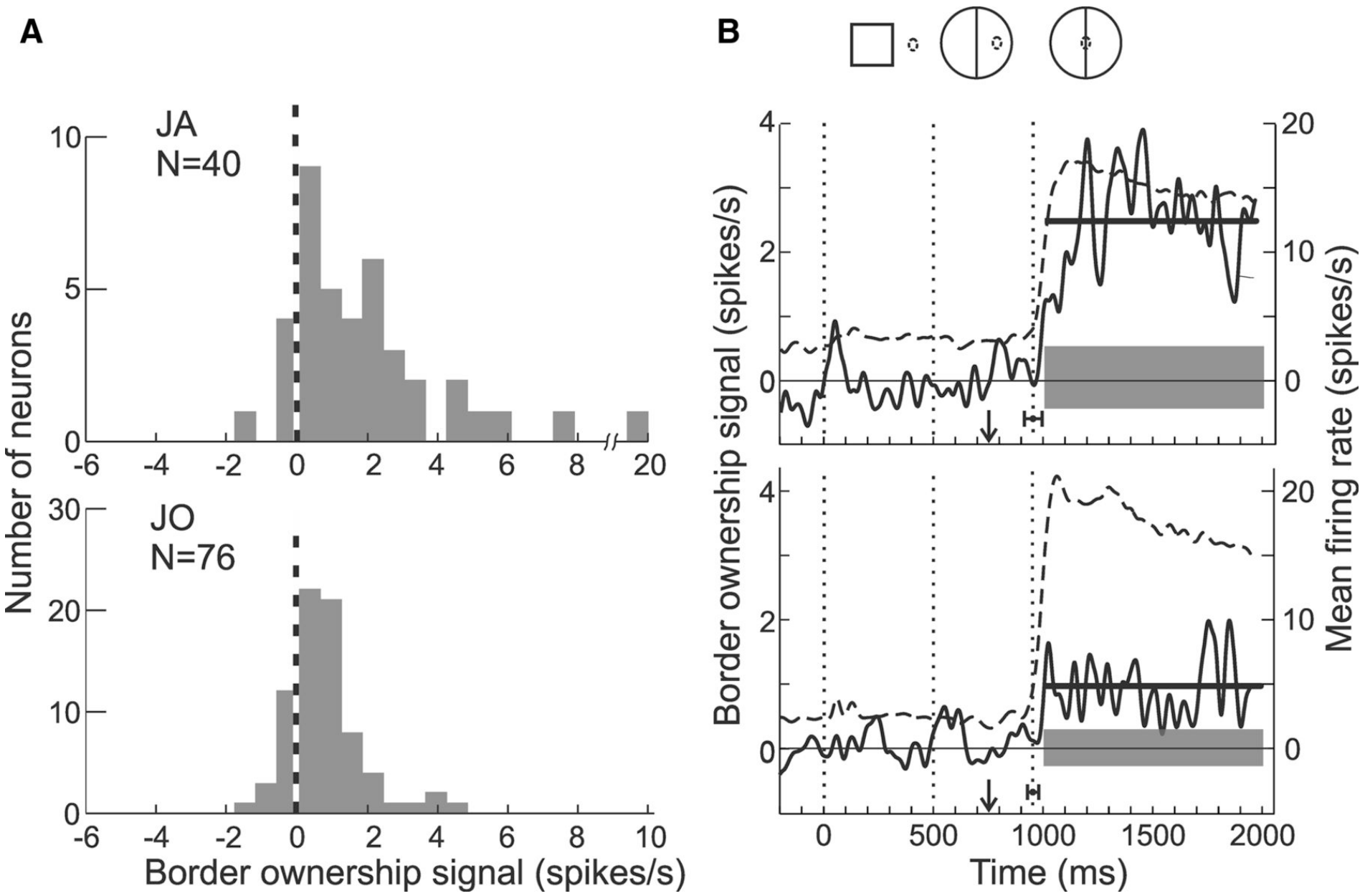

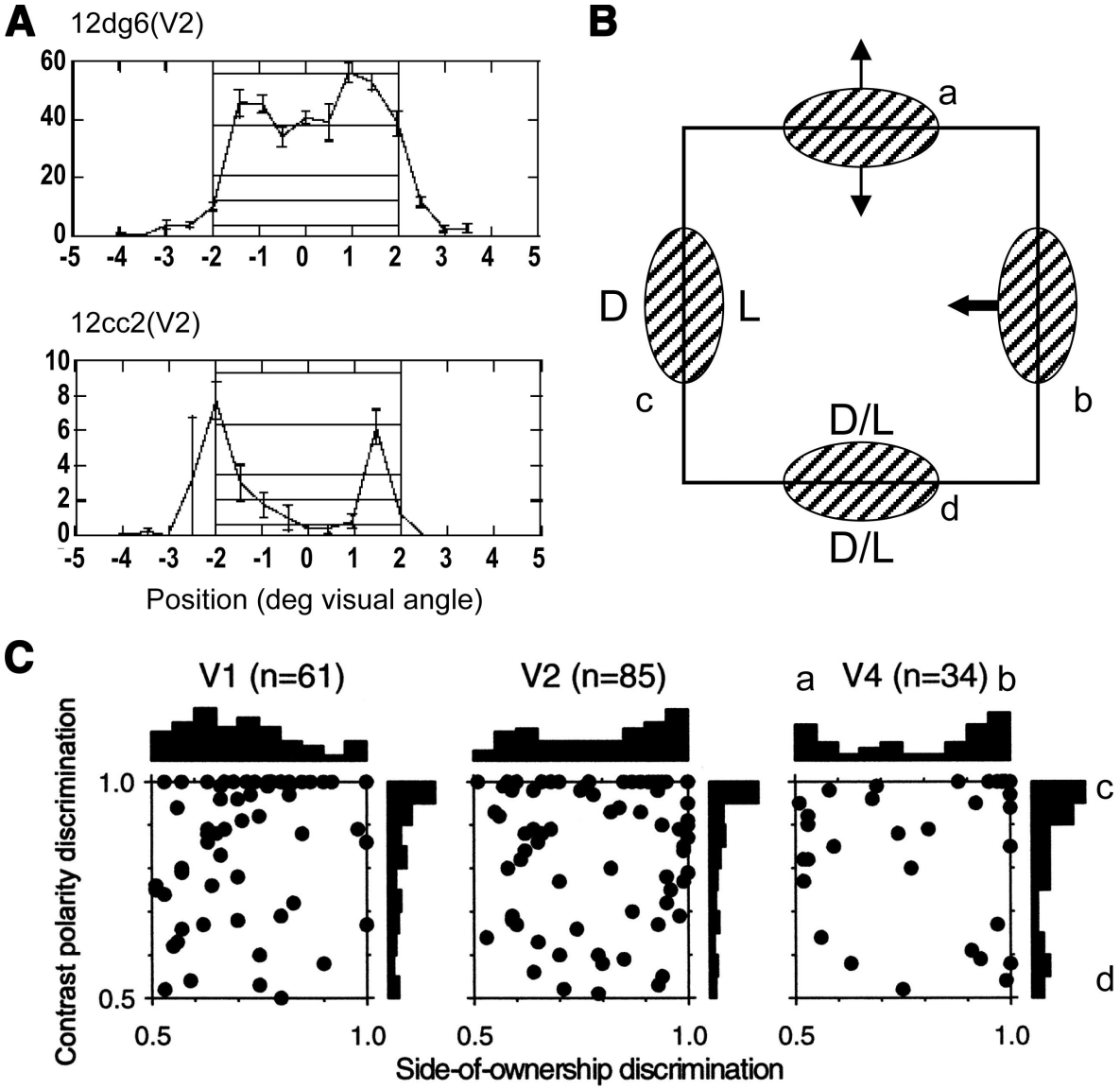

FIG. 7. Edge neurons and border ownership selectivity. *A*: response of a surface and an edge neuron (V2) as a function of the position of a square figure. [From Friedman et al. (71), with permission from Blackwell Publishing.] *B*: schematic indication of four types of neurons (stripes indicate RF) signaling the direction of the figure with respect to the edge (*b*) or not (*a*) and signaling the polarity of the figure (*c*) or not (*d*). *C*: distribution of contrast polarity discrimination (*c*-*d*) and side of ownership discrimination (*b*-*a*) in V1, V2, and V4. [Modified from Zhou et al. (350).]

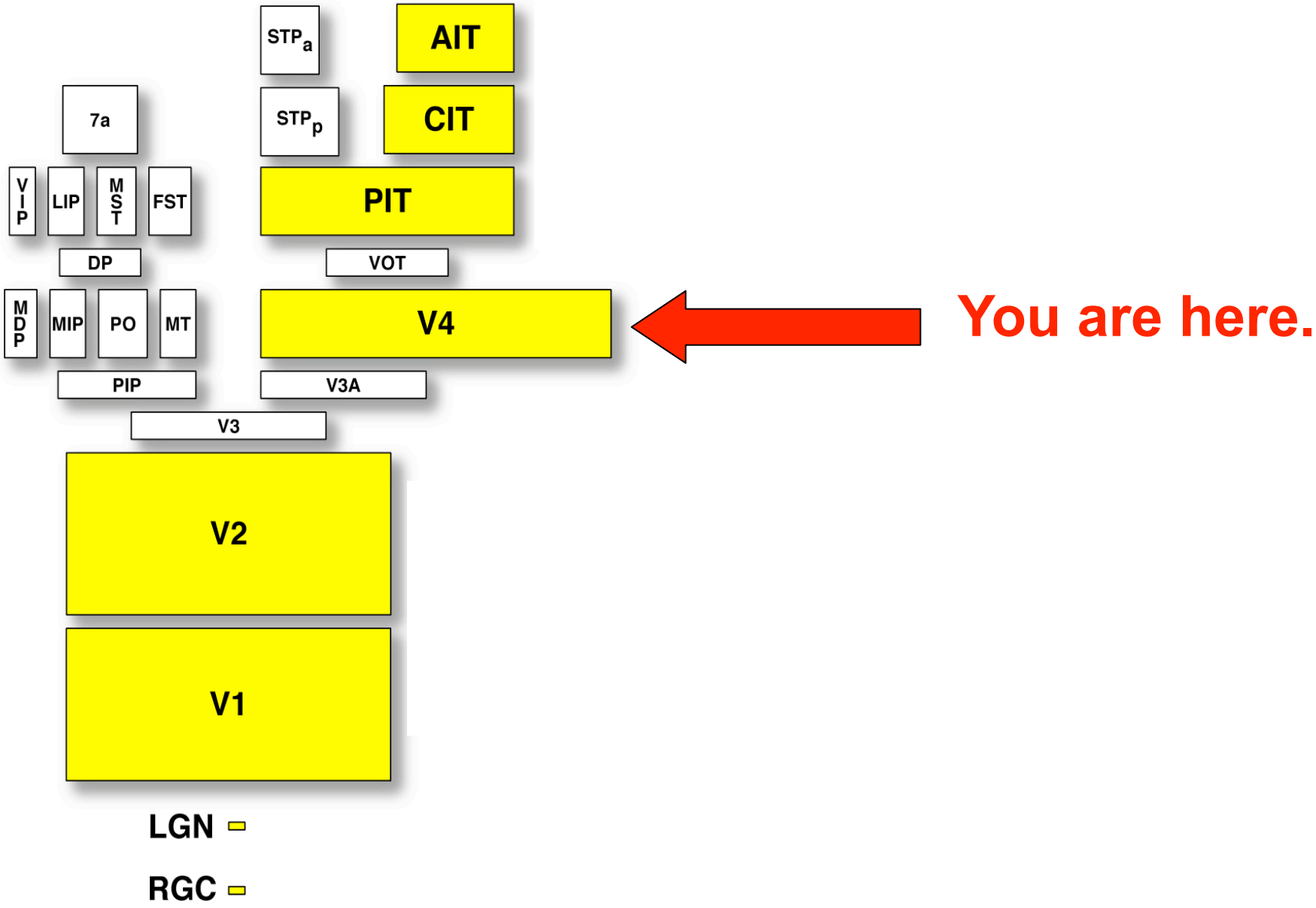
STPa
AIT
7a
STPp
CIT
VIP
LIP
MST
FST
PIT
DP
VOT
MDP
MIP
PO
MT
V4
You are here.
PIP
V3A
V3
V2
V1
LGN
RGC

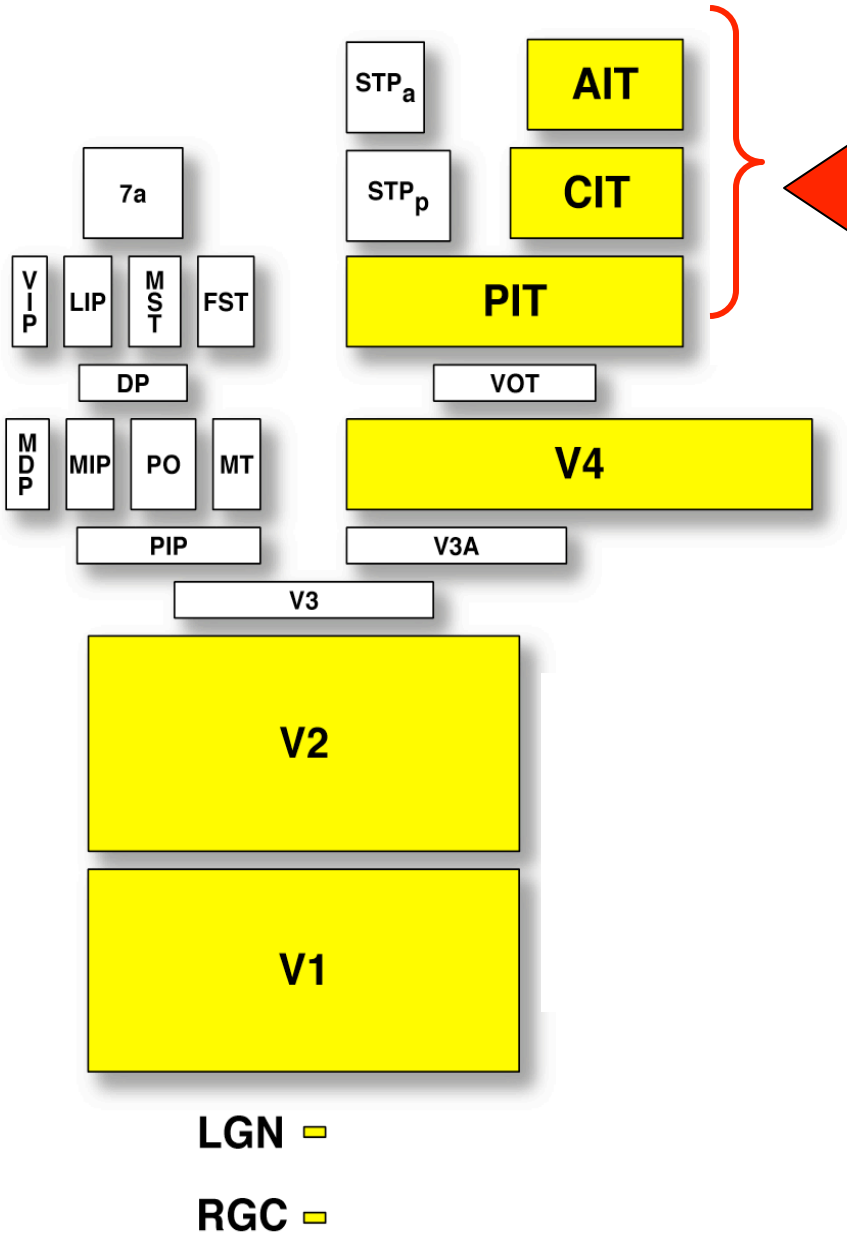
STP a
AIT
7a
STP p
CIT
VIP
LIP
MST
FST
PIT
DP
VOT
MDP
MIP
PO
MT
V4
PIP
V3A
V3
V2
V1
LGN
RGC

You are here.

IT statistics (rhesus monkey)

~ 7.7 cm^2 (in each hemisphere)

~ 8% of neocortex (~ 15% of visual cortex)

~ 90 million neurons

Subregions: (PIT, CIT, AIT) (TEO, TE)

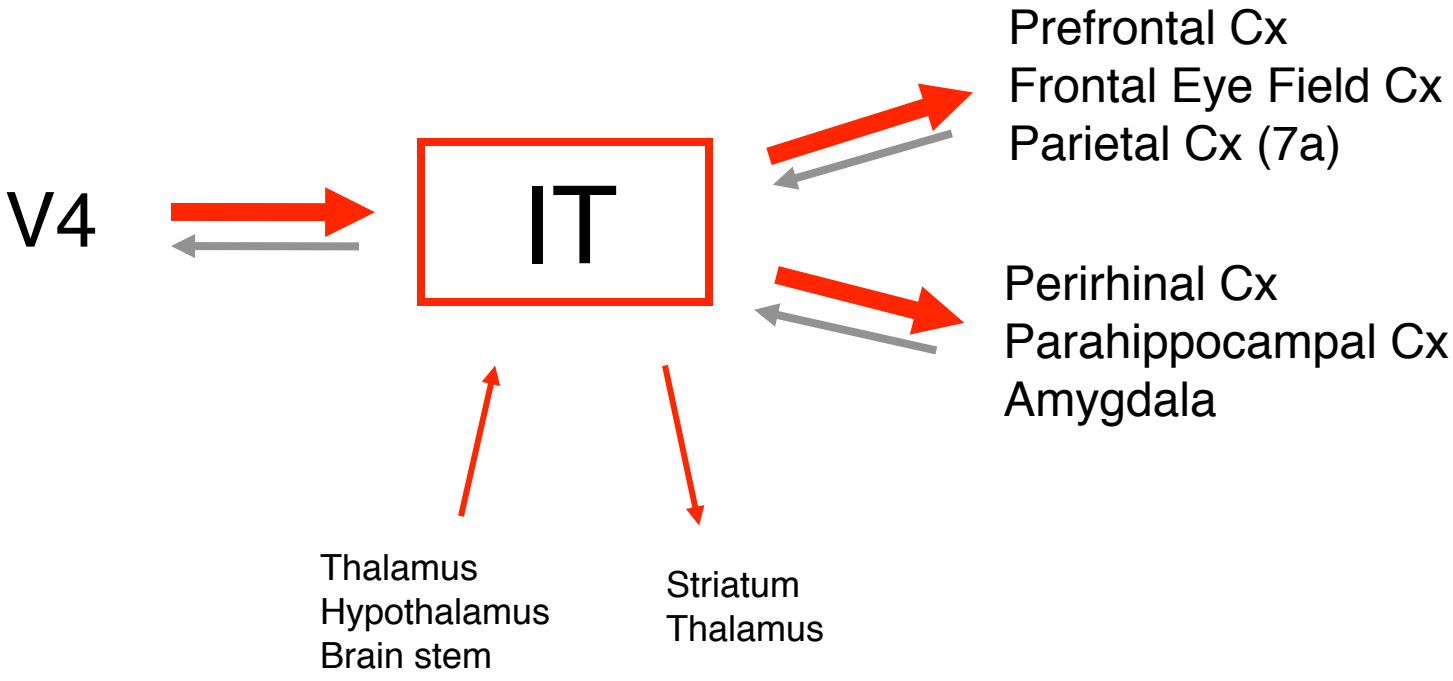

IT is about central vision

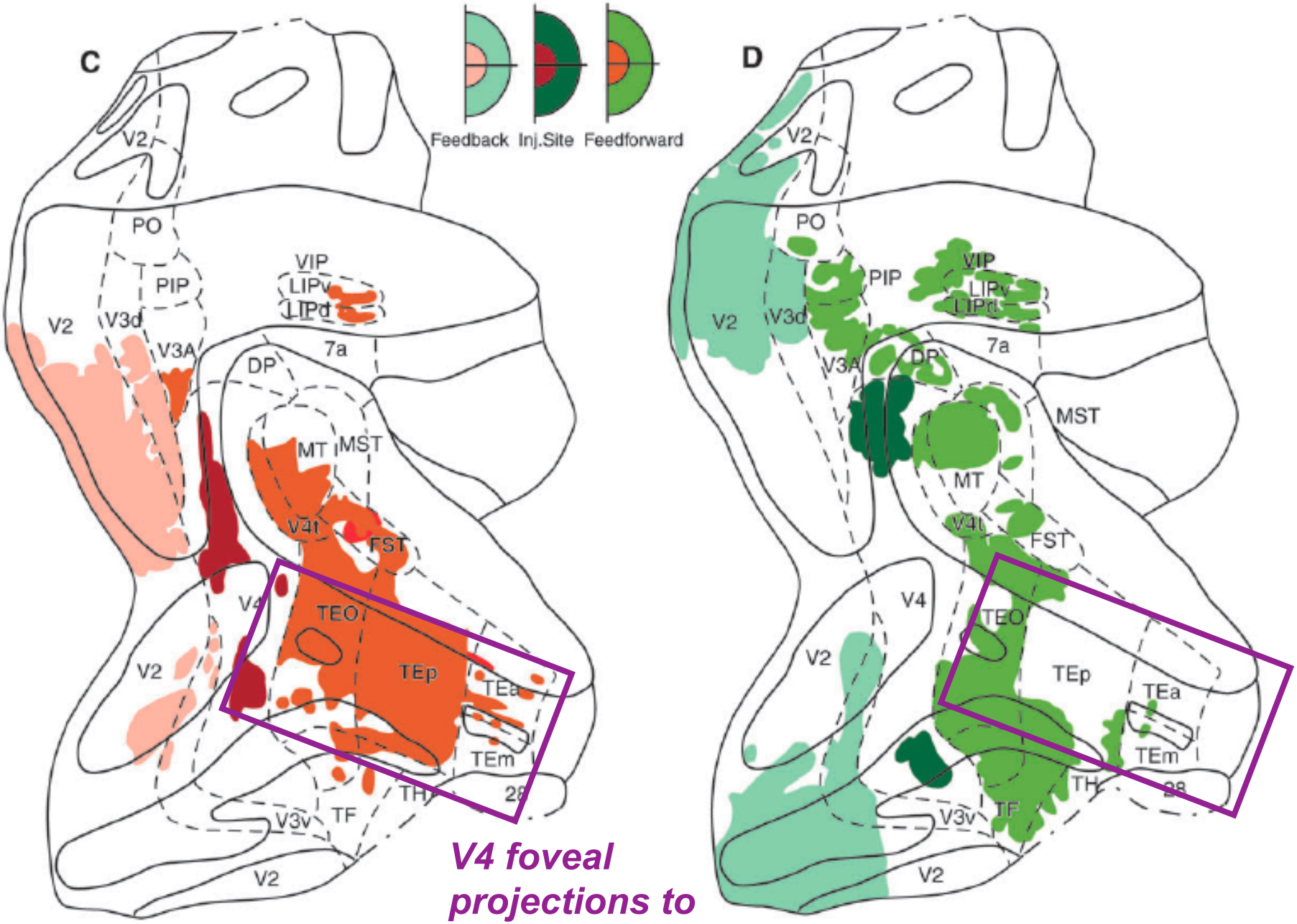

V4 foveal projections to IT

Ungerleider et al (2007)

The "complexity" of the stimuli needed to activate neurons increases along the ventral stream

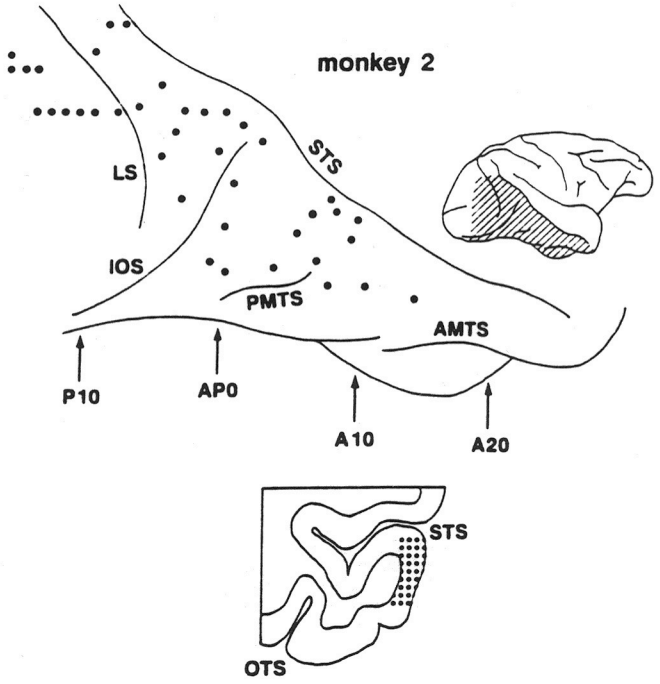

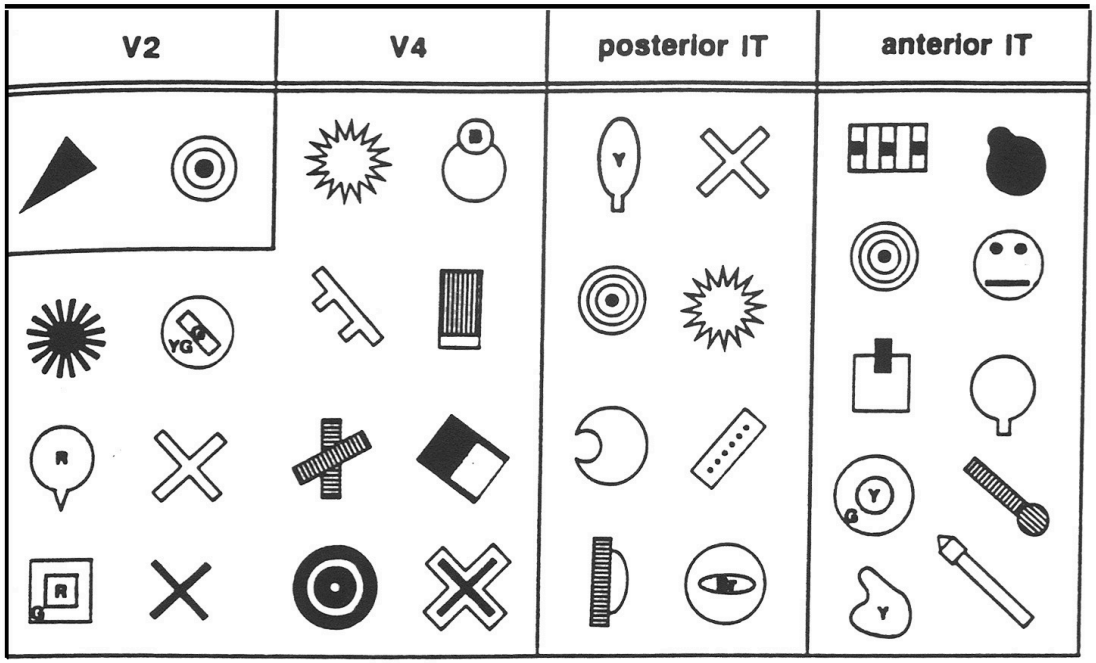

Kobatake and Tanaka (1994)

Average RF size also increases along the ventral stream

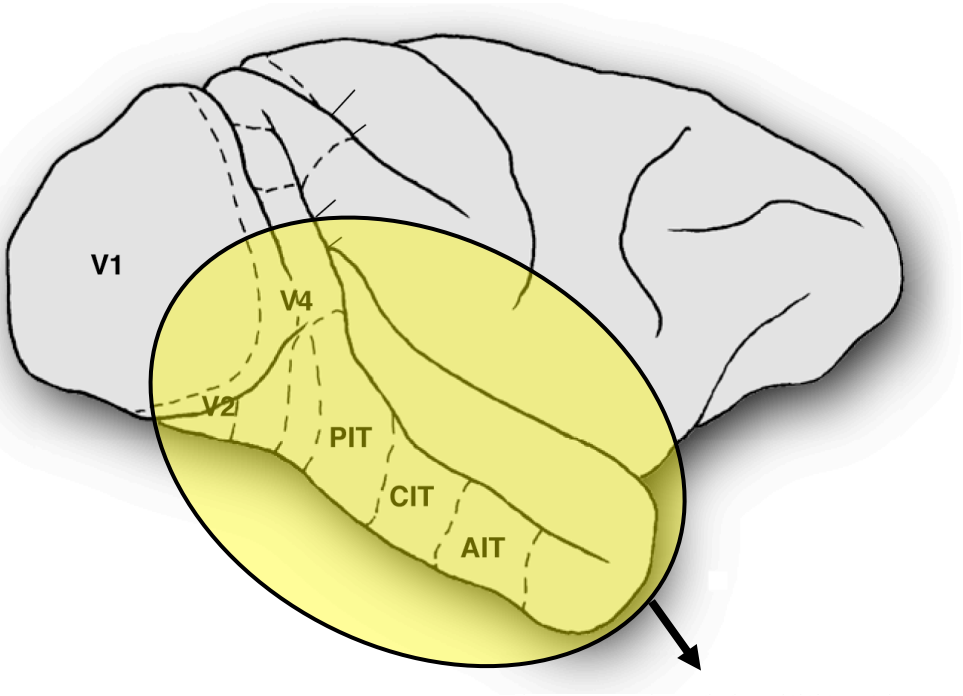

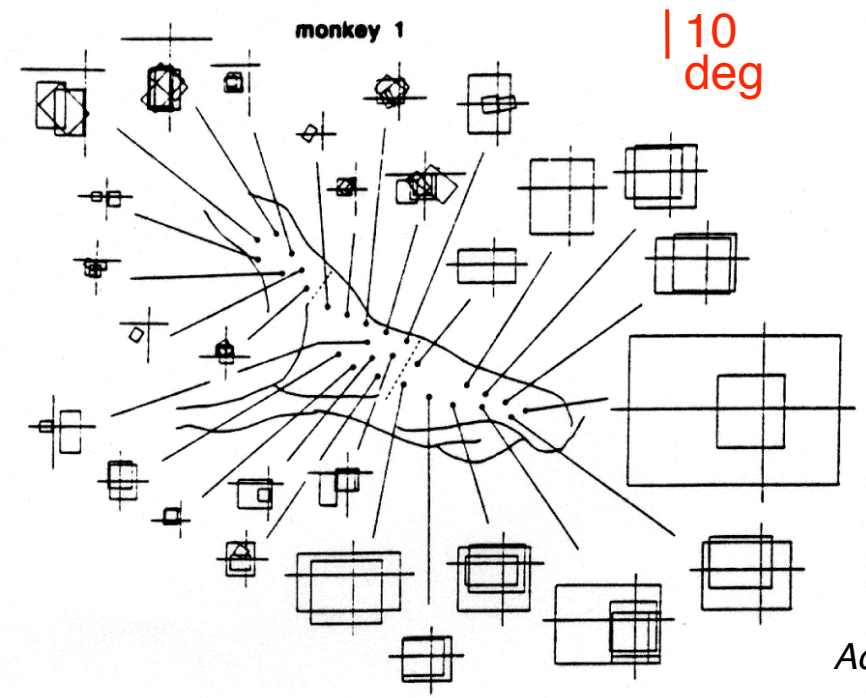

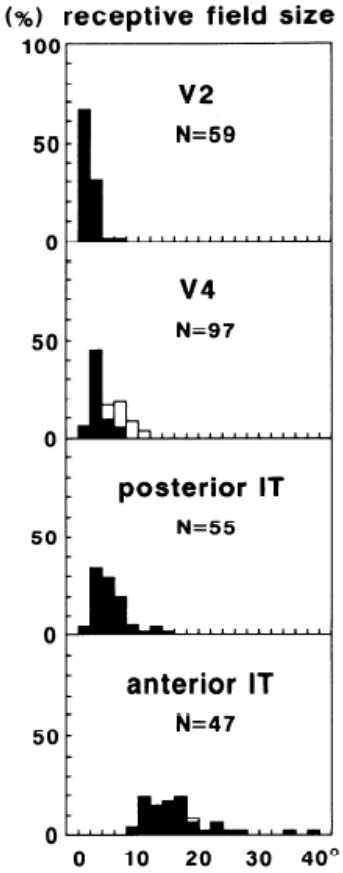

Adapted from Kobatake et al. (1994)

Stimulus selectivity in inferotemporal cortex
Gross, Rocha-Miranda & Bender 1972

Increasing ability to drive this IT neuron -->

“The use of [these] stimuli was begun one day when, having failed to drive a unit with any light stimulus, we waved a hand at the stimulus screen and elicited a very vigorous response from the previously unresponsive neuron...

“We then spent the next 12 hours testing various paper cutouts in an attempt to find the trigger feature for this unit. When the entire set of stimuli used were ranked according to the strength of the response that they produced, we could not find a simple physical dimension that correlated with this rank order. However, the rank order of adequate stimuli did correlate with similarity (for us) to the shadow of a monkey hand." (Gross et al., 1972)

IT neurons can be tuned to very specific combinations of features (high selectivity)

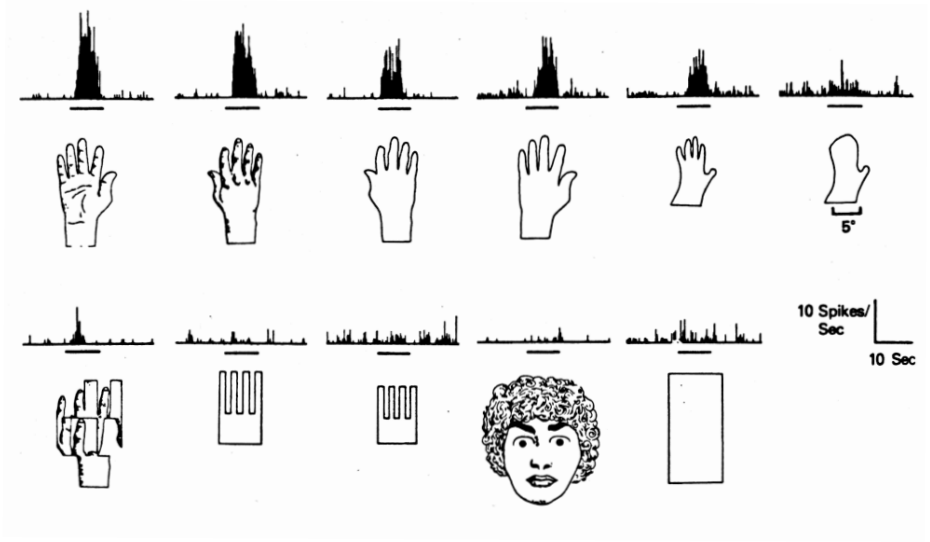

Desimone et al. (1984)

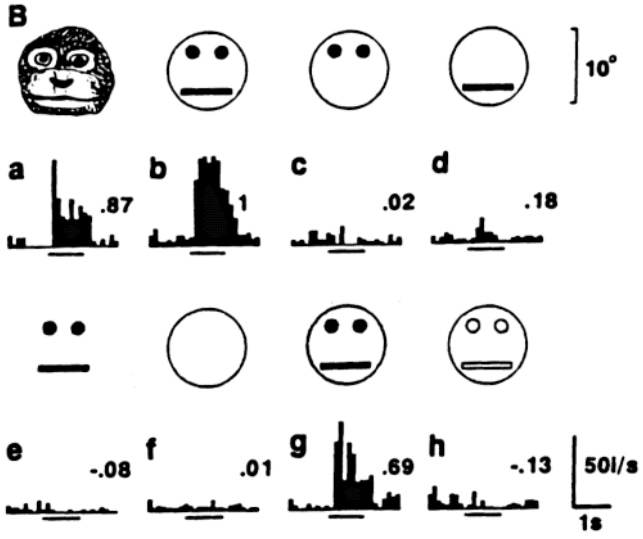

Kobatake et al. (1994)

Selectivity for objects in two IT neurons
(Tamura and Tanaka, 2001)

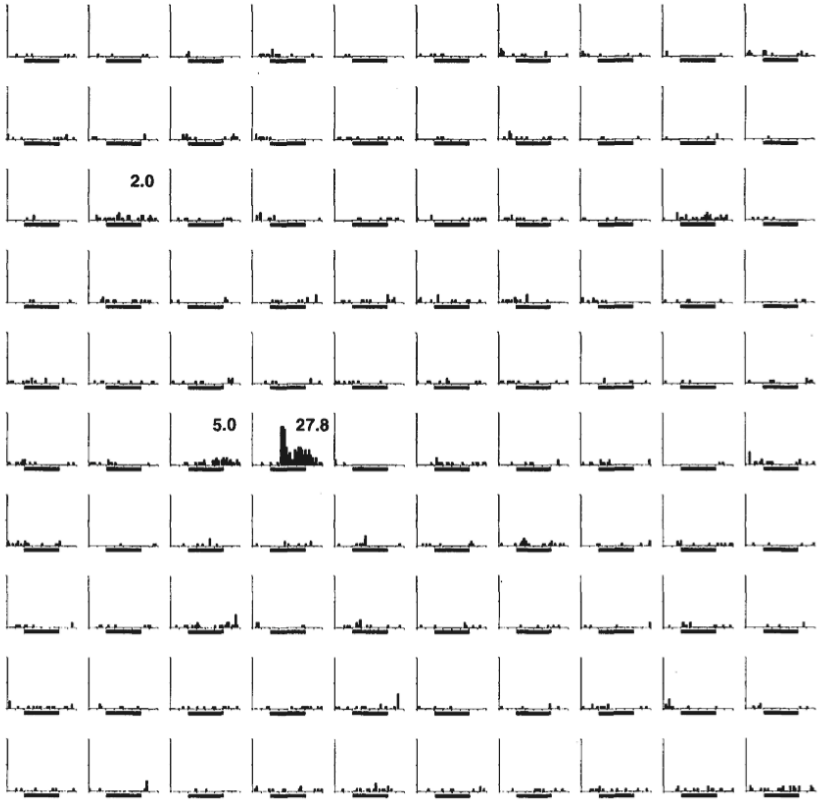

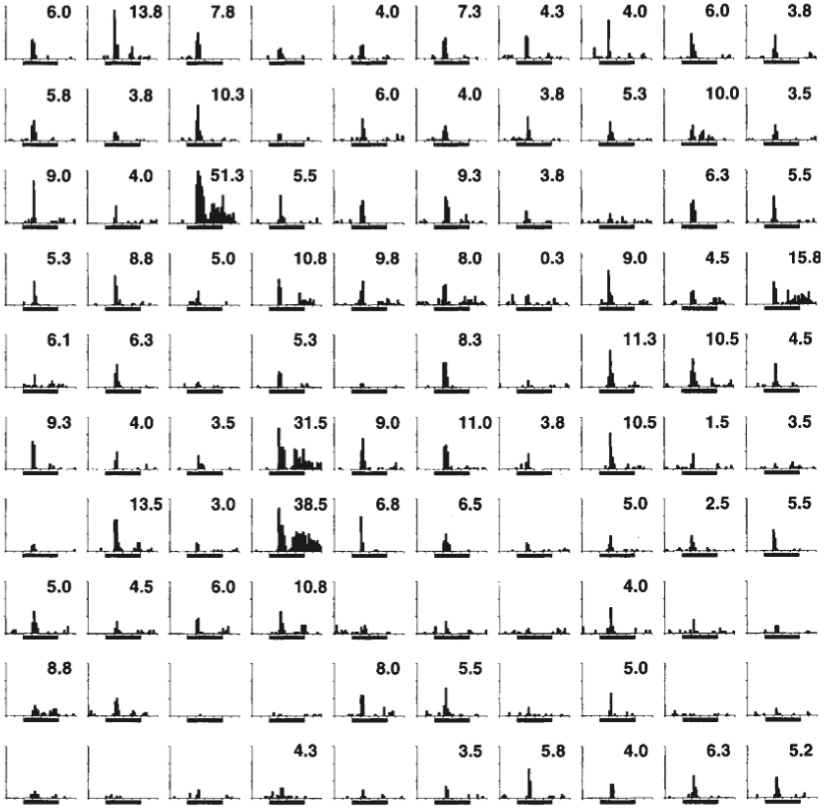

Cortical representations: sparseness

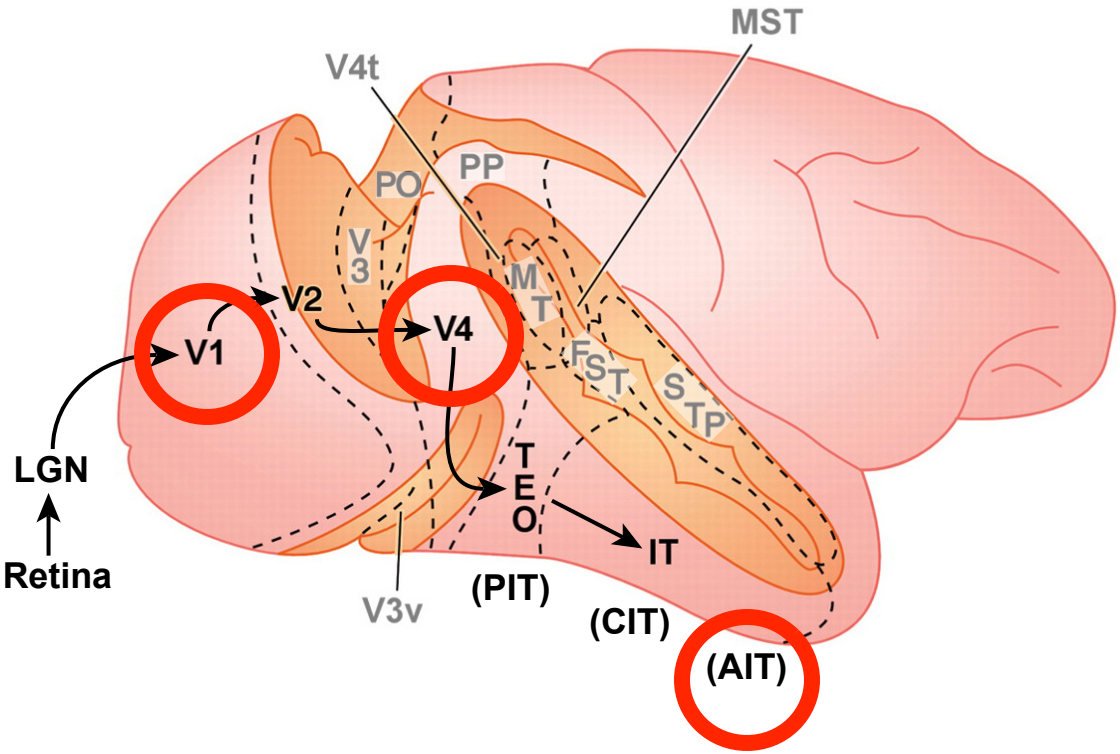

Sparseness of neural response in V1

V1

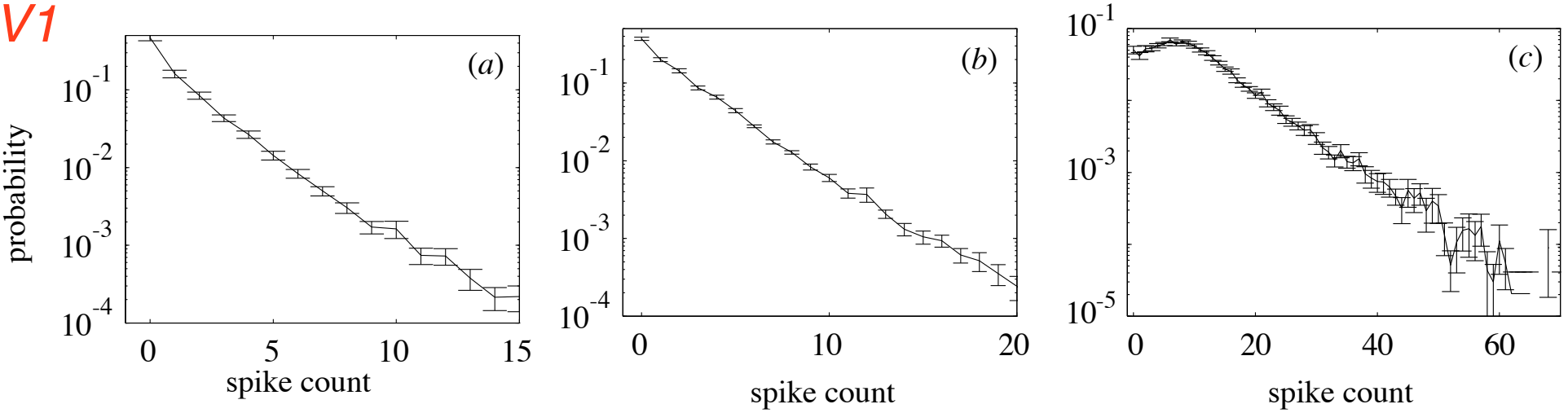

Baddeley et al, 1997

IT neurons are tolerant to identity-preserving transformations

Position *Scale* *Context*

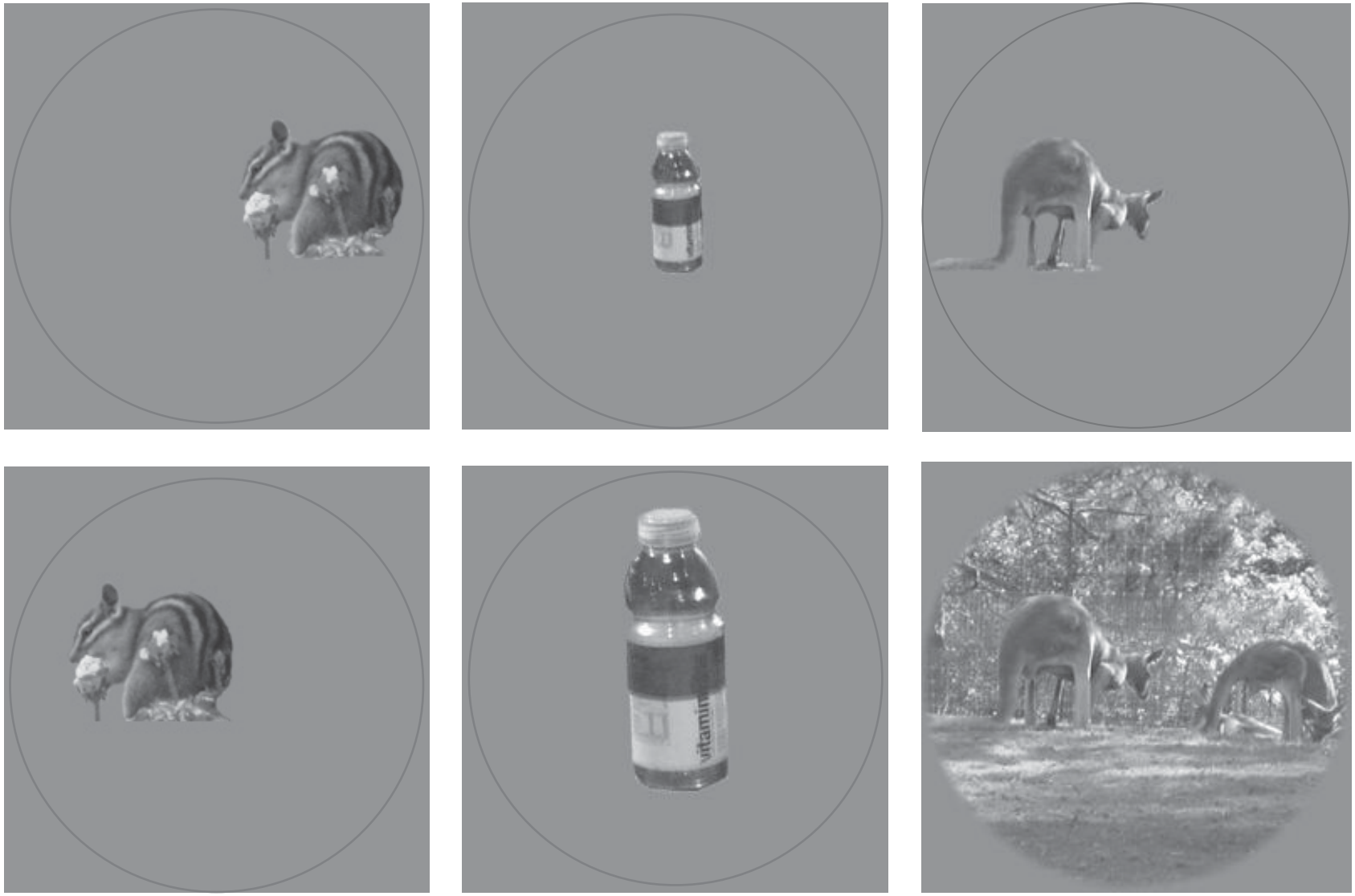

Rust & DiCarlo, 2012

"Sparseness" is not a direct measure of "selectivity"

Neuron 1

Neuron 2

Rust & DiCarlo, 2012

"Sparseness" is not a direct measure of "selectivity"

Neuron 1

Neuron 2

Sparseness: 2/4

Rust & DiCarlo, 2012

"Sparseness" is not a direct measure of "selectivity"

Neuron 1

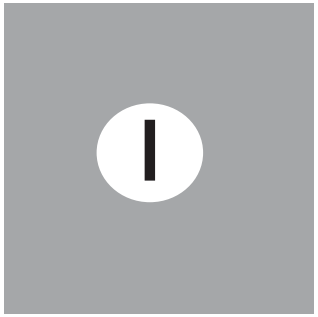

Neuron 2

Sparseness: 2/4

Rust & DiCarlo, 2012

"Sparseness" is not a direct measure of "selectivity"

Neuron 1

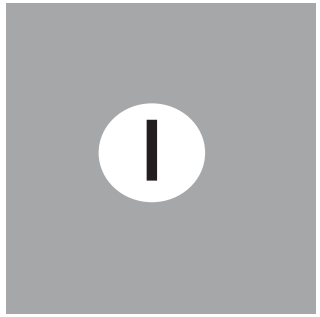

Neuron 2

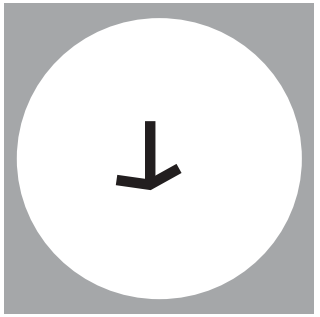

Sparseness: 2/4

Rust & DiCarlo, 2012

Selectivity and tolerance are confounded in complex images

Neuron 1

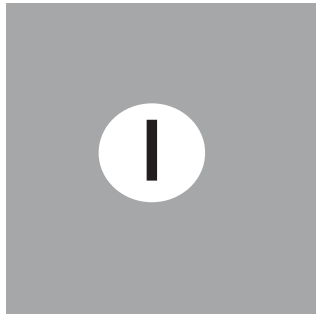

Neuron 2

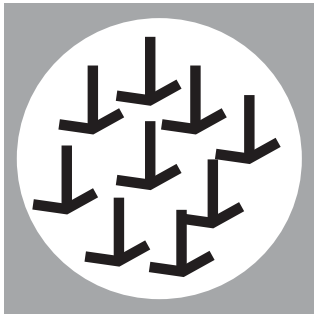

Sparseness: 2/4

Rust & DiCarlo, 2012

Variations in sparseness across the visual pathway?

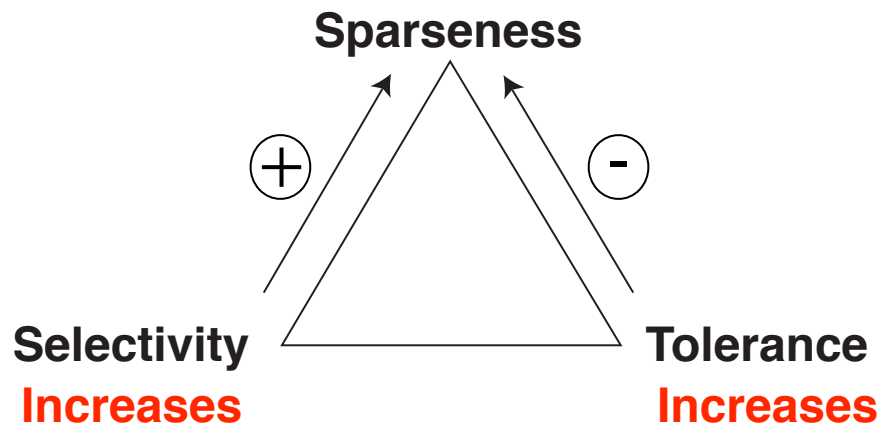

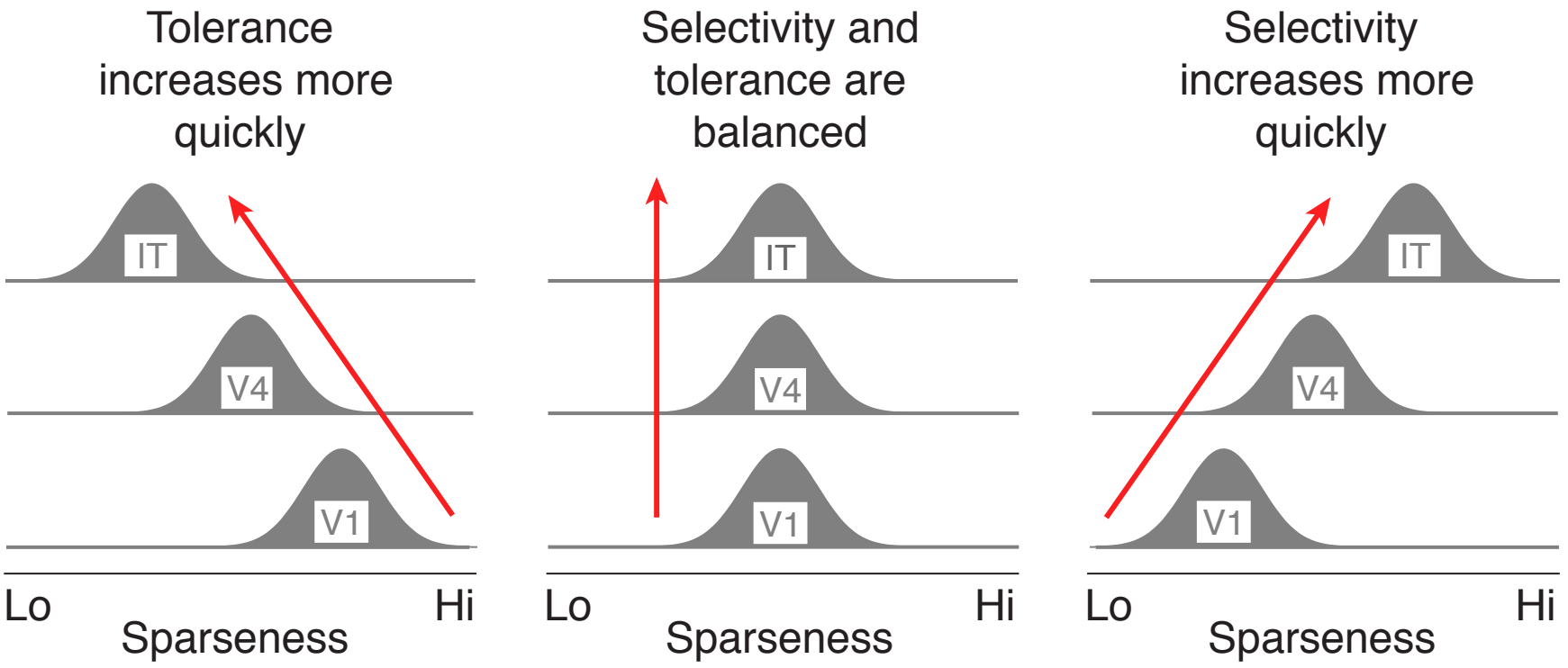

Rust & DiCarlo, 2012

Measuring sparseness

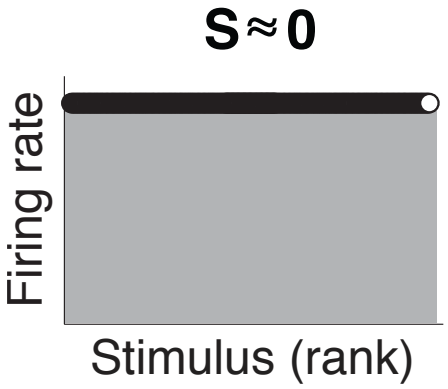

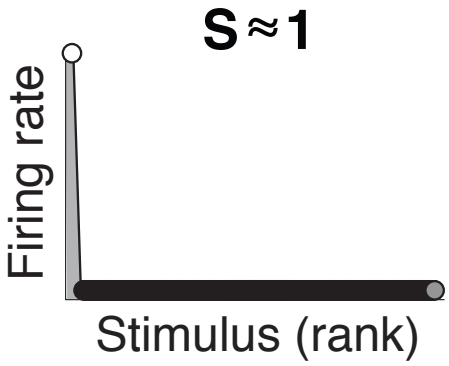

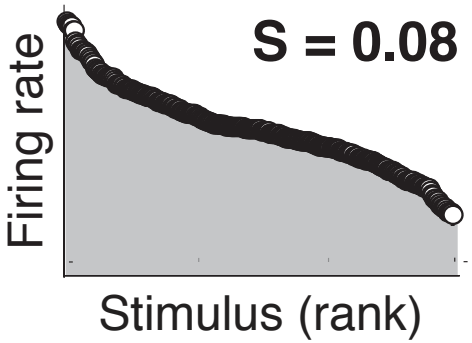

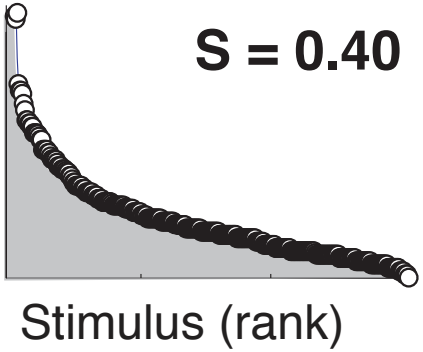

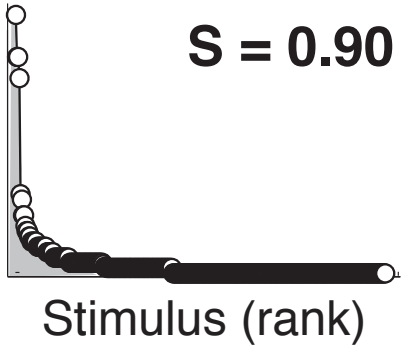

Rolls & Tovee 1995; Vinje & Gallant 2000; Lehky, Sejnowski & Desimone 2005

Sparseness is the same in V4 and IT

V4

n=153

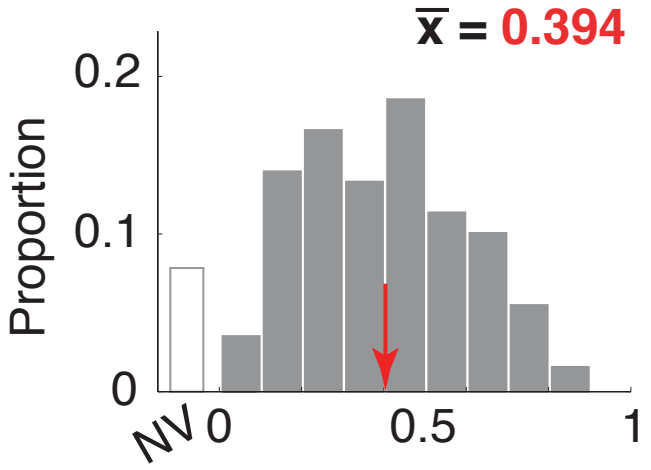

IT

n=151

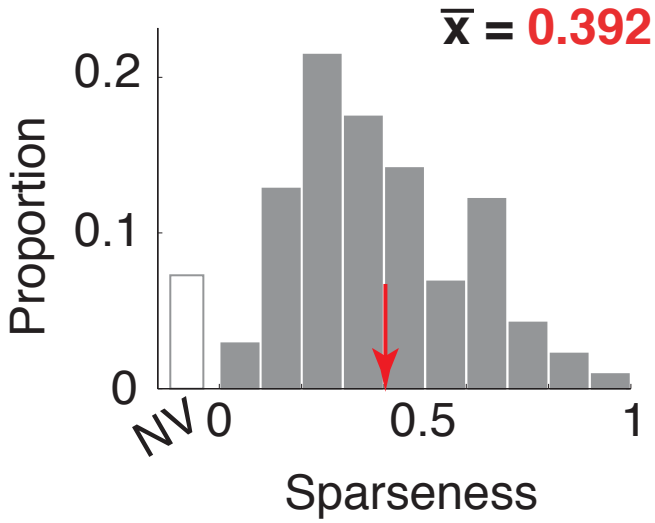

V4 and IT neurons respond to ~10% of natural images at firing rates over 50% of their peak

Rust & DiCarlo, 2012

Sparseness is the same in V1 and IT

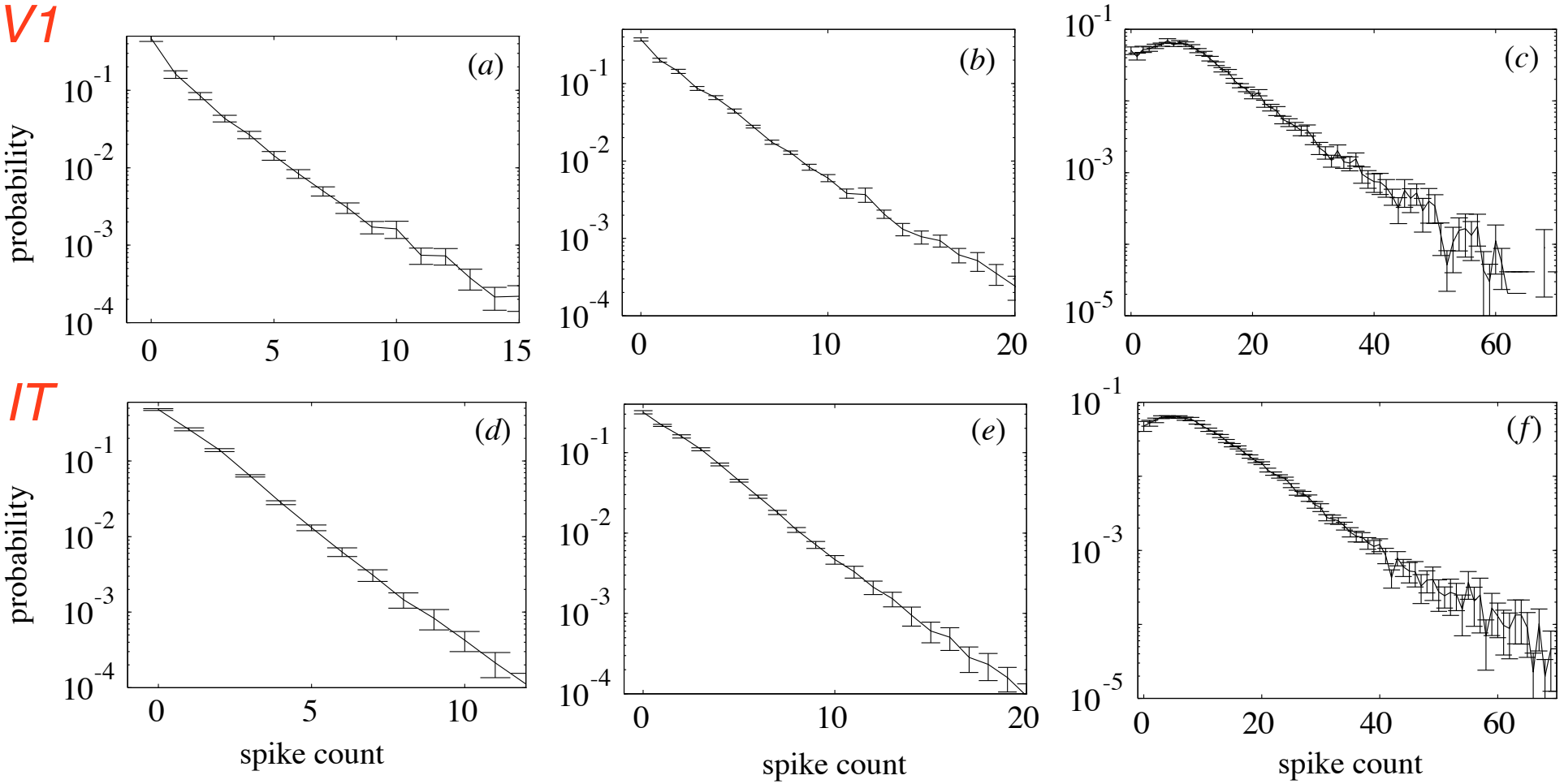

Baddeley et al, 1997

Sparseness is constant along the visual pathway

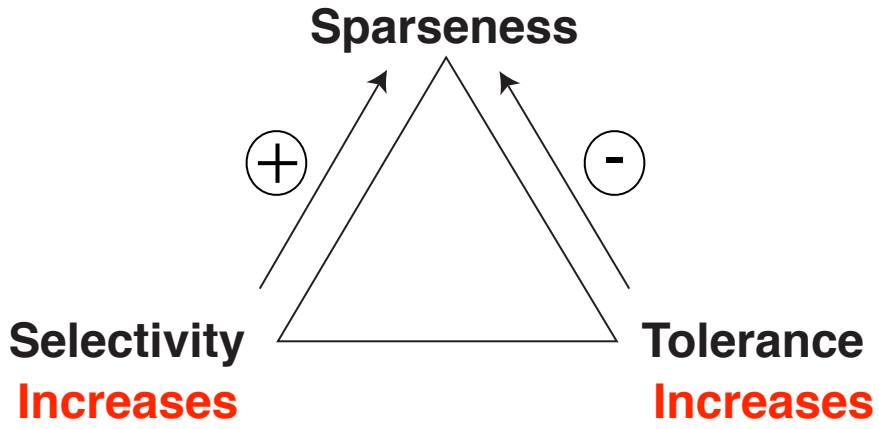

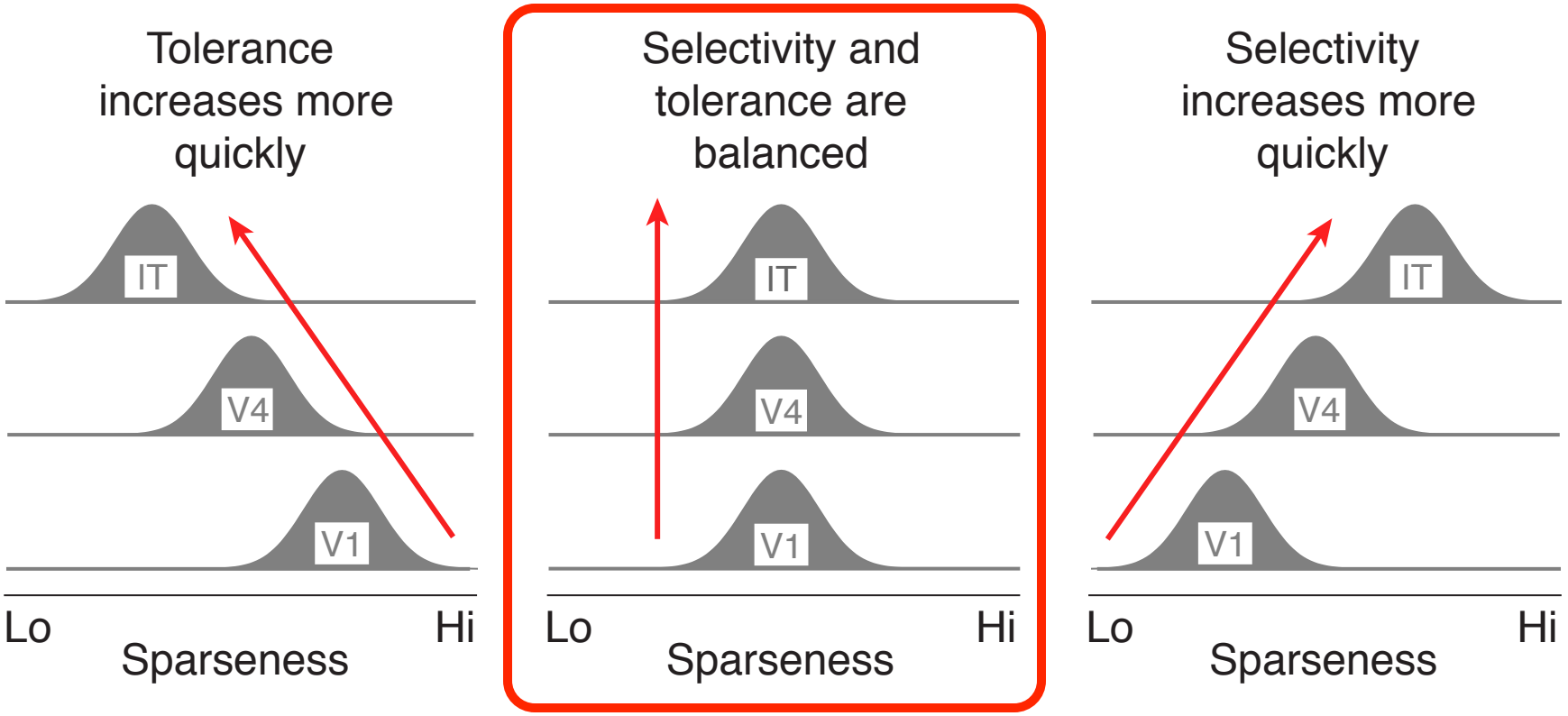

Rust & DiCarlo, 2012

Bandwidth of tuning for
complex/natural images

Sparseness

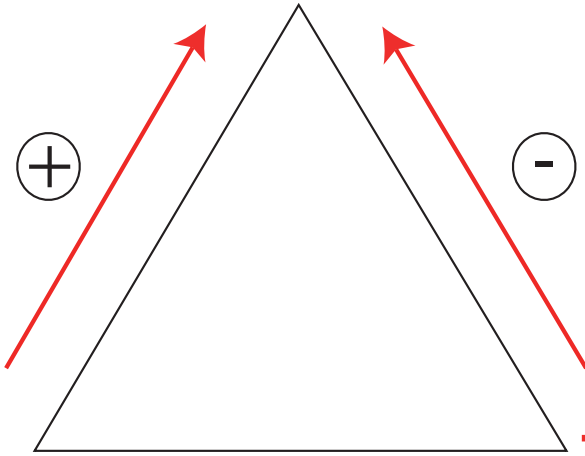

Selectivity

Tolerance

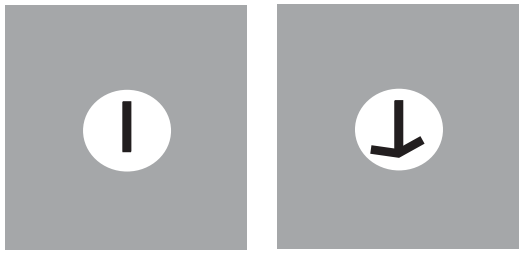

Complexity of image
features driving a
neuron

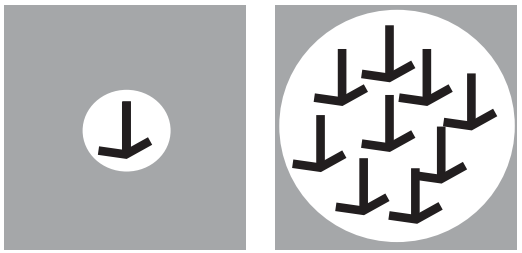

Insensitivity to identity-
preserving transformations

Rust & DiCarlo, 2012

The form processing pathway maintains an "equally distributed" representation of images